



State-of-the-Art review of Numerical Methods in Structural Dynamics

BETELEY TAMIRU MEKONNEN

A project submitted to the School of Graduate Studies of Addis Ababa University in Partial Fulfillment of the Requirement for the Degree of Master of Engineering in Civil Engineering (Structures)

November 2021



**ADDIS ABABA UNIVERSITY
SCHOOL OF GRADUATE STUDIES
FACULTY OF TECHNOLOGY
DEPARTMENT OF CIVIL ENGINEERING**

State-of-the-Art review of Numerical Methods in Structural Dynamics

By
BETELY TAMRU MEKONNEN

NOVEMBER 2021

The undersigned have examined the paper entitled '**State-of-the-Art review of Numerical Methods in Structural Dynamics**' presented by **Betely Tamru**, a candidate for the degree of **Master of Engineering** and hereby certify that it is worthy of acceptance.

Dr. Shifferaw Taye
Advisor

Signature

Date

External Examiner

Signature

Date

Internal Examiner

Signature

Date

Chairman

Signature

Date

DECLARATION

I certify that this paper work entitled '**State-of-the-Art review of Numerical Methods in Structural Dynamics**' is my own work except for citations which have been duly acknowledged. The work has not been presented elsewhere for assessment and award of any degree or diploma.

Betely Tamru
Author

Signature

Date

Contents

Acknowledgements	iii
Abstract	iv
List of Figures	v
List of Tables	viii
1. Introduction	1
1.1 Background.....	1
1.2 Statement of the problem	2
1.3 Research questions	2
1.4 Objective of the research	3
1.5 Application of the study	3
1.6 Delimitations and limitations of the study	4
2. Literature Review	5
2.1 Time stepping methods	5
2.2 Mode superposition method	7
2.3 Stability and Accuracy of numerical algorithms.....	8
2.4 Non-linear system.....	8
3. Methodology	10
4. Proposed Methods	12
4.1 Method based on interpolation of excitation 1 (linear system with non-classical damping)	12
4.2 Method based on interpolation of excitation 2 (non-linear system)	15
4.3 Method based on interpolation of excitation 3 (non-linear system)	21
5. Analysis and Results	27
6. Illustrative example solutions	47
6.1 Single degree of freedom system.....	47
6.2 Multi-degree of freedom system (Undamped).....	50
6.3 Multi-degree of freedom system (Non-classically damped).....	57
6.4 Clamped-free bar	65
6.5 Two-story-building system(dissipation of unwanted frequencies).....	72

6.6 Non-linear spring system	78
6.7 Five-story shear building (Non-linear)	81
7. Conclusion	75
8. References	86
Annex A	86

Acknowledgements

I would like to express my deep gratitude to Dr. Shifferaw Taye,

- for his kind support and cooperation vis-à-vis the preparation of this project paper
- for his invaluable knowledge transfer during his tenure as our lecturer

I would also like to thank Dr. Adil Zekaria, Dr. Girma Zerayohannes, Dr. Esayas Gebreyouhannes, Dr. Abraham Gebre and Dr. Bedilu Habte for sharing their wisdom, knowledge and experience during my stay in Addis Ababa University.

I would also like to extend my thanks to the staff of the civil engineering department for their help in overcoming the problems related to administration issues.

Furthermore, I am deeply indebted to my family members, friends and co-workers whose encouragements and advices were very crucial to my study.

Abstract

In this paper, a state-of-the-art review is carried out on numerical methods comprising the Central Difference, Houbolt, Newmark, Wilson- θ , HHT- α , WBZ- α , Generalized- α , Bathe and Piecewise Exact Methods. Three algorithms (related to Piecewise Exact Method and Power Series Method) are developed for linear and nonlinear systems.

To analyze the performance of the methods, the stability and accuracy of the above-mentioned methods are studied and some solutions for illustrative examples are presented.

The HHT- α , WBZ- α , Generalized- α and Bathe methods have controllable dissipation in higher methods. The piecewise exact method (method based on interpolation of excitation) and the proposed methods are effective in providing accurate results (compared to other methods) for the truncated modal space.

List of Figures

Figure 5.1 Spectral radii of Central Difference Method, case $\xi=0$	30
Figure 5.2 Spectral radii of Houbolt Method, case $\xi=0$	30
Figure 5.3 Spectral radii of N-M, HHT-M, WBZ-M and G-M, case $\xi=0$ and $\rho_{inf}=1$	31
Figure 5.4 Spectral radii of N-M, HHT-M, WBZ-M and G-M, case $\xi=0$ and $\rho_{inf}=0.7$	31
Figure 5.5 Spectral radii of N-M, HHT-M, WBZ-M and G-M, case $\xi=0$ and $\rho_{inf}=0.5$	32
Figure 5.6 Spectral radii of N-M, HHT-M, WBZ-M and G-M, case $\xi=0$ and $\rho_{inf}=0.3$	32
Figure 5.7 Spectral radii of Bathe-M, case $\xi=0$ and $0<\alpha s<1$	33
Figure 5.8 Spectral radii of Bathe-M, case $\xi=0$ and $\alpha s>1$	34
Figure 5.9 Spectral radii of Wilson-M, case $\xi=0$ and $\theta=1,1.37,1.4,1.5$	34
Figure 5.10 Amplitude decay of Central Difference Method, case $\xi=0$	35
Figure 5.11 Amplitude decay of Houbolt Method, case $\xi=0$	35
Figure 5.12 Amplitude decay of N-M, HHT-M, WBZ-M and G-M, case $\xi=0$ and $\rho_{inf}=1$	36
Figure 5.13 Amplitude decay of N-M, HHT-M, WBZ-M and G-M, case $\xi=0$ and $\rho_{inf}=0.7$	36
Figure 5.14 Amplitude decay of N-M, HHT-M, WBZ-M and G-M, case $\xi=0$ and $\rho_{inf}=0.5$	37
Figure 5.15 Amplitude decay of N-M, HHT-M, WBZ-M and G-M, case $\xi=0$ and $\rho_{inf}=0.3$	37
Figure 5.16 Amplitude decay of Bathe-M, case $\xi=0$ and $0<\alpha s<1$	38
Figure 5.17 Amplitude decay of Bathe-M, case $\xi=0$ and $\alpha s>1$	38
Figure 5.18 Amplitude decay of Wilson-M, case $\xi=0$ and $\theta=1,1.37,1.4,1.5$	39
Figure 5.19 Period elongation of Central Difference Method, case $\xi=0$	39
Figure 5.20 Period elongation of Houbolt Method, case $\xi=0$	40
Figure 5.21 Period elongation of N-M, HHT-M, WBZ-M and G-M, case $\xi=0$ and $\rho_{inf}=1$	40
Figure 5.22 Period elongation of N-M, HHT-M, WBZ-M and G-M, case $\xi=0$ and $\rho_{inf}=0.7$	41
Figure 5.23 Period elongation of N-M, HHT-M, WBZ-M and G-M, case $\xi=0$ and $\rho_{inf}=0.5$	41
Figure 5.24 Period elongation of N-M, HHT-M, WBZ-M and G-M, case $\xi=0$ and $\rho_{inf}=0.3$	42
Figure 5.25 Period elongation of Bathe-M, case $\xi=0$ and $0<\alpha s<1$	42
Figure 5.26 Period elongation of Bathe-M, case $\xi=0$ and $\alpha s>1$	43
Figure 5.27 Period elongation of Wilson-M, case $\xi=0$ and $\theta=1,1.37,1.4,1.5$	43
Figure 5.28 Spectral radii of Central Difference Method, case $\xi=0,0.02,0.05,0.1,0.2$	44
Figure 5.29 Spectral radii of Houbolt Method, case $\xi=0,0.02,0.05,0.1,0.2$	44
Figure 5.30 Spectral radii of Newmark Method, case $\xi=0,0.02,0.05,0.1,0.2$	45
Figure 5.31 Spectral radii of Wilson Method ($\theta=1.37$), case $\xi=0,0.02,0.05,0.1,0.2$	45
Figure 5.32 Spectral radii of Bathe Method ($\alpha s=0.01$), case $\xi=0,0.02,0.05,0.1,0.2$	46

Figure 6.1.1 Displacement response of single degree of freedom, $\Delta t=0.3$	48
Figure 6.1.2 Displacement response of single degree of freedom, $\Delta t=0.5$	48
Figure 6.1.3 Displacement response of single degree of freedom, $\Delta t=1.2$	49
Figure 6.2.(a) Multi-degree of freedom system	50
Figure 6.2.1 Displacement response of multi-degree of freedom system Ut1, $\Delta t=0.25$	52
Figure 6.2.2 Displacement response of multi-degree of freedom system Ut2, $\Delta t=0.25$	53
Figure 6.2.3 Displacement response of multi-degree of freedom system Ut1, $\Delta t=0.4$	53
Figure 6.2.4 Displacement response of multi-degree of freedom system Ut2, $\Delta t=0.4$	54
Figure 6.2.5 Displacement response of multi-degree of freedom system Ut1, $\Delta t=0.9$	54
Figure 6.2.6 Displacement response of multi-degree of freedom system Ut2, $\Delta t=0.9$	55
Figure 6.3.(a) Multi-degree of freedom system (NCD)	57
Figure 6.3.1 Displacement response of multi-degree of freedom system (NCD) Ut1, $\Delta t=0.3$	61
Figure 6.3.2 Displacement response of multi-degree of freedom system (NCD) Ut2, $\Delta t=0.3$	61
Figure 6.3.3 Displacement response of multi-degree of freedom system (NCD) Ut1, $\Delta t=0.5$	62
Figure 6.3.4 Displacement response of multi-degree of freedom system (NCD) Ut2, $\Delta t=0.5$	62
Figure 6.3.5 Displacement response of multi-degree of freedom system (NCD) Ut1, $\Delta t=1.5$	63
Figure 6.3.6 Displacement response of multi-degree of freedom system (NCD) Ut2, $\Delta t=1.5$	63
Figure 6.4.(a) Multi-degree of freedom system (NCD)	65
Figure 6.4.1 Displacement response of clamped-free bar – Analytic Solution, Proposed method 1, Newmark, Central difference	67
Figure 6.4.2 Velocity response of clamped-free bar – Analytic Solution, Proposed method 1, Newmark, Central difference	67
Figure 6.4.3 Displacement response of clamped-free bar – Analytic, N-M, HHT-M, WBZ-M and G-M, $\rho_{inf}=0.7$	68
Figure 6.4.4 Velocity response of clamped-free bar – Analytic, N-M, HHT-M, WBZ-M and G-M, $\rho_{inf}=0.7$	68
Figure 6.4.5 Displacement response of clamped-free bar – Analytic, N-M, HHT-M, WBZ-M and G-M, $\rho_{inf}=0.5$	69
Figure 6.4.6 Velocity response of clamped-free bar – Analytic, N-M, HHT-M, WBZ-M and G-M, $\rho_{inf}=0.5$	69
Figure 6.4.7 Displacement response of clamped-free bar – Analytic, N-M, HHT-M, WBZ-M and G-M, $\rho_{inf}=0.3$	70
Figure 6.4.8 Velocity response of clamped-free bar – Analytic, N-M, HHT-M, WBZ-M and G-M, $\rho_{inf}=0.3$	70

Figure 6.4.9 Displacement response of clamped-free bar – Analytic, N-M, HHT-M, WBZ-M and G-M, $\rho_{inf}=0$ with Standar Bathe and Houbolt...	71
Figure 6.4.10 Velocity response of clamped-free bar – Analytic, N-M, HHT-M, WBZ-M and G-M, $\rho_{inf}=0$ with Standar Bathe and Houbolt.....	71
Figure 6.5 (a) Two story building system	72
Figure 6.5.1 Two story building system, Bathe Method ($\gamma=1/2, \beta=1/4, \alpha_s=0.5$)	74
Figure 6.5.2 Two story building system, Central Difference Method	74
Figure 6.5.3 Two story building system, Generalized-alpha Method ($\gamma=1/2, \beta=1/4, \alpha_f=1/2, \alpha_m=1/2$)	75
Figure 6.5.4 Two story building system, Houbolt Method	75
Figure 6.5.5 Two story building system, Newmark Method ($\gamma=1/2, \beta=1/4$)	76
Figure 6.5.6 Two story building system, Newmark Method ($\gamma=21/38, \beta=100/361$)	76
Figure 6.5.7 Two story building system, Wilson Method ($\theta=1.37$)	77
Figure 6.6 (a) Non-linear spring	78
Figure 6.6.1 Displacement response of non-linear spring – Reference, CD-M, N-M, PM2, PM3- time step (0.1s)	79
Figure 6.6.2 Displacement response of non-linear spring – Reference, CD-M, N-M, PM2, PM3- time step (0.3s)	80
Figure 6.6.3 Displacement response of non-linear spring – Reference, CD-M, N-M, PM2, PM3- time step (0.5s)	80
Figure 6.7 (a)	81
Figure 6.7 (b)	81
Figure 6.7.1 Displacement response (5) of five story shear building – Reference, CD-M, N-M, PM2- time step (0.05s)	83
Figure 6.7.2 Displacement response (5) of five story shear building – Reference, CD-M, N-M, PM2- time step (0.s)	84
Figure 6.7.3 Displacement response (5) of five story shear building – Reference, CD-M, N-M, PM2- time step (0.2s)	84
Figure A.3.2.1 Regions of stability of Central Difference and Newmark methods	129
Figure A.3.2.2 Regions of stability of Newmark methods in β and γ	133
Figure A.4.2.1 Newton Raphson iteration of a single degree of freedom system.....	145

List of Tables

Table 4.1.1 Interpolation of excitation 1- Linear system for non classical damping.....	14
Table 4.2.1 Interpolation of excitation 2- Non-Linear system	19
Table 4.3.1 Interpolation of excitation 3- Non-Linear system	26
Table A.1.1.1 Central Difference Method	89
Table A.1.2.1 Houbolt Method	91
Table A.1.3.1 Newmark Method	94
Table A.1.4.1 Wilson Method	97
Table A.1.5.1 HHT- α Method	99
Table A.1.6.1 WBZ- α Method	101
Table A.1.7.1 Generalized- α Method	103
Table A.1.8.1 Bathe Implicit Method	105
Table A.1.9.1 Coefficient in recurrence formulas (Interpolation of excitation	107
Table A.4.1.1 Central Difference Method (Non-linear system)	142
Table A.4.2.1 Newmark Method (Non-linear system)	147
Table A.4.2.2 Generalized- α Method (Non-linear system)	150
Table A.4.2.3 Bathe Implicit Method (Non-linear system)	154

1. Introduction

1.1 Background

The study of structural dynamics is of paramount importance for the design of civil engineering structure, especially when the structures are subjected to seismic load.

In practical problems, a need - to evaluate the behavior of a structure subjected to dynamic loads (such as earthquake, wind, blast or machinery) - arises.

To investigate the performance of a structure, it is necessary to enhance the efficiency of the numerical algorithm, which is an integral component of the model.

The forcing function encountered in many engineering problems is arbitrary and cannot be expressed in terms of smooth functions (for example: cosine and sine functions). Such problems require numerical algorithm and can be handled (if the system is linear) by the mode superposition method.

Furthermore, in many practical problems, the system is nonlinear due to the fact that the stiffness matrix of the structure doesn't remain constant if it is heavily loaded. In these situations, it is difficult to use the mode superposition method and more accurate results can be obtained by applying direct numerical method of the equations of motion.

Several numerical techniques are used to solve the dynamic problems in many engineering applications.

In the problems of structural dynamics, the following governing equilibrium equations are solved:

$$M\ddot{U} + C\dot{U} + KU = R \quad \text{for linear system} \quad (1.1.1)$$

$$M\ddot{U} + C\dot{U} + F(U) = R \quad \text{for nonlinear system} \quad (1.1.2)$$

where M , C and K are the mass, damping and stiffness matrices; U , \dot{U} and \ddot{U} are the displacement, velocity and acceleration vectors of the system; R is the vector of loads applied on the system; $F(U)$ is the vector of the force function.

1.2 Statement of problem

Previous surveys exist where a rigorous mathematical background is provided. As new computational techniques have been developed, a review of numerical methods has become necessary.

The properties of the existing methods with regard to convergence, accuracy and stability (in linear system with proportional damping) are studied in a vast body of literature. Especially, the piece-wise exact method is considered as an accurate and unconditionally stable algorithm for linear system with proportional damping.

On the other hand, no definitive answers - concerning their performance in linear system (with non-classical damping) and non-linear system - are given.

This paper presents an analysis of existing numerical methods employed to simulate structural dynamics problems and introduces new algorithms which are unconditionally stable and accurate (for linear system (with non-classical damping) and non-linear system).

1.3 Research questions

The research questions for the project are the following:

Which of the existing methods are efficient when evaluated with respect to stability, accuracy and controllable dissipation of higher modes?

Can we develop a piecewise exact method for all linear systems (with classical damping and non-classical damping)?

Is it possible to formulate a piecewise exact method for non-linear system (elastic and inelastic)?

1.4 Objective of the Research

The general objectives of this project are to study the stability and accuracy of the existing numerical methods of structural dynamics (in linear and nonlinear systems), to propose efficient methods (for linear system) and to explore the possibilities of developing an exact method for non-linear system.

The specific objectives of this project are summarized in the following manner:

- To calculate the spectral radius, period elongation and amplitude decay of the existing methods
- To compare the numerical methods based on control parameters
- To develop unconditionally stable and accurate algorithms (for linear and nonlinear systems)
- To compare the analytical and numerical solutions by studying specific problems related to single degree of freedom system, multi degree of freedom system (without damping), multi degree of freedom system (non-classical damping), multi degree of freedom system (finite element system) and nonlinear system

1.5 Application of the study

The paper compares the stability and accuracy of the existing methods. It identifies the advantages and disadvantages of the existing methods. The current piecewise exact method (method based on interpolation of excitation) is a scheme which is widely used in Modal Time History Analysis (for linear system with classical damping) due to its high efficiency and accuracy.

Piecewise exact methods are developed for linear system (with non-classical damping) and non-linear system. The method formulated for the non-classical system can be easily used in structural analysis software like the existing piecewise exact method. On the other hand, the method developed for the non-linear system might be cumbersome. However, due to its accuracy and stability, it can be the preferred method in the dynamic analysis of non-linear system.

1.5 Delimitations and Limitations of the study

Delimitations

- a) Even though many algorithms (possibly hundreds) are developed by researchers around the world, only nine methods are reviewed in this paper. The selected methods are/were widely utilized in the dynamic analysis of structures and studied in known textbooks.
- b) Experimental studies are not carried out to evaluate the efficiency of the methods. Closed form or highly precise solutions are used as a reference when evaluating the accuracy of the algorithms.
- c) The paper focuses on time stepping methods and it doesn't review the methods used for the determination of eigenvalues and eigenvectors (which is an integral part of modal analysis).

Limitations

- a) The effectiveness of the algorithms in complex structures is not examined. The illustrative examples should have included the analysis of complex structures.

2. Literature Review

The differential equation (1.1.1) can be solved in closed form if the excitation is a simple function. Otherwise, time stepping methods are necessary for complex excitations such as earthquake ground motion. Furthermore, uncoupling of modal equations is not possible if the system has non-classical damping or it responds into the nonlinear range. In this case, direct integration methods are required to obtain solution of the differential equation.

2.1 Time stepping methods

In the time-stepping methods, the required physical quantities (Displacement, Velocity, and Acceleration) are determined by a step-by-step procedure. Any time-stepping method is based on the following ideas:

- The dynamic equation is satisfied only at discrete time points (Δt apart) instead of at any time t .
- The variations of displacements, velocities and accelerations are assumed within each time step.

Most time-stepping methods can be divided into two main categories:

- Explicit method: the equation of motion at time t (for which the displacements are already calculated) is used
- Implicit method: the equation of motion at $t+\Delta t$ (for which the quantities are unknown) is employed

In order to check the reliability of the direct integration methods, the convergence, stability and accuracy are studied.

The efficiency of a numerical method depends on the following requirements:

- Convergence (the solution of the numerical method should tend to the exact value as the time step tends to zero)
- Stability (The numerical solution should not increase greatly when the algorithm progresses)

- Accuracy (The numerical algorithm should give results that agree with the exact solution especially in lower modes)
- Controllable dissipation in higher modes

The following time-stepping methods are (or were) often used in the analysis of the problems of structural dynamics:

- **Central difference method:** The central difference method is an explicit time-stepping method based on the finite difference expressions used to approximate the accelerations and velocities in terms of displacements (**KJ Bathe 2014**) [1].
- **Houbolt method:** It was proposed by **JC Houbolt in 1950** [9]. The accelerations and the velocities are expressed in terms of the displacements at $t - 2\Delta t$, $t - \Delta t$, t and $t + \Delta t$. The expressions of the accelerations and the velocities are derived by using a third order interpolation of displacement.
- **Newmark method:** The method - developed by **N. M. Newmark in 1959** [4] - is one of the widely used integration methods in structural dynamics. The expressions of the method are determined by truncating the Taylor series of the displacements and the velocities. Two parameters β and γ are included to control the functioning of the algorithm.
- **Wilson- θ method:** In this method, the acceleration is assumed to vary linearly in the time interval t to $t + \theta\Delta t$ (**K. J. Bathe and E. L. Wilson**) [10]. The equation of equilibrium is satisfied at $t + \theta\Delta t$. When $\theta = 1$, the Wilson method is equivalent to the linear acceleration method or the Newmark method (with $\beta = \frac{1}{6}$ and $\gamma = \frac{1}{2}$).
- **HHT- α method:** The equation of equilibrium is modified and satisfied at some intermediate points within the time interval Δt . A parameter α_f is introduced in order to modify the velocities, the displacements and the forces. The equations of Newmark method for the accelerations (at $t + \Delta t$) and the velocities (at $t + \Delta t$) are used to solve the equation of equilibrium. The method possesses algorithmic damping properties which can be controlled. (**Hans M. Hilber, Thomas G. R. Hughes and Robert L. Taylor, 1976**)[8]

- **WBZ- α method:** The approach used in HHT- α method is repeated in this method except that a parameter α_m is introduced to change the accelerations. In a manner similar to HHT- α method, the equations of Newmark method are employed to solve the equation of equilibrium. **(WL Wood, M Bossak, OC Zienkiewicz 1980)[14]**
- **Generalized- α method:** It includes elements of HHT- α and WBZ- α methods. The two methods were combined in order to obtain an algorithm with an improved performance. **(J Chung, GM Hulbert 1993)[15]**
- **Bathe method:** Bathe implicit method is a composite method in which various methods are combined in each time step **(G Noh, KJ Bathe 2018)[11]**. In the first sub-step which ends at $t + \alpha_s \Delta t$, Newmark's method is applied. In the second sub-step, the 3-point Euler backward method is employed.
- **Piecewise Exact Method (Method based on interpolation of excitation):** In this scheme, the exact solutions of the equilibrium equation are determined based on the assumption that the excitation function varies linearly over the time interval $[t, t + \Delta t]$. **(AK Chopra 2012) [5]**

(Note: A detailed review of the numerical methods is found in A.1)

2.2 Mode superposition

The above-mentioned methods (except the piecewise exact method) are suitable for carrying out of the direct integration of the equilibrium equation (for multi-degree-of-freedom system).

Another approach to solve the equilibrium equation is to transform it into an uncoupled set of modal equations **(KJ Bathe 2014) [1]**.

The modal equations can be uncoupled if the damping effects are neglected or the damping is proportional **(AK Chopra 2012) [5]**.

(Note: A detailed review of the mode superposition method is found in A.2)

2.3 Stability and Accuracy of numerical algorithms

The stability of an integration method is the condition in which any "initial" conditions at time t given by errors in the displacements, velocities, and accelerations do not increase in the integration **(KJ Bathe 2014) [1]**.

An algorithm is said to be unconditionally stable if it leads to bounded solutions irrespective of the size of the time step. **(M. Géradin and D.J. Rixen 2015)[12]**

In order to analyze the stability of an algorithm, the amplification matrix should be studied. In addition to the stability, the amplitude decay and the period elongation depend on the spectral radii of the amplification matrix. **(H. M. Hilber and T.J.R. Hughes 1978)[7]**

(Note: A detailed analysis of stability and accuracy of numerical algorithms is found in A.3)

2.4 Non-linear system

Mode superposition method is suitable for linear systems with classical damping. It is impossible to uncouple the modal equations if the system responds in non-linear range. **(AK Chopra 2012) [5]**

The solutions of non-linear system are obtained using iterative procedures (such as Newton-Raphson method) if an implicit method is employed. While the Newton-Raphson method is effective for quick convergence, the modified version of the Newton-Raphson method may be utilized due to its simplicity. **(KJ Bathe 2014) [1]**

As the central difference method is an explicit method, no iteration is required to determine the solutions of the non-linear system. Thus, the central difference is considered as the simplest scheme for analysis of non-linear MDF systems. **(AK Chopra 2012) [5]** However, it requires a very small time step to provide meaningful results.

The Newmark trapezoidal rule is unstable in some non-linear problems. For such problems, Bathe method is found to be effective in providing stable solutions. **(KJ Bathe 2014) [1]**

(Note: A detailed review of the application of the numerical algorithms in non-linear system is found in A.4)

3. Methodology

The methodology can be described as follows:

- i) Three methods are developed (based on the assumption that the load varies linearly):
 - The first method is based on the state-space model used for the analysis of nonclassically damped linear system. **(AK Chopra 2012) [5]** It is suitable for all linear problems unlike the original method based on interpolation of excitation. The exact solutions of the differential equations are determined at each time t_i .
 - The second method uses the first method to determine the linear part of the solution and adds another term for the nonlinear part which is calculated by using Newton-Raphson method.
 - The third method is related to the power series method of differential equations. The displacements, the velocities and the accelerations are expanded by utilizing Taylor series.
- ii) The properties of the existing methods are studied:
 - The eigenvalues for each amplification matrix of previously discussed (existing) algorithms are expressed as a function of $\Delta t/T$ by using MATLAB.

The amplification matrix A can be written in the following manner:

$$A = \begin{bmatrix} aa & ab & ac \\ ad & ae & af \\ ag & ah & ak \end{bmatrix} \quad (3.1)$$

The expressions for aa, ab, ac, ad, ae, af, ag, ah and ak are determined based on the algorithms discussed in the previous section.

- The spectral radius, the amplitude decay and the period elongation are determined and plotted with respect to $\frac{\Delta t}{T}$ using MATLAB. Accordingly, the

performances of the algorithms are evaluated by comparing the plotted curves.

- The efficiencies of the algorithms having the same ρ_{inf} are compared by plotting them together.
- iii) In illustrative examples, the theoretical (closed-form) and highly precise solutions of the differential equations are determined and plotted with the results obtained from the numerical methods. The closed-form and highly precise solutions are provided based on the procedure of structural dynamics. The codes for the numerical methods are written in MATLAB platform.

4. Proposed Methods

4.1 Method based on interpolation of excitation 1 (linear system with non-classical damping)

This numerical procedure is a generalized version of the method based on interpolation of excitation.

The motivation behind the development of this method is that the original method based on interpolation of excitation is not suitable to a system with non-classical damping.

The excitation function is determined by;

$$R(\tau) = R_t + \frac{\Delta R_t}{\Delta t} \tau \quad 4.1.1$$

where

$$\Delta R_t = R_{t+\Delta t} - R_t \quad 4.1.2$$

and the time variable τ varies from 0 to Δt .

The equations of motion are written in the following manner:

$$M\ddot{U} - M\dot{U} = 0 \quad 4.1.3$$

$$M\ddot{U} + C\dot{U} + KU = R \quad 4.1.4$$

A state space formulation of the equations of motion can be obtained by combining the above equations:

$$a\hat{U} + b\hat{U} = e(\tau) \quad 4.1.5$$

in which \hat{U} and $e(t)$ are vectors defined as follows

$$\hat{U} = \begin{Bmatrix} \dot{U} \\ U \end{Bmatrix} \text{ and } e(\tau) = \begin{Bmatrix} 0 \\ R(\tau) \end{Bmatrix} \quad 4.1.6$$

and where a and b are determined in the following manner

$$a = \begin{bmatrix} 0 & M \\ M & C \end{bmatrix} \quad b = \begin{bmatrix} -M & 0 \\ 0 & K \end{bmatrix} \quad 4.1.7$$

The general solution of the above equation is:

$$\hat{U}(\tau) = \kappa e^{\lambda\tau} \quad 4.1.8$$

in which λ is an eigenvalue and κ is the eigenvector.

$$\kappa = \begin{Bmatrix} \lambda\psi \\ \psi \end{Bmatrix} \quad 4.1.9$$

ψ is a vector representing the modal displacements.

Substituting (4.1.8) into (4.1.5), we obtain the following eigenvalue problem:

$$\lambda a\kappa + bk = 0 \quad 4.1.10$$

The vector \hat{U} can be expressed by the following equation:

$$\hat{U}(\tau) = \sum_{n=1}^{2N} \kappa_n \hat{q}_n(\tau) = \boldsymbol{\kappa} \hat{q}(\tau) \quad 4.1.11$$

where $\boldsymbol{\kappa} = [\kappa_1 \kappa_2 \dots \kappa_{2N}]$, $\hat{q} = [\hat{q}_1 \hat{q}_2 \dots \hat{q}_{2N}]^T$ and \hat{q}_n are scalar multipliers which can be determined from the initial conditions.

After substituting the above equation into (4.1.5), we get the following relation:

$$a\kappa \hat{q} + bk \hat{q} = e(\tau) \quad 4.1.12$$

By multiplying the terms of the above equation by $\boldsymbol{\kappa}^T$, we obtain:

$$(\boldsymbol{\kappa}^T a\kappa) \hat{q} + (\boldsymbol{\kappa}^T bk) \hat{q} = \boldsymbol{\kappa}^T e(\tau) \quad 4.1.13$$

The orthogonality property of the eigenvectors leads to the following 2N uncoupled equations:

$$A_{nn} \hat{q} + B_{nn} \hat{q} = R_{nn(t)} + \Delta R_{nn(t)} \tau \quad 4.1.14$$

where

$$A_{nn} = (\boldsymbol{\kappa}^T a\kappa) \quad B_{nn} = (\boldsymbol{\kappa}^T bk) \quad R_{nn(t)} = \boldsymbol{\kappa}^T e_t \quad \Delta R_{nn(t)} = \frac{\boldsymbol{\kappa}^T \Delta e_t}{\Delta t} \quad \Delta e_t = \begin{Bmatrix} 0 \\ \Delta R_t \end{Bmatrix} \quad 4.1.15$$

The solution of 4.1.14 (with initial condition $\hat{U}(0) = \hat{U}_t$) is as follows:

$$\hat{q}_{n(t)}(\tau) = \frac{1}{A_{nn}} \left[R_{nn(t)} \left(\frac{A_{nn}}{B_{nn}} \right) - \Delta R_{nn(t)} \left(\frac{A_{nn}}{B_{nn}} \right)^2 + \Delta R_{nn(t)} \left(\frac{A_{nn}}{B_{nn}} \right) \tau \right] + C_{nn(t)} e^{-\frac{A_{nn}}{B_{nn}} \tau} \quad 4.1.16$$

where

$$C_{nn(t)} = \hat{q}_{n(t)}(0) - \frac{1}{A_{nn}} \left[R_{nn(t)} \left(\frac{A_{nn}}{B_{nn}} \right) - \Delta R_{nn(t)} \left(\frac{A_{nn}}{B_{nn}} \right)^2 \right] \text{ and } \hat{q}_{n(t)}(0) = \frac{\boldsymbol{\kappa}^T a \hat{U}_t}{\boldsymbol{\kappa}^T a\kappa} \quad 4.1.17$$

Using (4.1.11) we obtain the following relation:

$$\hat{U}_{t+\Delta t} = \hat{U}(\Delta t) = \sum_{n=1}^{2N} \kappa_n \hat{q}_{n(t)}(\Delta t) \quad 4.1.18$$

Table 4.1.1 INTERPOLATION OF EXCITATION 1-LINEAR SYSTEM FOR NON-CLASSICAL DAMPING

1 Initial calculations

1.1 Form stiffness matrix \mathbf{K} , mass matrix \mathbf{M} , and damping matrix \mathbf{C}

1.2 Form matrix \mathbf{a} and matrix \mathbf{b}

$$\mathbf{a} = \begin{bmatrix} \mathbf{0} & \mathbf{M} \\ \mathbf{M} & \mathbf{C} \end{bmatrix} \quad \mathbf{b} = \begin{bmatrix} -\mathbf{M} & \mathbf{0} \\ \mathbf{0} & \mathbf{K} \end{bmatrix}$$

1.3 Solve the eigenvalue problem:

$$\lambda \mathbf{a} \mathbf{k} + \mathbf{b} \mathbf{k} = \mathbf{0}$$

1.4 $\dot{\mathbf{U}}_0 = \mathbf{M}^{-1}(\mathbf{R}_0 - \mathbf{C}\dot{\mathbf{U}}_0 - \mathbf{K}\mathbf{U}_0)$

2 For each time step, $j=0,1,2$

2.1 Calculate $\Delta \mathbf{R}_t, \mathbf{e}_t, \Delta \mathbf{e}_t$

$$\Delta \mathbf{R}_t = \mathbf{R}_{t+\Delta t} - \mathbf{R}_t$$

$$\mathbf{e}_t = \begin{bmatrix} \mathbf{0} \\ \mathbf{R}_t \end{bmatrix}$$

$$\Delta \mathbf{e}_t = \begin{bmatrix} \mathbf{0} \\ \Delta \mathbf{R}_t \end{bmatrix}$$

3 For each iteration, $n=1,2,\dots, 2N$

3.1 $A_{nn} = (\boldsymbol{\kappa}^T \mathbf{a} \boldsymbol{\kappa})$

3.2 $B_{nn} = (\boldsymbol{\kappa}^T \mathbf{b} \boldsymbol{\kappa})$

3.3 $R_{nn(t)} = (\boldsymbol{\kappa}^T \mathbf{e}_t)$

3.4 $\Delta R_{nn(t)} = \frac{\boldsymbol{\kappa}^T \Delta \mathbf{e}_t}{\Delta t}$

3.5 $q_{n(t)}(0) = \frac{\boldsymbol{\kappa}^T \mathbf{a} \dot{\mathbf{U}}_t}{\boldsymbol{\kappa}^T \mathbf{a} \boldsymbol{\kappa}}$

3.6 $C_{nn(t)} = q_{n(t)}(0) - \frac{1}{A_{nn}} \left[R_{nn(t)} \left(\frac{A_{nn}}{B_{nn}} \right) - \Delta R_{nn(t)} \left(\frac{A_{nn}}{B_{nn}} \right)^2 \right]$

3.7 $\hat{q}_{n(t)}(\Delta t) = \frac{1}{A_{nn}} \left[R_{nn(t)} \left(\frac{A_{nn}}{B_{nn}} \right) - \Delta R_{nn(t)} \left(\frac{A_{nn}}{B_{nn}} \right)^2 + \Delta R_{nn(t)} \left(\frac{A_{nn}}{B_{nn}} \right) \Delta t \right] + C_{nn(t)} e^{-\frac{A_{nn} \Delta t}{B_{nn}}}$

3.8 $\mathbf{U}_{t+\Delta t} = \sum_{n=1}^{2N} \boldsymbol{\kappa}_n \hat{q}_{n(t)}(\Delta t)$

4.2 Method based on interpolation of excitation 2 (non-linear system)

An efficient numerical method can be established for non-linear system by applying the method based on interpolation of excitation.

In the same manner, the excitation function is determined by;

$$\mathbf{R}(\tau) = \mathbf{R}_t + \frac{\Delta \mathbf{R}_t}{\Delta t} \tau \quad 4.2.1$$

where

$$\Delta \mathbf{R}_t = \mathbf{R}_{t+\Delta t} - \mathbf{R}_t \quad 4.2.2$$

and the time variable τ varies from 0 to Δt .

The equilibrium equation to be solved is:

$$\mathbf{M}\ddot{\mathbf{U}} + \mathbf{C}\dot{\mathbf{U}} + \mathbf{F}(\mathbf{U}) = \mathbf{R} \quad 4.2.3$$

Let

$$\mathbf{U} = \mathbf{U}_L + \mathbf{U}_N \quad 4.2.4$$

where

$$\mathbf{M}\ddot{\mathbf{U}}_L + \mathbf{C}\dot{\mathbf{U}}_L + \mathbf{F}(\mathbf{U}_t) + \mathbf{K}_t(\mathbf{U}_L - \mathbf{U}_t) = \mathbf{R} \quad 4.2.5$$

U_L , U_N are the linear and non-linear components of the displacement vector. U_L is to be determined using the method outlined in the previous section. K_t represents the tangent stiffness which is determined as follows:

$$\mathbf{K}_t = \left[\frac{\partial \mathbf{F}}{\partial \mathbf{U}} \right] \Big|_{\mathbf{U}_t} \quad 4.2.6$$

The displacement vectors are determined from the Taylor series:

$$\mathbf{U} = \mathbf{U}_t + \dot{\mathbf{U}}_t \tau + \frac{1}{2} \ddot{\mathbf{U}}_t \tau^2 + \frac{1}{6} \dddot{\mathbf{U}}_t \tau^3 \dots \dots \dots \quad 4.2.7$$

$$\mathbf{U}_L = \mathbf{U}_t + \dot{\mathbf{U}}_t \tau + \frac{1}{2} \ddot{\mathbf{U}}_t \tau^2 + \frac{1}{6} \ddot{\mathbf{U}}_{Lt} \tau^3 \dots \dots \dots \quad 4.2.8$$

$$\mathbf{U}_N = \frac{1}{6} \ddot{\mathbf{U}}_{Nt} \tau^3 + \frac{1}{24} \mathbf{U}^{IV}_{Nt} \tau^4 \dots \dots \dots \quad 4.2.9$$

By truncating the above Taylor series, we obtain:

$$\mathbf{U}_N = \frac{1}{6} \mathbf{Y}_{t+\Delta t} \tau^3 \quad 4.2.10$$

Determination of $U_{L,t+\Delta t}$

In order to determine U_L , the following equation needs to be solved:

$$M\ddot{U}_L + C\dot{U}_L + F(U_t) + K_t(U_L - U_t) = R \quad 4.2.11$$

Alternatively, the equations of motion are expressed in the following manner:

$$M\dot{U}_L - M\dot{U}_L = \mathbf{0} \quad 4.2.12$$

$$M\ddot{U}_L + C\dot{U}_L + F(U_t) + K_t(U_L - U_t) = R \quad 4.2.13$$

(Repeated for convenience) A state space formulation of the equations of motion can be obtained by combining the above equations:

$$a\hat{U}_L + b\hat{U}_L = e_1(\tau) \quad 4.2.14$$

in which \hat{U} and $e(t)$ are vectors defined as follows:

$$\hat{U}_L = \begin{Bmatrix} \dot{U}_L \\ U_L \end{Bmatrix} \text{ and } e_1(\tau) = \begin{Bmatrix} \mathbf{0} \\ R(\tau) - F(U_t) + K_t U_t \end{Bmatrix} \quad 4.2.15$$

and where a and b are determined in the following manner

$$a = \begin{bmatrix} \mathbf{0} & M \\ M & C \end{bmatrix} \quad b = \begin{bmatrix} -M & \mathbf{0} \\ \mathbf{0} & K_t \end{bmatrix} \quad 4.2.16$$

The general solution of the above equation is:

$$\hat{U}_L(\tau) = \kappa e^{\lambda\tau} \quad 4.2.17$$

in which λ is an eigenvalue and κ is the eigenvector.

$$\kappa = \begin{Bmatrix} \lambda\psi \\ \psi \end{Bmatrix} \quad 4.2.18$$

ψ is a vector representing the modal displacements.

Substituting the above equation into 4.2.14, we obtain the following eigenvalue problem:

$$\lambda a \kappa + b \kappa = \mathbf{0} \quad 4.2.19$$

The vector \hat{U} can be expressed by the following equation:

$$\hat{U}_L(\tau) = \sum_{n=1}^{2N} \kappa_n \hat{q}_n(\tau) = \kappa \hat{q}(\tau) \quad 4.2.20$$

where $\kappa = [\kappa_1 \kappa_2 \dots \kappa_{2N}]$, $\hat{q} = [\hat{q}_1 \hat{q}_2 \dots \hat{q}_{2N}]^T$ and \hat{q}_n are scalar multipliers which can be determined from the initial conditions.

After substituting the above equation 4.2.14, we get the following relation:

$$\mathbf{a}\boldsymbol{\kappa}\hat{\mathbf{q}} + \mathbf{b}\boldsymbol{\kappa}\hat{\mathbf{q}} = \mathbf{e}_1(\tau) \quad 4.2.21$$

By multiplying the terms of the above equation by $\boldsymbol{\kappa}^T$, we obtain:

$$(\boldsymbol{\kappa}^T \mathbf{a}\boldsymbol{\kappa})\hat{\mathbf{q}} + (\boldsymbol{\kappa}^T \mathbf{b}\boldsymbol{\kappa})\hat{\mathbf{q}} = \boldsymbol{\kappa}^T \mathbf{e}(\tau) \quad 4.2.22$$

The orthogonality property of the eigenvectors leads to the following 2N uncoupled equations:

$$A_{nn}\hat{\mathbf{q}} + B_{nn}\hat{\mathbf{q}} = R_{nn(t)} + \Delta R_{nn(t)}\tau \quad 4.2.23$$

where

$$A_{nn} = (\boldsymbol{\kappa}^T \mathbf{a}\boldsymbol{\kappa}) \quad B_{nn} = (\boldsymbol{\kappa}^T \mathbf{b}\boldsymbol{\kappa}) \quad R_{nn(t)} = \boldsymbol{\kappa}^T \mathbf{e}_t \quad \Delta R_{nn(t)} = \frac{\boldsymbol{\kappa}^T \Delta \mathbf{e}_t}{\Delta t} \quad \Delta \mathbf{e}_t = \begin{Bmatrix} \mathbf{0} \\ \Delta \mathbf{R}_t \end{Bmatrix} \quad 4.2.24$$

The solution of 4.2.23 (with initial condition $\hat{\mathbf{U}}(0) = \hat{\mathbf{U}}_t$) is as follows:

$$\hat{\mathbf{q}}_{n(t)}(\tau) = \frac{1}{A_{nn}} \left[R_{nn(t)} \left(\frac{A_{nn}}{B_{nn}} \right) - \Delta R_{nn(t)} \left(\frac{A_{nn}}{B_{nn}} \right)^2 + \Delta R_{nn(t)} \left(\frac{A_{nn}}{B_{nn}} \right) \tau \right] + C_{nn(t)} e^{-\frac{A_{nn}\tau}{B_{nn}}} \quad 4.2.25$$

where

$$C_{nn(t)} = \hat{\mathbf{q}}_{n(t)}(0) - \frac{1}{A_{nn}} \left[R_{nn(t)} \left(\frac{A_{nn}}{B_{nn}} \right) - \Delta R_{nn(t)} \left(\frac{A_{nn}}{B_{nn}} \right)^2 \right] \text{ and } \hat{\mathbf{q}}_{n(t)}(0) = \frac{\boldsymbol{\kappa}^T \mathbf{a}\hat{\mathbf{U}}_t}{\boldsymbol{\kappa}^T \mathbf{a}\boldsymbol{\kappa}} \quad 4.2.26$$

Using (4.2.25) we obtain the following relation:

$$\hat{\mathbf{U}}_{L t+\Delta t} = \hat{\mathbf{U}}(\Delta t) = \sum_{n=1}^{2N} \boldsymbol{\kappa}_n \hat{\mathbf{q}}_{n(t)}(\Delta t) \quad 4.2.27$$

Determination of $\mathbf{U}_{N t+\Delta t}$

The equation of equilibrium can be rewritten in the following manner:

$$\mathbf{F}_p(\mathbf{U}_{t+\Delta t}) = \mathbf{R}_{t+\Delta t} \quad 4.2.28$$

where

$$\mathbf{F}_p(\mathbf{U}_{t+\Delta t}) = \mathbf{M}\ddot{\mathbf{U}}_{t+\Delta t} + \mathbf{C}\dot{\mathbf{U}}_{t+\Delta t} + \mathbf{F}(\mathbf{U}_{t+\Delta t}) \quad 4.2.29$$

$$\mathbf{U}_{t+\Delta t} = \mathbf{U}_{L t+\Delta t} + \mathbf{U}_{N t+\Delta t} = \mathbf{U}_{L t+\Delta t} + \frac{1}{6} \mathbf{Y}_{t+\Delta t} \Delta t^3 \quad 4.2.30$$

$$\dot{\mathbf{U}}_{t+\Delta t} = \dot{\mathbf{U}}_{L t+\Delta t} + \dot{\mathbf{U}}_{N t+\Delta t} = \dot{\mathbf{U}}_{L t+\Delta t} + \frac{1}{2} \mathbf{Y}_{t+\Delta t} \Delta t^2 \quad 4.2.31$$

$$\ddot{\mathbf{U}}_{t+\Delta t} = \ddot{\mathbf{U}}_{L t+\Delta t} + \ddot{\mathbf{U}}_{N t+\Delta t} = \ddot{\mathbf{U}}_{L t+\Delta t} + \mathbf{Y}_{t+\Delta t} \Delta t \quad 4.2.32$$

By finding the derivative of F_p with respect to the unknown quantity $Y_{t+\Delta t}$, we get:

$$\frac{\partial F_p(\mathbf{U}_{t+\Delta t})}{\partial \mathbf{Y}_{t+\Delta t}} = \mathbf{M} \frac{\partial \ddot{\mathbf{U}}_{t+\Delta t}}{\partial \mathbf{Y}_{t+\Delta t}} + \mathbf{C} \frac{\partial \dot{\mathbf{U}}_{t+\Delta t}}{\partial \mathbf{Y}_{t+\Delta t}} + \frac{\partial F(\mathbf{U}_{t+\Delta t})}{\partial \mathbf{Y}_{t+\Delta t}} \quad 4.2.33$$

Using (4.2.31) and (4.2.32), we find:

$$\frac{\partial \ddot{\mathbf{U}}_{t+\Delta t}}{\partial \mathbf{Y}_{t+\Delta t}} = \Delta t \quad 4.2.34$$

$$\frac{\partial \dot{\mathbf{U}}_{t+\Delta t}}{\partial \mathbf{Y}_{t+\Delta t}} = \frac{\Delta t^2}{2} \quad 4.2.35$$

Substituting the above two equations in (4.2.33) and using (A.4.2.4) results in:

$$\mathbf{K}_{p\ t+\Delta t} = \frac{\partial F_p(\mathbf{U}_{t+\Delta t})}{\partial \mathbf{Y}_{t+\Delta t}} = \Delta t \mathbf{M} + \frac{\Delta t^2}{2} \mathbf{C} + \frac{\Delta t^3}{6} \mathbf{K}_{t+\Delta t} \quad 4.2.36$$

The Newton-Raphson equation (A.4.2.3) can be rewritten as follows:

$$\mathbf{K}_{p\ t+\Delta t}^{(i)} \Delta \mathbf{Y}^{(i)} = \mathbf{R}_{t+\Delta t} - \mathbf{F}_p(\mathbf{U}_{t+\Delta t}^{(i)}) = \mathbf{f}_{p\ t+\Delta t}^{(i)} \quad 4.2.37$$

Using (4.2.30), (4.2.31), (4.2.32) and (4.2.37), it is found that:

$$\begin{aligned} \mathbf{f}_{p\ t+\Delta t}^{(i)} &= \mathbf{R}_{t+\Delta t} - \mathbf{F} \left(\mathbf{U}_{L\ t+\Delta t} + \frac{1}{6} \mathbf{Y}_{t+\Delta t}^{(i)} \Delta t^3 \right) - \left[\Delta t \mathbf{M} + \frac{1}{2} \Delta t^2 \mathbf{C} \right] \mathbf{Y}_{t+\Delta t}^{(i)} \\ &\quad - \mathbf{M} \ddot{\mathbf{U}}_{L\ t+\Delta t} - \mathbf{C} \dot{\mathbf{U}}_{L\ t+\Delta t} \end{aligned} \quad 4.2.38$$

After $\mathbf{Y}_{t+\Delta t}$ is determined based on (4.2.37) and (4.2.38), $\mathbf{U}_{t+\Delta t}$, $\dot{\mathbf{U}}_{t+\Delta t}$ and $\ddot{\mathbf{U}}_{t+\Delta t}$ can be calculated using the equations (4.2.30) (4.2.31) and (4.2.32).

Table 4.2.1 INTERPOLATION OF EXCITATION 2-NON LINEAR SYSTEM

1 Initial calculations

1.1 Form mass matrix \mathbf{M} , and damping matrix \mathbf{C}

$$1.2 \ddot{\mathbf{U}}_0 = \mathbf{M}^{-1}(\mathbf{R}_0 - \mathbf{C}\dot{\mathbf{U}}_0 - \mathbf{F}(\mathbf{U}_0))$$

2 For each time step,

2.1 Form matrix a and matrix b

$$\mathbf{a} = \begin{bmatrix} \mathbf{0} & \mathbf{M} \\ \mathbf{M} & \mathbf{C} \end{bmatrix} \quad \mathbf{b} = \begin{bmatrix} -\mathbf{M} & \mathbf{0} \\ \mathbf{0} & \mathbf{K}_t \end{bmatrix}$$

2.2 Solve the eigenvalue problem:

$$\lambda \mathbf{a} \mathbf{k} + \mathbf{b} \mathbf{k} = \mathbf{0}$$

2.3 Calculate $\Delta \mathbf{R}_t, \mathbf{e}_{t+\Delta t}, \Delta \mathbf{e}_{t+\Delta t}$

$$\Delta \mathbf{R}_t = \mathbf{R}_{t+\Delta t} - \mathbf{R}_t$$

$$\mathbf{e}_t = \begin{bmatrix} \mathbf{0} \\ \mathbf{R}_t \end{bmatrix}$$

$$\mathbf{e}_{1t} = \begin{bmatrix} \mathbf{0} \\ \mathbf{R}_t - \mathbf{F}(\mathbf{U}_t) + \mathbf{K}_t \mathbf{U}_t \end{bmatrix}$$

$$\Delta \mathbf{e}_t = \begin{bmatrix} \mathbf{0} \\ \Delta \mathbf{R}_t \end{bmatrix}$$

2.4 For each iteration, $n=1,2,\dots, 2N$

$$2.4.1 \quad A_{nn}(t) = (\boldsymbol{\kappa}^T \mathbf{a} \boldsymbol{\kappa})$$

$$2.4.2 \quad B_{nn}(t) = (\boldsymbol{\kappa}^T \mathbf{b} \boldsymbol{\kappa})$$

$$2.4.3 \quad R_{nn}(t) = (\boldsymbol{\kappa}^T \mathbf{e}_{1t})$$

$$2.4.4 \quad \Delta R_{nn}(t) = \frac{\boldsymbol{\kappa}^T \Delta \mathbf{e}_t}{\Delta t}$$

$$2.4.5 \quad q_n(t)(0) = \frac{\boldsymbol{\kappa}^T \mathbf{a} \hat{\mathbf{U}}_t}{\boldsymbol{\kappa}^T \mathbf{a} \boldsymbol{\kappa}}$$

$$2.4.6 \quad C_{nn}(t) = q_n(t)(0) - \frac{1}{A_{nn}} \left[R_{nn}(t) \left(\frac{A_{nn}}{B_{nn}} \right) - \Delta R_{nn}(t) \left(\frac{A_{nn}}{B_{nn}} \right)^2 \right]$$

$$2.4.7 \quad \hat{q}_n(t)(\Delta t) = \frac{1}{A_{nn}} \left[R_{nn}(t) \left(\frac{A_{nn}}{B_{nn}} \right) - \Delta R_{nn}(t) \left(\frac{A_{nn}}{B_{nn}} \right)^2 + \Delta R_{nn}(t) \left(\frac{A_{nn}}{B_{nn}} \right) \Delta t \right] + C_{nn}(t) e^{-\frac{A_{nn} \Delta t}{B_{nn}}}$$

$$2.5 \quad \hat{\mathbf{U}}_{L t+\Delta t} = \sum_{n=1}^{2N} \kappa_n \hat{q}_{n(t)} (\Delta t)$$

$$2.6 \quad \dot{\hat{\mathbf{U}}}_{L t+\Delta t} = \mathbf{a}^{-1}(\mathbf{e}_{1 t+\Delta t} - \mathbf{b} \hat{\mathbf{U}}_{L t+\Delta t})$$

$$2.7 \text{ Calculate } \mathbf{U}_{L t+\Delta t}, \dot{\mathbf{U}}_{L t+\Delta t} \text{ and } \ddot{\mathbf{U}}_{L t+\Delta t}$$

2.8 Initial calculations

$$2.8.1 \quad i = 1, \mathbf{Y}_{t+\Delta t}^{(1)} = \mathbf{0}$$

$$2.8.2 \quad \mathbf{R}_{p t+\Delta t} = \mathbf{R}_{t+\Delta t} - (\mathbf{M} \ddot{\mathbf{U}}_{L t+\Delta t} + \mathbf{C} \dot{\mathbf{U}}_{L t+\Delta t})$$

2.9 For each iteration, $i=1,2,\dots$

$$2.9.1 \quad \mathbf{f}_{p t+\Delta t}^{(i)} = \mathbf{R}_{p t+\Delta t} - \mathbf{F}(\mathbf{U}_{L t+\Delta t} + \frac{1}{6} \mathbf{Y}_{t+\Delta t}^{(i)} \Delta t^3) - (\Delta t \mathbf{M} + \frac{1}{2} \Delta t^2 \mathbf{C}) \mathbf{Y}_{t+\Delta t}^{(i)}$$

2.9.2 Check convergence; If criteria are not satisfied, follow steps 2.9.3 to 2.9.7;
Else, skip these steps and go to step 4

$$2.9.3 \quad \mathbf{K}_{p t+\Delta t}^{(i)} = \frac{\Delta t^3}{6} \mathbf{K}_{t+\Delta t}^{(i)} + \Delta t \mathbf{M} + \frac{1}{2} \Delta t^2 \mathbf{C}$$

$$2.9.4 \text{ solve } \mathbf{K}_{p t+\Delta t}^{(i)} \Delta \mathbf{Y}^{(i)} = \mathbf{f}_{p t+\Delta t}^{(i)}$$

$$2.9.5 \quad \mathbf{Y}_{t+\Delta t}^{(i+1)} = \mathbf{Y}_{t+\Delta t}^{(i)} + \Delta \mathbf{Y}^{(i)}$$

$$2.9.6 \text{ determine: } \mathbf{F}(\mathbf{U}_{L t+\Delta t} + \frac{1}{6} \mathbf{Y}_{t+\Delta t}^{(i+1)} \Delta t^3) \text{ and } \mathbf{K}_{t+\Delta t}^{(i+1)}$$

2.9.7 replace i by $i+1$ and repeat steps 3.1 to 3.6. denote final value $\mathbf{Y}_{t+\Delta t}$

$$2.10 \text{ Calculate } \mathbf{U}_{t+\Delta t}, \dot{\mathbf{U}}_{t+\Delta t} \text{ and } \ddot{\mathbf{U}}_{t+\Delta t}$$

$$\mathbf{U}_{t+\Delta t} = \mathbf{U}_{L t+\Delta t} + \frac{1}{6} \mathbf{Y}_{t+\Delta t} \Delta t^3$$

$$\dot{\mathbf{U}}_{t+\Delta t} = \dot{\mathbf{U}}_{L t+\Delta t} + \frac{1}{2} \mathbf{Y}_{t+\Delta t} \Delta t^2$$

$$\ddot{\mathbf{U}}_{t+\Delta t} = \ddot{\mathbf{U}}_{L t+\Delta t} + \mathbf{Y}_{t+\Delta t} \Delta t$$

4.3 Method based on interpolation of excitation 3 (non-linear system)

A numerical procedure -which is unconditionally stable- can be developed for non-linear system. In this method, the differential equation is solved by using the power series method.

We assume that the excitation function is linear during the short period $t \leq t_\tau \leq t + \Delta t$:

$$\mathbf{R}(\tau) = \mathbf{R}_t + \frac{\Delta \mathbf{R}_t}{\Delta t} \tau \quad 4.3.1$$

The equilibrium equation (to be considered) is:

$$\mathbf{M}\ddot{\mathbf{U}} + \mathbf{C}\dot{\mathbf{U}} + \mathbf{F}(\mathbf{U}) = \mathbf{R} \quad 4.3.2$$

The displacement, velocity and acceleration vectors are expressed in the form of Taylor series as follows:

$$\mathbf{U}(\tau) = \mathbf{a}_1 + \mathbf{a}_2\tau + \frac{1}{2}\mathbf{a}_3\tau^2 + \frac{1}{6}\mathbf{a}_4\tau^3 + \dots \quad 4.3.3$$

$$\dot{\mathbf{U}}(\tau) = \mathbf{a}_2 + \mathbf{a}_3\tau + \frac{1}{2}\mathbf{a}_4\tau^2 + \frac{1}{6}\mathbf{a}_5\tau^3 \dots \quad 4.3.4$$

$$\ddot{\mathbf{U}}(\tau) = \mathbf{a}_3 + \mathbf{a}_4\tau + \frac{1}{2}\mathbf{a}_5\tau^2 + \frac{1}{6}\mathbf{a}_6\tau^3 \dots \quad 4.3.5$$

where

$$\mathbf{a}_n = \mathbf{U}^{(n-1)}(0) \quad 4.3.6$$

Futhermore, the force-displacement function \mathbf{F} is expanded in the following manner:

$$\mathbf{F}(\mathbf{U}(\tau)) = \mathbf{b}_1 + \mathbf{b}_2\tau + \frac{1}{2}\mathbf{b}_3\tau^2 + \frac{1}{6}\mathbf{b}_4\tau^3 + \dots \quad 4.3.7$$

$$\mathbf{b}_n = [\mathbf{F}(\mathbf{U}(\tau))]^{(n-1)}_{\tau=0} \quad 4.3.8$$

Substituting (4.3.1), (4.3.3), (4.3.4) and (4.3.5) into (4.3.2) , we obtain:

$$\mathbf{M}\mathbf{a}_3 + \mathbf{C}\mathbf{a}_2 + \mathbf{b}_1 = \mathbf{R}_t \quad 4.3.9$$

$$\mathbf{M}\mathbf{a}_4 + \mathbf{C}\mathbf{a}_3 + \mathbf{b}_2 = \frac{\Delta \mathbf{R}_t}{\Delta t} \quad 4.3.10$$

$$\text{for } n \geq 5 \quad \mathbf{M}\mathbf{a}_n + \mathbf{C}\mathbf{a}_{n-1} + \mathbf{b}_{n-2} = 0 \quad 4.3.11$$

The above expression is considered as a recursion formula.

It is obvious that:

$$\mathbf{a}_1 = \mathbf{U}_t, \mathbf{a}_2 = \dot{\mathbf{U}}_t \text{ and } \mathbf{a}_3 = \ddot{\mathbf{U}}_t \quad 4.3.12$$

However, determining \mathbf{b}_n is a challenging task because the procedure of finding the derivative of $\mathbf{F}(\mathbf{U}(\tau))$ is cumbersome.

Determination of \mathbf{b}_n

In order to simplify the procedure of determining \mathbf{b}_n , we have to define a function which is a truncated form of Taylor series of \mathbf{U} :

$$\mathbf{U}_{p(n)}(\tau) = \sum_{s=1}^n \mathbf{a}_s \tau^{s-1} \quad 4.3.13$$

The important property resulting from the above relation is the following:

$$[\mathbf{U}_{p(n)}(\tau)]_{\tau=0}^{(s-1)} = [\mathbf{U}(\tau)]_{\tau=0}^{(s-1)} \text{ for } 1 \leq s \leq n \quad 4.3.14$$

Let $\mathbf{F}(\mathbf{U}(\tau)) = \langle F_1(\mathbf{U}(\tau)), F_2(\mathbf{U}(\tau)), \dots \dots \dots F_j(\mathbf{U}(\tau)) \rangle^T$ and

$$\mathbf{U}(\tau) = \langle U_1(\tau), U_2(\tau), \dots \dots \dots U_j(\tau) \rangle^T \quad 4.3.15$$

The derivatives $\mathbf{F}(\mathbf{U}(\tau))$ are determined in the following manner:

$$[F_i(\mathbf{U}(\tau))]^{(1)} = \sum_{k1=1}^j \frac{\partial F_i}{\partial U_{k1}} \frac{dU_{k1}}{d\tau} \quad 4.3.16$$

$$\begin{aligned} [F_i(\mathbf{U}(\tau))]^{(2)} &= \sum_{k1=1}^j \left(\left(\sum_{k2=1}^j \left(\frac{\partial^2 F_i}{\partial U_{k1} \partial U_{k2}} \frac{dU_{k2}}{d\tau} \right) \right) \frac{dU_{k1}}{d\tau} \right. \\ &\quad \left. + \frac{\partial F_i}{\partial U_{k1}} \frac{d^2 U_{k1}}{d\tau^2} \right) \quad 4.3.17 \end{aligned}$$

$$\begin{aligned}
& [F_i(\mathbf{U}(\tau))]^{(3)} \\
&= \sum_{k_1=1}^j \left(\left(\sum_{k_2=1}^j \left(\left(\sum_{k_3=1}^j \frac{\partial^3 F_i}{\partial U_{k_1} \partial U_{k_2} \partial U_{k_3}} \frac{dU_{k_3}}{d\tau} \right) \frac{dU_{k_2}}{d\tau} \right. \right. \right. \\
&\quad \left. \left. \left. + \frac{\partial^2 F_i}{\partial U_{k_1} \partial U_{k_2}} \frac{d^2 U_{k_2}}{d\tau^2} \right) \right) \frac{dU_{k_1}}{d\tau} + 2 \left(\sum_{k_2=1}^j \left(\frac{\partial^2 F_i}{\partial U_{k_1} \partial U_{k_2}} \frac{dU_{k_2}}{d\tau} \right) \right) \frac{d^2 U_{k_1}}{d\tau^2} \right. \\
&\quad \left. + \frac{\partial F_i}{\partial U_{k_1}} \frac{d^3 U_{k_1}}{d\tau^3} \right) \tag{4.3.18}
\end{aligned}$$

$$\begin{aligned}
& [F_i(\mathbf{U}(\tau))]^{(n)} \\
&= G_{in} \left(\frac{\partial^n F_i}{\partial U_{k_1} \partial U_{k_2} \dots \partial U_{k_n}}, \frac{\partial^{n-1} F_i}{\partial U_{k_1} \partial U_{k_2} \dots \partial U_{k_{(n-1)}}}, \dots, \frac{\partial F_i}{\partial U_{k_1}}, \right. \\
&\quad \left. \frac{dU_{k_1}}{d\tau}, \dots, \frac{d^n U_{k_1}}{d\tau^n} \right) \\
&= H_{in} \left(U_{k_1}, \frac{dU_{k_1}}{d\tau}, \dots, \frac{d^n U_{k_1}}{d\tau^n} \right) \tag{4.3.19}
\end{aligned}$$

The above equation leads to:

$$[F_i(\mathbf{U}(\tau))]_{\tau=0}^{(n)} = H_{in}([U(\tau)]_{\tau=0}^{(0)}, \dots, [U(\tau)]_{\tau=0}^{(n)}) \quad 4.3.20$$

Using (4.3.14) and (4.3.20), we get:

$$\begin{aligned} & [F(\mathbf{U}(\tau))]_{\tau=0}^{(n)} \\ &= \mathbf{H}_n([U_{p(n+1)}(\tau)]_{\tau=0}^{(0)}, \dots, [U_{p(n+1)}(\tau)]_{\tau=0}^{(n)}) \end{aligned} \quad 4.3.21$$

(4.3.8) and (4.3.21) imply that:

$$[F(\mathbf{U}(\tau))]_{\tau=0}^{(n)} = [F(\mathbf{U}_{p(n+1)}(\tau))]_{\tau=0}^{(n)} \quad 4.3.22$$

$$\mathbf{b}_n = [F(\mathbf{U}(\tau))]_{\tau=0}^{(n-1)} = [F(\mathbf{U}_{p(n)}(\tau))]_{\tau=0}^{(n-1)} \quad 4.3.23$$

Iteration for the determination of $\mathbf{U}_{t+\Delta t}$

The initial conditions of the iteration can be specified as follows:

$$\mathbf{U}_{t+\Delta t}^{(1)} = \mathbf{a}_1 + \mathbf{a}_2\Delta t + \frac{1}{2}\mathbf{a}_3\Delta t^2 = \mathbf{U}_t + \dot{\mathbf{U}}_t\Delta t + \frac{1}{2}\ddot{\mathbf{U}}_t\Delta t^2 \quad 4.3.24$$

$$\dot{\mathbf{U}}_{t+\Delta t}^{(1)} = \mathbf{a}_2 + \mathbf{a}_3\Delta t = \dot{\mathbf{U}}_t + \ddot{\mathbf{U}}_t\Delta t \quad 4.3.25$$

$$\ddot{\mathbf{U}}_{t+\Delta t}^{(1)} = \mathbf{a}_3 = \ddot{\mathbf{U}}_t \quad 4.3.26$$

The improved displacement, velocity and acceleration are calculated using the following relations which are derived from (4.3.3), (4.3.4) and (4.3.5) :

$$\mathbf{U}_{t+\Delta t}^{(i+1)} = \mathbf{U}_{t+\Delta t}^{(i)} + \frac{\mathbf{a}_{i+3}\Delta t^{i+2}}{(i+2)!} \quad 4.3.27$$

$$\dot{\mathbf{U}}_{t+\Delta t}^{(i+1)} = \dot{\mathbf{U}}_{t+\Delta t}^{(i)} + \frac{\mathbf{a}_{i+3}\Delta t^{i+1}}{(i+1)!} \quad 4.3.28$$

$$\ddot{\mathbf{U}}_{t+\Delta t}^{(i+1)} = \ddot{\mathbf{U}}_{t+\Delta t}^{(i)} + \frac{\mathbf{a}_{i+3}\Delta t^i}{(i)!} \quad 4.3.29$$

\mathbf{a}_{i+3} can be calculated using (4.3.10) and (4.3.11):

$$\text{for } i = 1 \quad \mathbf{a}_4 = \mathbf{M}^{-1} \left(\frac{\Delta \mathbf{R}_t}{\Delta t} - (\mathbf{C}\mathbf{a}_3 + \mathbf{b}_2) \right) \quad 4.3.30$$

$$\text{for } i \geq 2 \quad \mathbf{a}_{i+3} = -\mathbf{M}^{-1}(\mathbf{C}\mathbf{a}_{i+2} + \mathbf{b}_{i+1}) \quad 4.3.31$$

\mathbf{b}_{i+1} is determined based on (4.3.23):

$$\mathbf{b}_{i+1} = [\mathbf{F}(\mathbf{U}(\tau))]_{\tau=0}^{(i)} = [\mathbf{F}(\mathbf{U}_{p(i+1)}(\tau))]_{\tau=0}^{(i)} \quad 4.3.32$$

The increment of displacement can be computed in the following manner:

$$\Delta \mathbf{U}^{(i)} = \mathbf{U}_{t+\Delta t}^{(i+1)} - \mathbf{U}_{t+\Delta t}^{(i)} = \frac{\mathbf{a}_{i+3} \Delta t^{i+2}}{(i+2)!} \quad 4.3.33$$

The iteration is stopped when the criteria specified in section (2.4.2.1) is satisfied.

Table 4.3.1 INTERPOLATION OF EXCITATION 3-NON LINEAR SYSTEM

1 Initial calculations

1.1 Form mass matrix \mathbf{M} , and damping matrix \mathbf{C}

$$1.2 \ddot{\mathbf{U}}_0 = \mathbf{M}^{-1}(\mathbf{R}_0 - \mathbf{C}\dot{\mathbf{U}}_0 - \mathbf{F}(\mathbf{U}_0))$$

2 For each time step,

2.1 Initial calculations $\mathbf{a}_1 = \mathbf{U}_t$, $\mathbf{a}_2 = \dot{\mathbf{U}}_t$, $\mathbf{a}_3 = \ddot{\mathbf{U}}_t$

$$2.2 \mathbf{U}_{t+\Delta t}^{(1)} = \mathbf{a}_1 + \mathbf{a}_2\Delta t + \frac{1}{2}\mathbf{a}_3\Delta t^2$$

$$\dot{\mathbf{U}}_{t+\Delta t}^{(1)} = \mathbf{a}_2 + \mathbf{a}_3\Delta t$$

$$\ddot{\mathbf{U}}_{t+\Delta t}^{(1)} = \mathbf{a}_3$$

$$\mathbf{b}_2 = [\mathbf{F}(\mathbf{U}_{p(i+1)}(\tau))]_{\tau=0}^{(1)}$$

$$\mathbf{a}_4 = \mathbf{M}^{-1}\left(\frac{\Delta \mathbf{R}_t}{\Delta t} - (\mathbf{C}\mathbf{a}_3 + \mathbf{b}_2)\right)$$

$$2.3 \mathbf{U}_{t+\Delta t}^{(2)} = \mathbf{a}_1 + \mathbf{a}_2\Delta t + \frac{1}{2}\mathbf{a}_3\Delta t^2 + \frac{1}{6}\mathbf{a}_4\Delta t^3$$

$$\dot{\mathbf{U}}_{t+\Delta t}^{(2)} = \mathbf{a}_2 + \mathbf{a}_3\Delta t + \frac{1}{2}\mathbf{a}_4\Delta t^2$$

$$\ddot{\mathbf{U}}_{t+\Delta t}^{(2)} = \mathbf{a}_3 + \mathbf{a}_4\Delta t$$

2.4 Check convergence; If criteria are not satisfied, follow steps 3.3 to 3.7; Else, skip these steps and go to step 4

3 For each iteration, $i=2,3,\dots$

$$3.1 \mathbf{b}_{i+1} = [\mathbf{F}(\mathbf{U}_{p(i+1)}(\tau))]_{\tau=0}^{(i)}$$

$$3.2 \mathbf{a}_{i+3} = -\mathbf{M}^{-1}(\mathbf{C}\mathbf{a}_{i+2} + \mathbf{b}_{i+1})$$

$$3.3 \mathbf{U}_{t+\Delta t}^{(i+1)} = \mathbf{U}_{t+\Delta t}^{(i)} + \frac{\mathbf{a}_{i+3}\Delta t^{i+2}}{(i+2)!}$$

$$3.4 \dot{\mathbf{U}}_{t+\Delta t}^{(i+1)} = \dot{\mathbf{U}}_{t+\Delta t}^{(i)} + \frac{\mathbf{a}_{i+3}\Delta t^{i+1}}{(i+1)!}$$

$$3.5 \ddot{\mathbf{U}}_{t+\Delta t}^{(i+1)} = \ddot{\mathbf{U}}_{t+\Delta t}^{(i)} + \frac{\mathbf{a}_{i+3}\Delta t^i}{(i)!}$$

$$3.6 \Delta \mathbf{U}^{(i)} = \mathbf{U}_{t+\Delta t}^{(i+1)} - \mathbf{U}_{t+\Delta t}^{(i)} = \frac{\mathbf{a}_{i+3}\Delta t^{i+2}}{(i+2)!}$$

3.7 Check convergence; If criteria are not satisfied, follow steps 3.1 to 3.6; Else, skip these steps and stop iteration

3.8 replace i by $i+1$ and repeat steps 3.1 to 3.6. denote final value $\mathbf{U}_{t+\Delta t}$, $\dot{\mathbf{U}}_{t+\Delta t}$ and $\ddot{\mathbf{U}}_{t+\Delta t}$

5. Analysis and Results

The spectral radii, the amplitude decay and the period elongation of the Central Difference, Houbolt, Newmark, Wilson- θ , HHT- α , WBZ- α , Generalized- α and Bathe Methods are determined and plotted with respect to $\frac{\Delta t}{T}$. The results are summarized in the figures.

Evidently, the numerical dissipation of all algorithms tends to be lower, when $\frac{\Delta t}{T}$ approaches to zero. However, when the ratio $\frac{\Delta t}{T}$ increases, the various algorithms show different characteristics. Fig 5.1 indicates that the central difference method is conditionally stable. (In this case, it can be shown that the ratio $\frac{\Delta t}{T}$ should not be greater than $\frac{1}{\pi}$). In fig 5.2, it is observed that the Houbolt method is unconditionally stable but it introduces greater amplitude decay and period elongation compared to the central difference method as demonstrated in Fig 5.10, Fig 5.11, Fig 5.19 and Fig 5.20.

The Wilson algorithm ($\theta=1$) which is equivalent to the Newmark ($\gamma=1/2$, $\beta=1/6$) becomes unstable when the ratio $\frac{\Delta t}{T}$ is greater than 0.55. Furthermore, the Wilson algorithm shows unconditional stability when θ is greater than 1.37. But, the amplitude decay and the period elongation of Wilson method tend to increase with θ (Fig 5.18 and Fig 5.27).

In fig 5.3, no amplitude decay is observed for Newmark ($\gamma=1/2$, $\beta=1/4$), HHT($\gamma=1/2$, $\beta=1/4, \alpha_f=0$), WBC($\gamma=1/2$, $\beta=1/4, \alpha_m=0$) and Generalized ($\gamma=1/2$, $\beta=1/4, \alpha_f=1/2, \alpha_m=1/2$). Furthermore, the mentioned algorithm introduces the same period elongation.

Concerning the numerical dissipation of the Newmark, HHT, WBC and Generalized methods, it is observed that the Generalized- α method possesses superior performance because of the following reasons:

- For the same ρ_{inf} , the amplitude decay of the Generalized- α method is small compared to those of the other methods in all cases except when ρ_{inf} is equal to 0.3. (It should be noted that HHT method becomes conditionally stable when $\rho_{inf}=0.3$)
- For the same ρ_{inf} , the period elongation of the Generalized- α method is almost similar to those of the other methods
- The lower modes can be accurately determined and the higher modes dissipated.

Regarding the Bathe method, the amplitude decay is minimal (near to zero) when α_s is equal to 0.01 and 1.01. The amplitude decay increases as α_s approaches to a value approximately equal to 0.6 (Fig 5.16). The same increase is observed when α_s is greater than 1.01 (Fig 5.17). However, according to Fig 5.25 and Fig 5.26, it should be noted that the period elongation of Bathe ($\gamma=1/2, \beta=1/4, 0.01 < \alpha_s < 1$) is lesser than that of Bathe ($\gamma=1/2, \beta=1/4, \alpha_s > 1$).

With regard to the effect of damping on the stability of a numerical method, the spectral radii have been determined by taking into account the damping coefficient. Except for the Houbolt method, the spectral radii of a numerical scheme have a tendency to decrease when the damping coefficient increases. (Fig 5.28, 5.30, 5.31, 5.32)

But for Houbolt method, the spectral radii decrease as the damping coefficient increases, provided that $\frac{\Delta t}{T}$ is approximately less than 0.4. The reverse is true for the condition in which $\frac{\Delta t}{T}$ is approximately greater than 0.4. (Fig 5.29)

The original method based on interpolation of excitation **(AK Chopra 2012) [5]** and the first proposed method **(method based on interpolation of excitation-1)** are the most precise algorithm. They are unconditionally stable, don't introduce amplitude decay and period elongation due to the following reasons:

- The exact solutions are provided for the piecewise representation of the excitation.

- In section A.3.2, it is stated that the stability of an algorithm is studied by taking into consideration the case of free vibration. In this situation, the solutions given the algorithms are equivalent to the closed-form solution. Thus, instability, amplitude decay and period elongation do not occur.

However, the methods based on interpolation of excitation are suitable for truncated modal space. The unwanted (or spurious) frequencies are eliminated by modal superposition method in which the important modal equations are solved precisely.

The behavior of the existing algorithms in nonlinear systems is not well known. Some methods may be effective than other schemes in specific problems. However, if the algorithms shows good properties in linear system, they are likely to be accurate and stable in nonlinear problems.

The third proposed method (**method based on interpolation of excitation-3**) provides an exact result if the excitation is accurately described. In this case, it is assumed that the load varies linearly in the time step interval. In this method, the solutions are obtained when the Taylor series of the displacement, the velocity and acceleration vectors converges. Consequently, the method can be considered as an unconditionally stable and accurate scheme for linear and nonlinear problems. Nonetheless, the major drawback of this method is that it is difficult to calculate the derivative of the force function for each iteration in the time step.

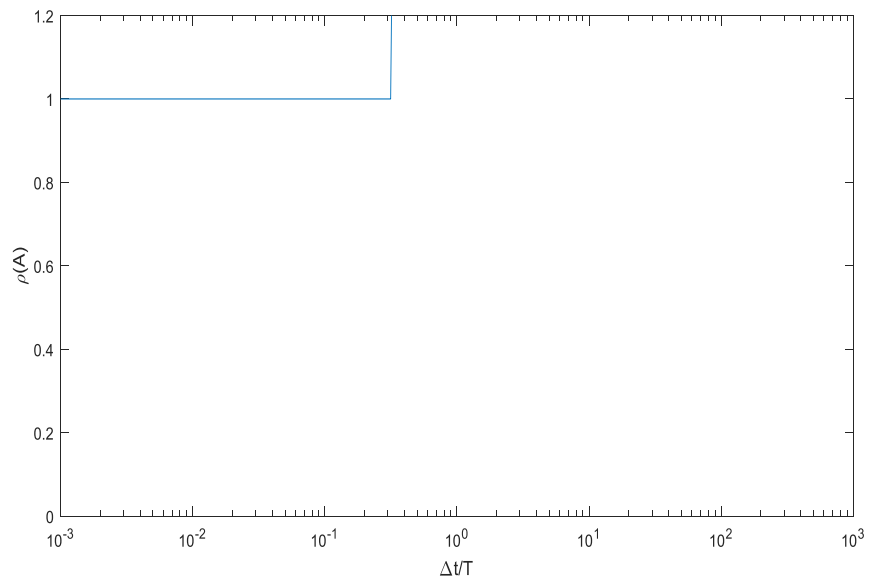


Figure 5.1 Spectral radii of Central Difference Method, case $\xi=0$

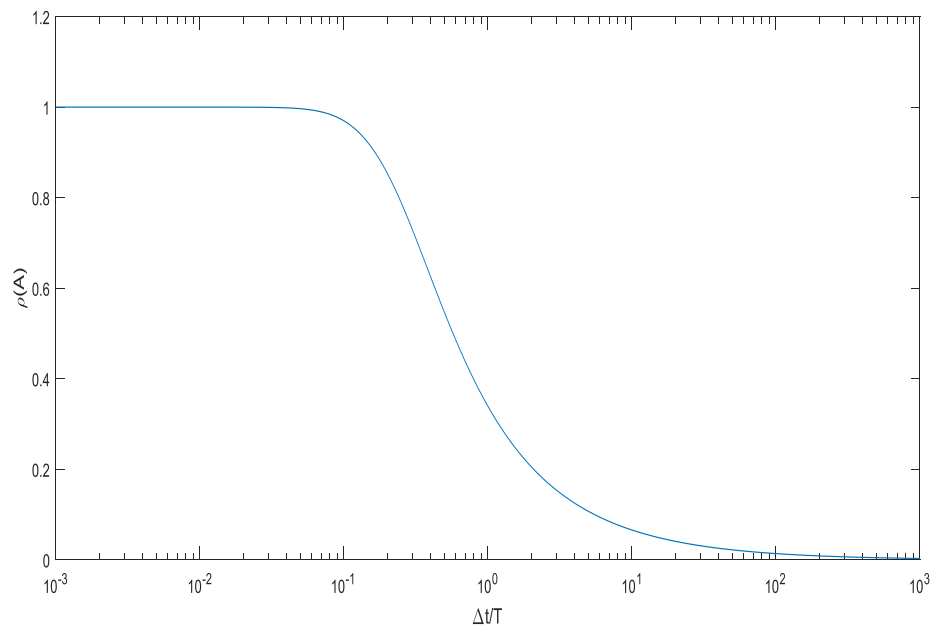


Figure 5.2 Spectral radii of Houbolt Method, case $\xi=0$

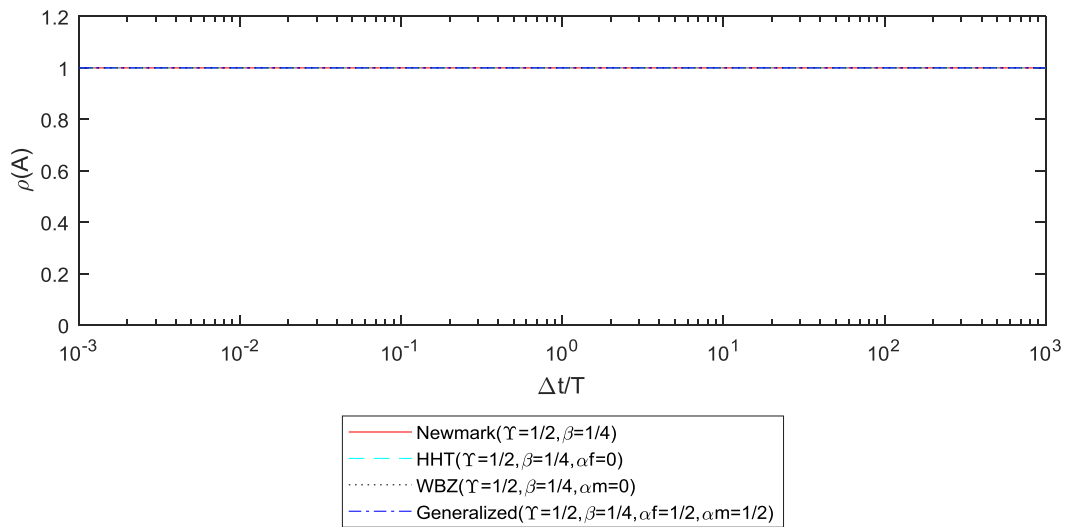


Figure 5.3 Spectral radii of N-M,HHT-M,WBZ-M and G-M,case $\xi=0$ and $\rho_{inf}=1$

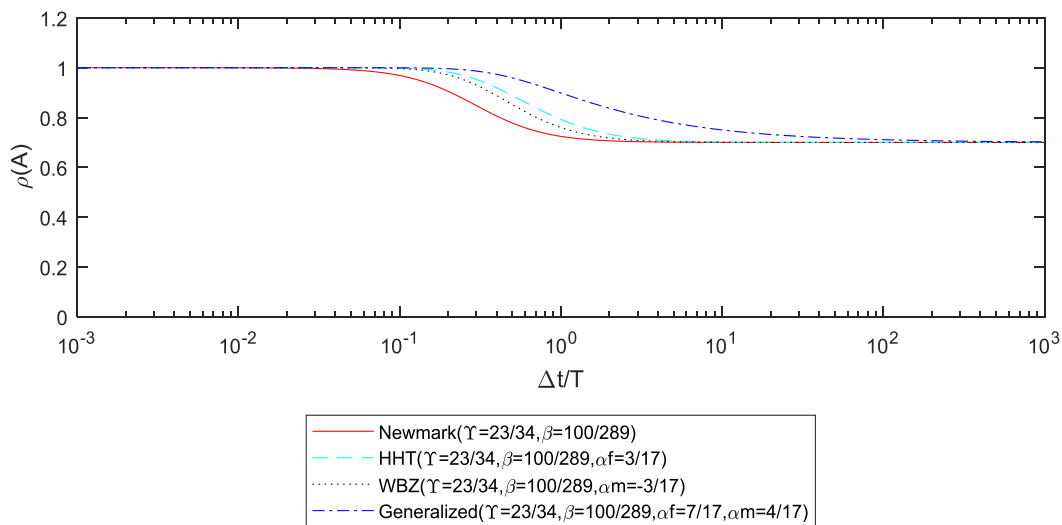


Figure 5.4 Spectral radii of N-M,HHT-M,WBZ-M and G-M,case $\xi=0$ and $\rho_{inf}=0.7$

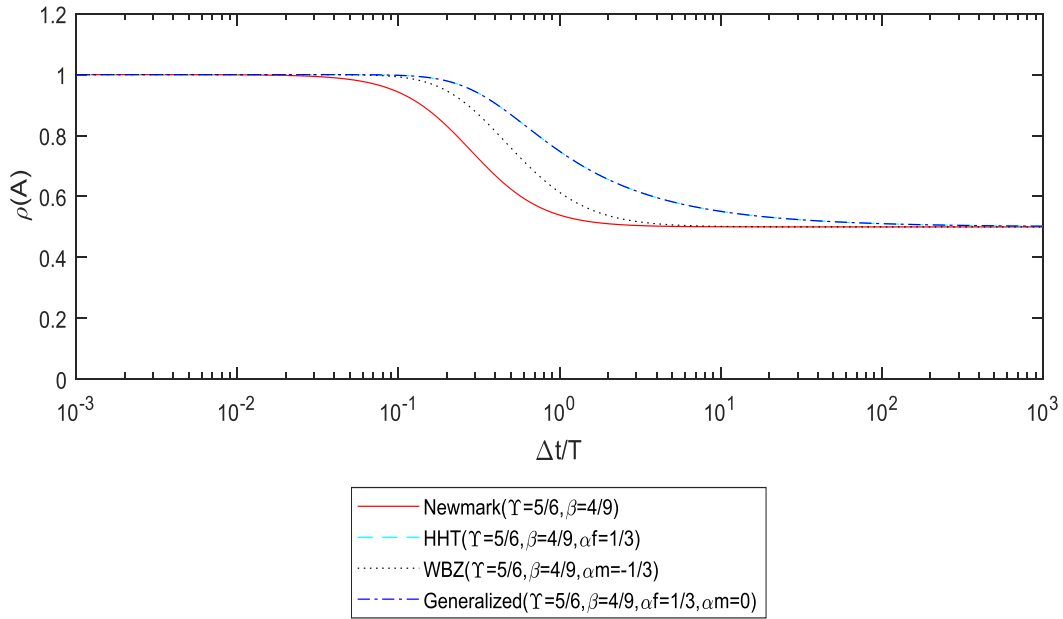


Figure 5.5 Spectral radii of N-M,HHT-M,WBZ-M and G-M,case $\xi=0$ and $\rho_{inf}=0.5$

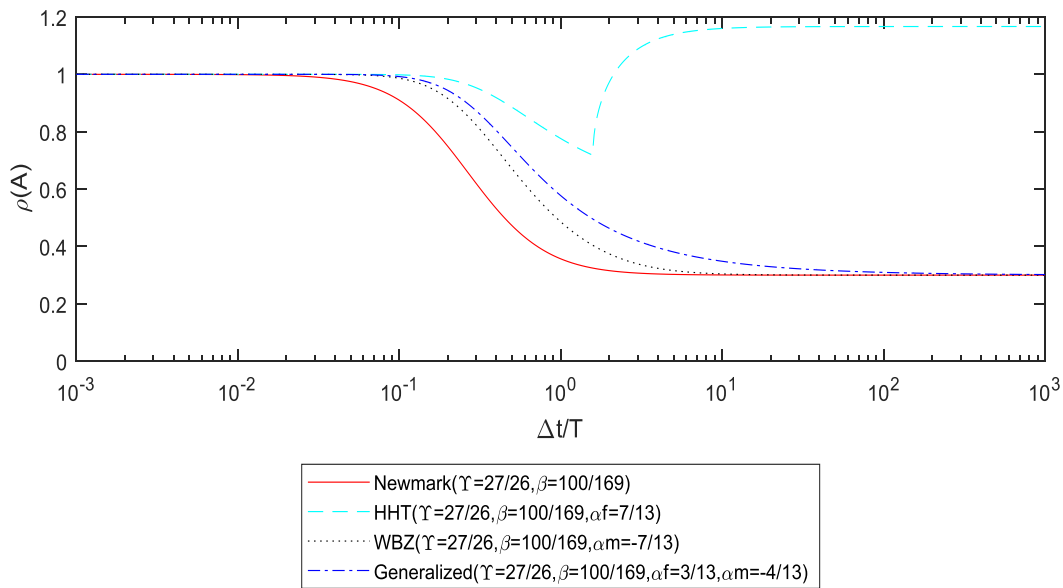


Figure 5.6 Spectral radii of N-M,HHT-M,WBZ-M and G-M,case $\xi=0$ and $\rho_{inf}=0.3$

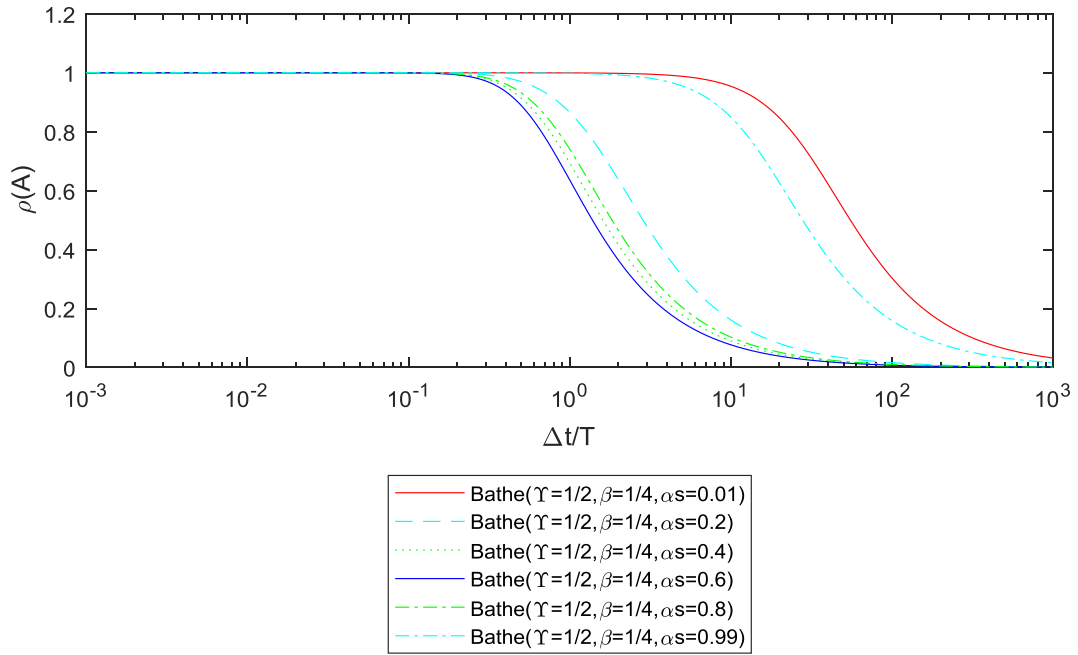


Figure 5.7 Spectral radii of Bathe-M, case $\xi=0$ and $0 < \alpha s < 1$

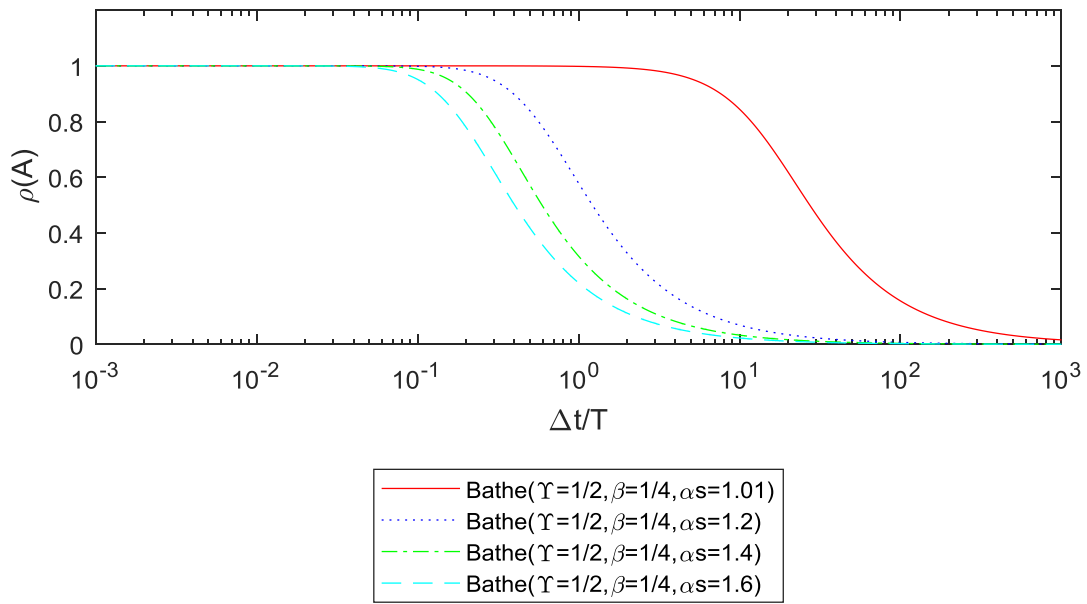


Figure 5.8 Spectral radii of Bathe-M, case $\xi=0$ and $\alpha s > 1$

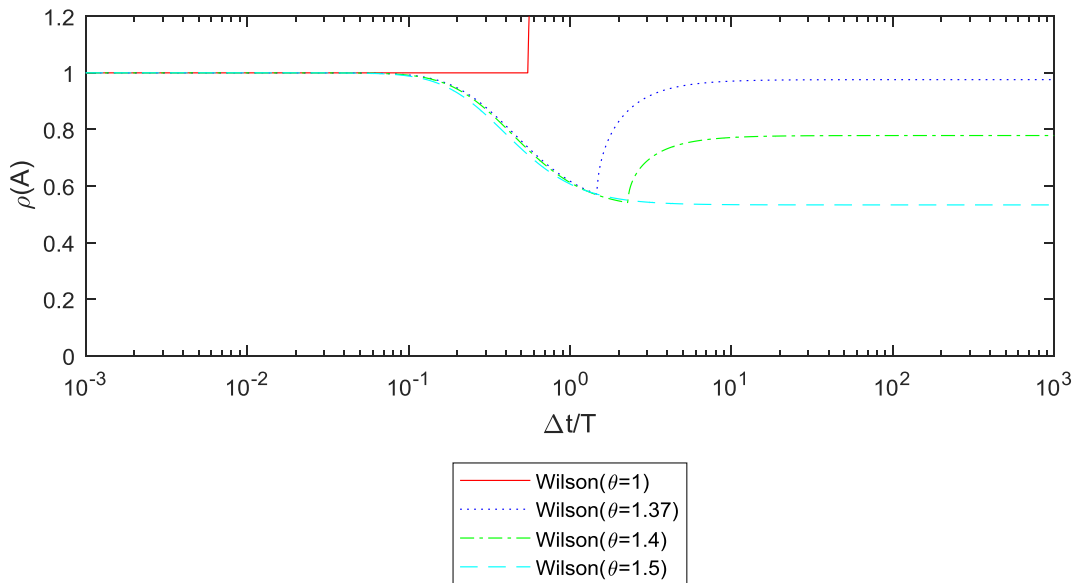


Figure 5.9 Spectral radii of Wilson-M, case $\xi=0$ and $\theta=1, 1.37, 1.4, 1.5$

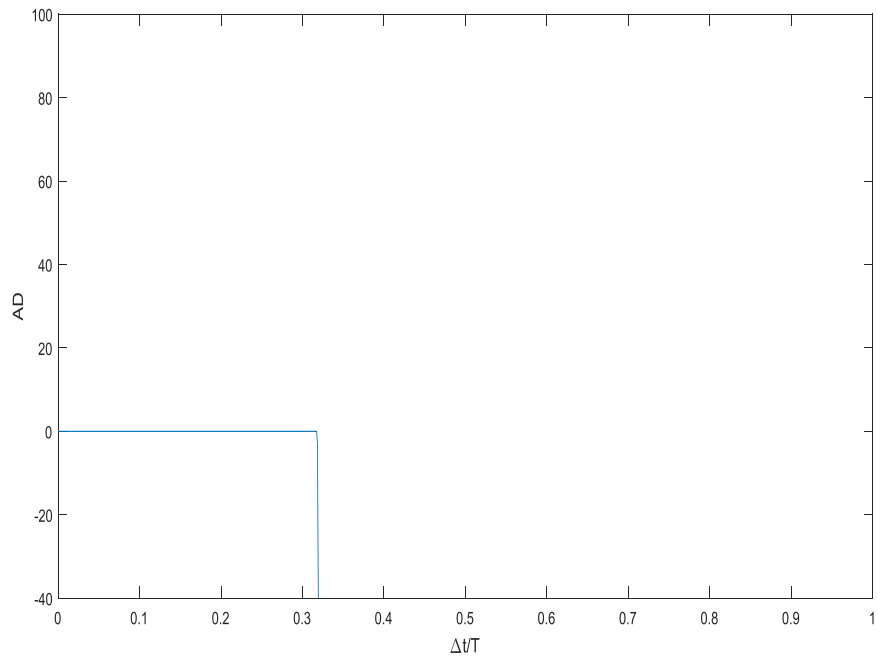


Figure 5.10 Amplitude Decay of Central Difference Method, case $\xi=0$

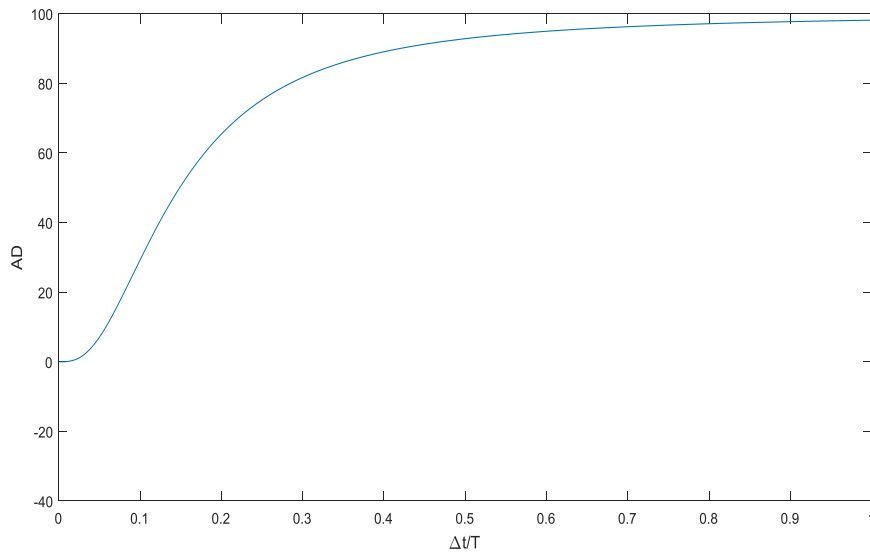


Figure 5.11 Amplitude Decay of Houbolt Method, case $\xi=0$

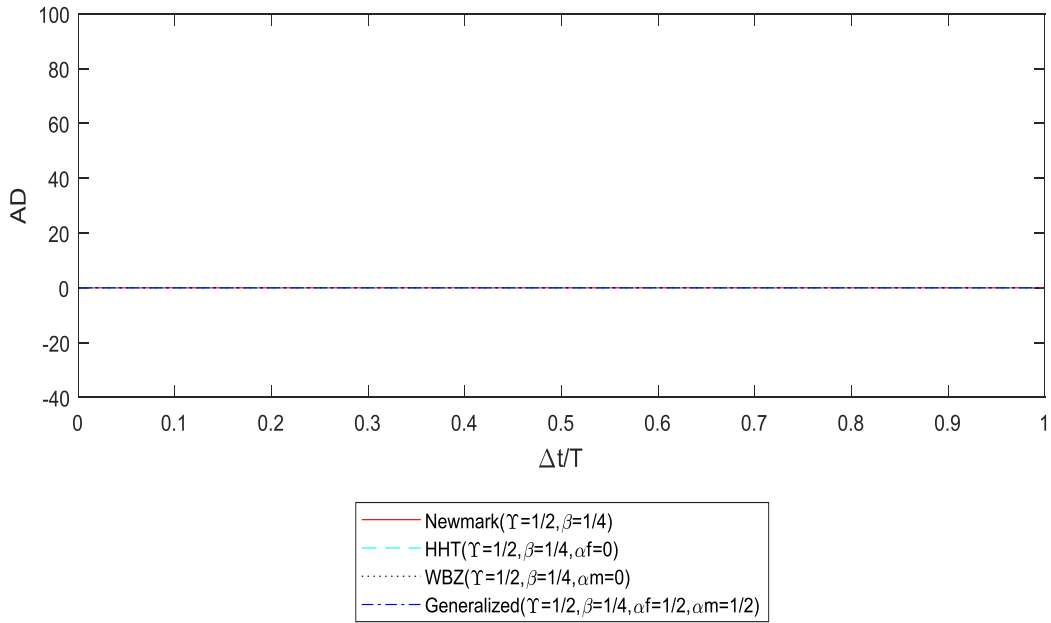


Figure 5.12 Amplitude Decay of N-M,HHT-M,WBZ-M and G-M,case $\xi=0$ and $\rho_{inf}=1$

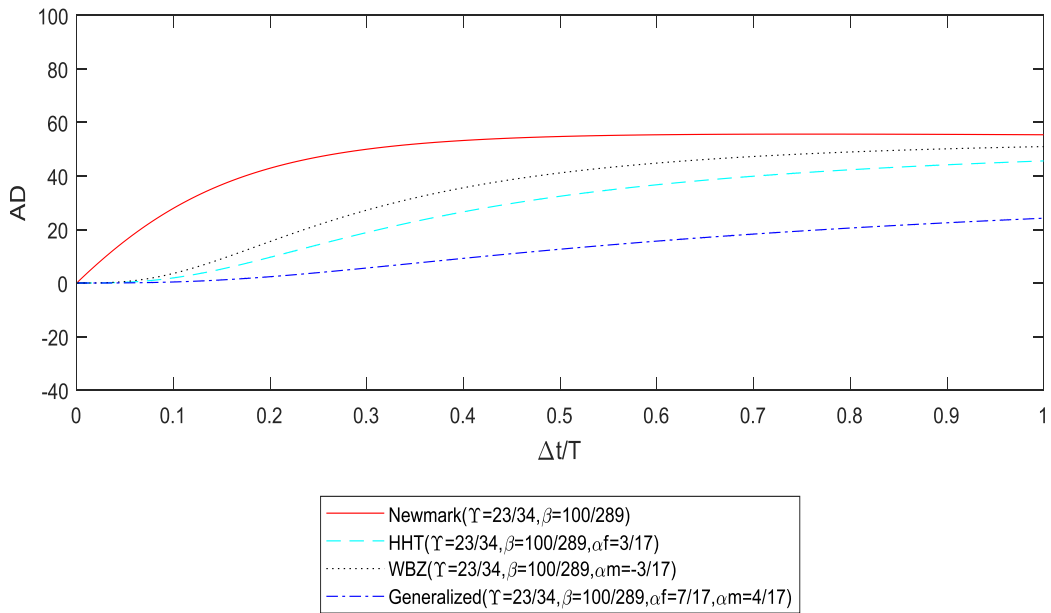


Figure 5.13 Amplitude Decay of N-M,HHT-M,WBZ-M and G-M,case $\xi=0$ and $\rho_{inf}=0.7$

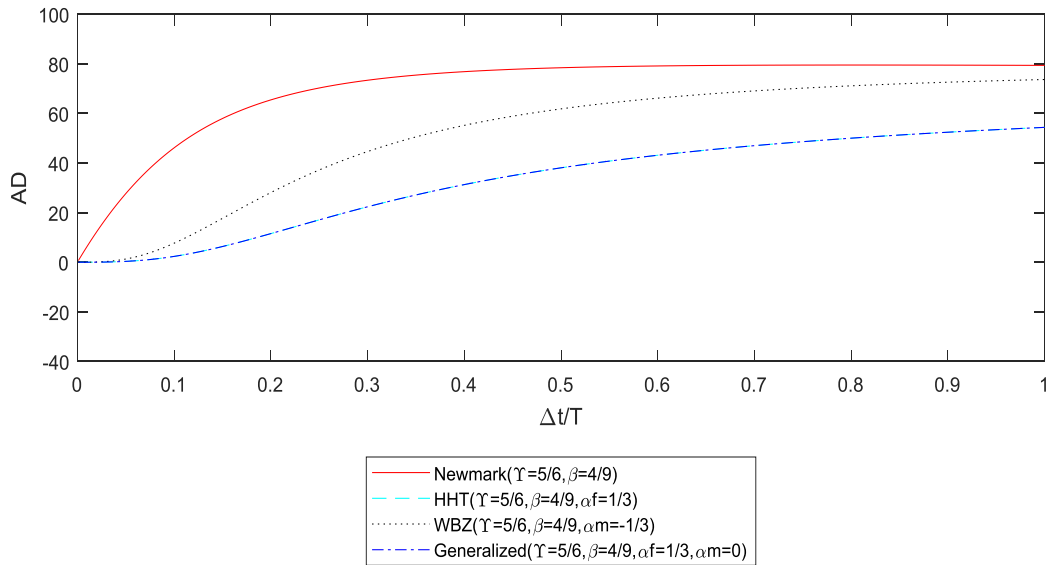


Figure 5.14 Amplitude Decay of N-M,HHT-M,WBZ-M and G-M,case $\xi=0$ and $\rho_{inf}=0.5$

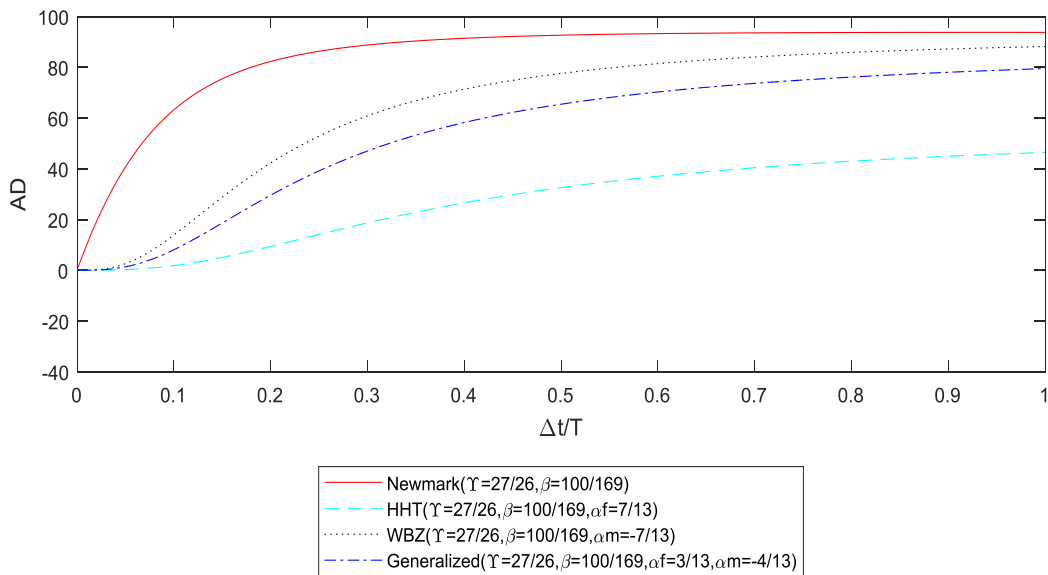


Figure 5.15 Amplitude Decay of N-M,HHT-M,WBZ-M and G-M,case $\xi=0$ and $\rho_{inf}=0.3$

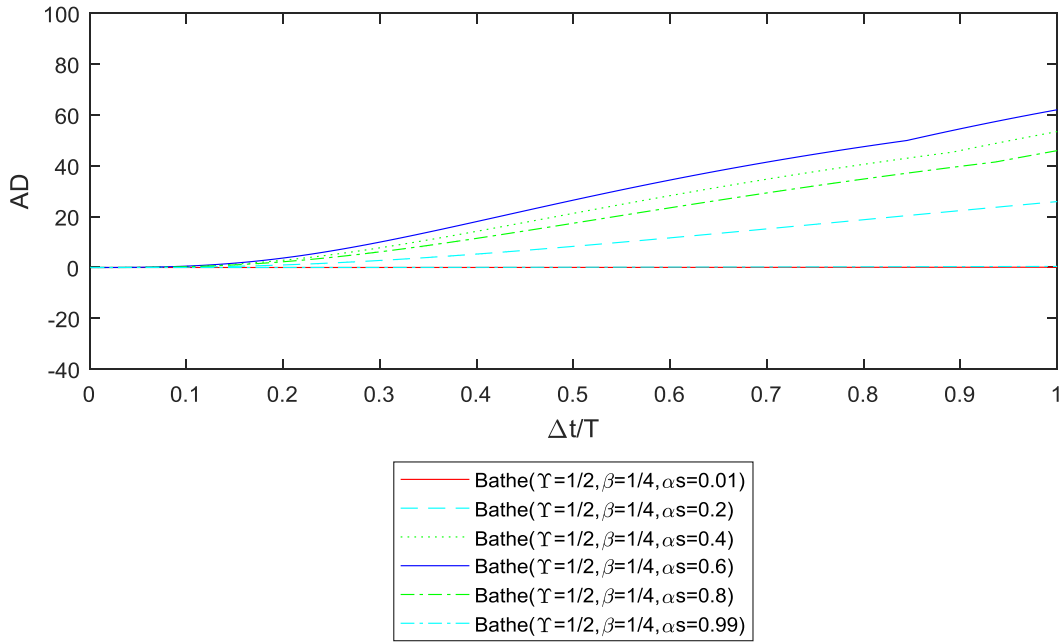


Figure 5.16 Amplitude Decay of Bathe-M, case $\xi=0$ and $0 < \alpha s < 1$

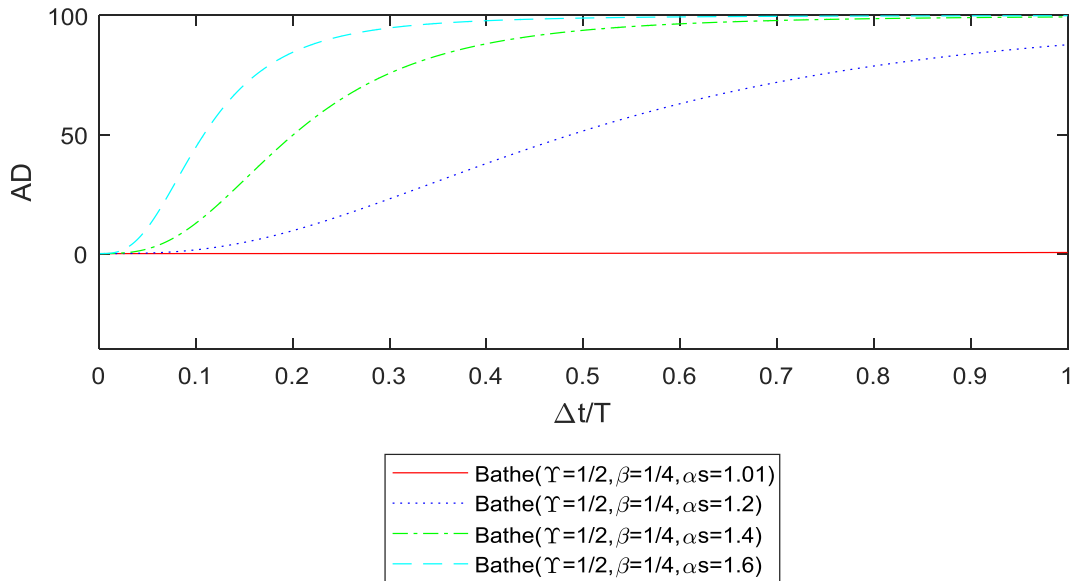


Figure 5.17 Amplitude Decay of Bathe-M, case $\xi=0$ and $\alpha s > 1$

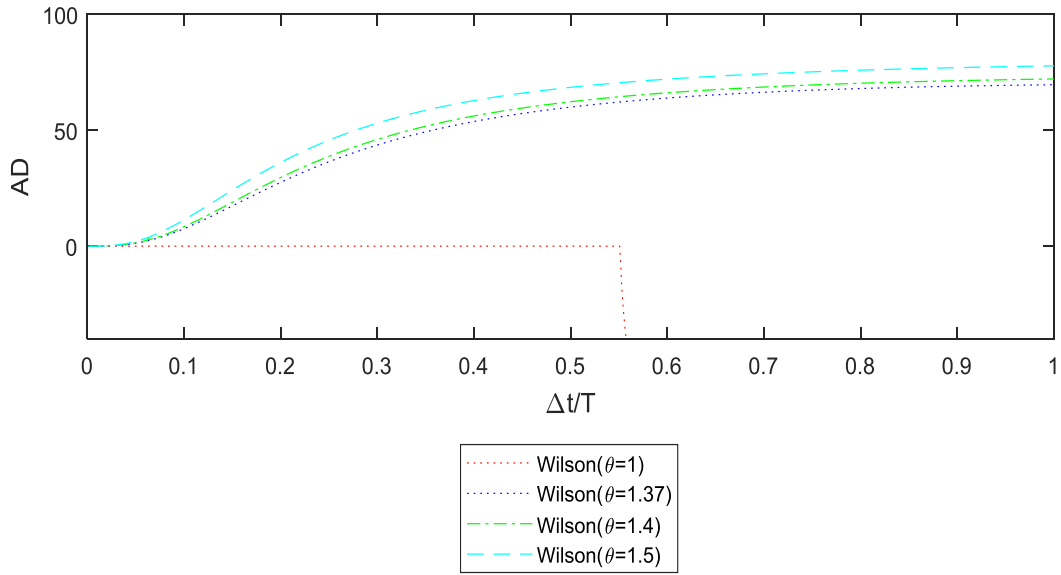


Figure 5.18 Amplitude Decay of Wilson-M, case $\xi=0$ and $\theta=1,1.37,1.4,1.5$

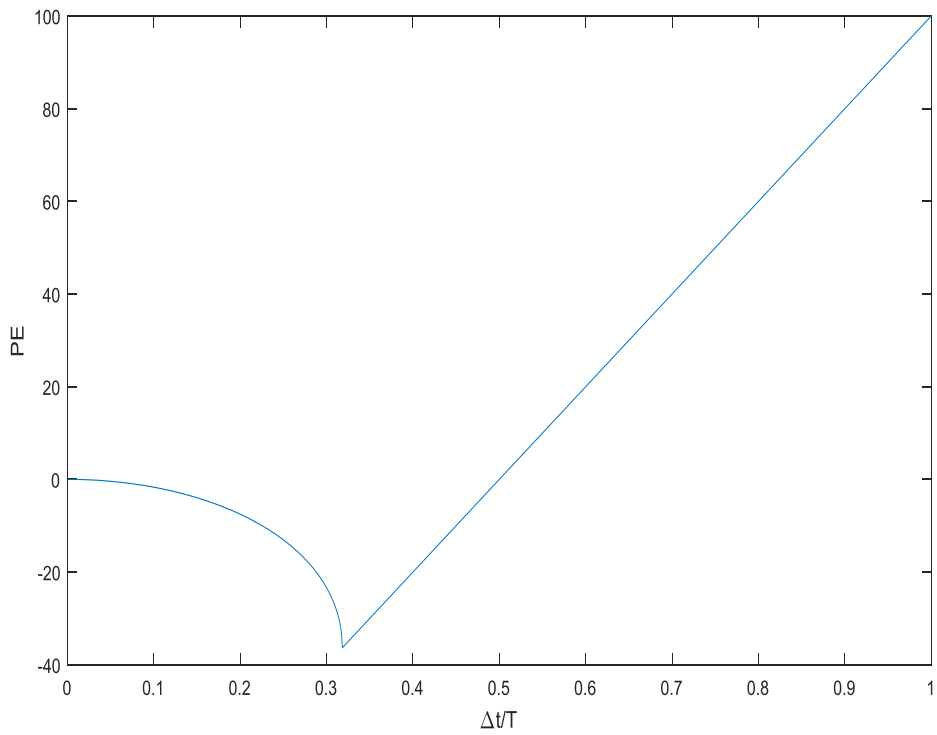


Figure 5.19 Period Elongation of Central Difference Method, case $\xi=0$

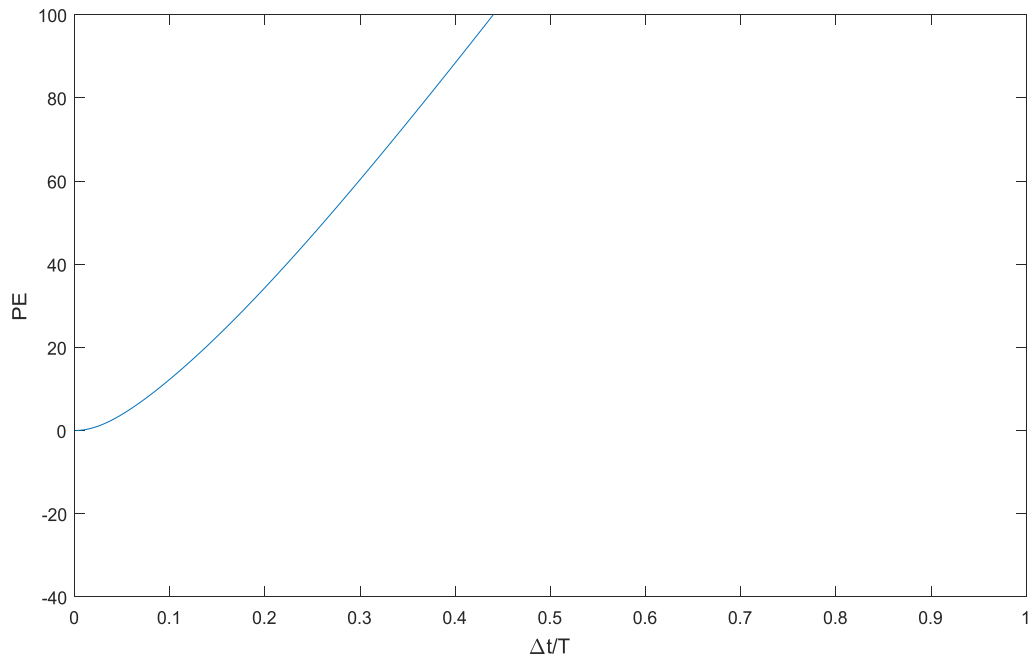


Figure 5.20 Period Elongation of Houbolt Method, case $\xi=0$

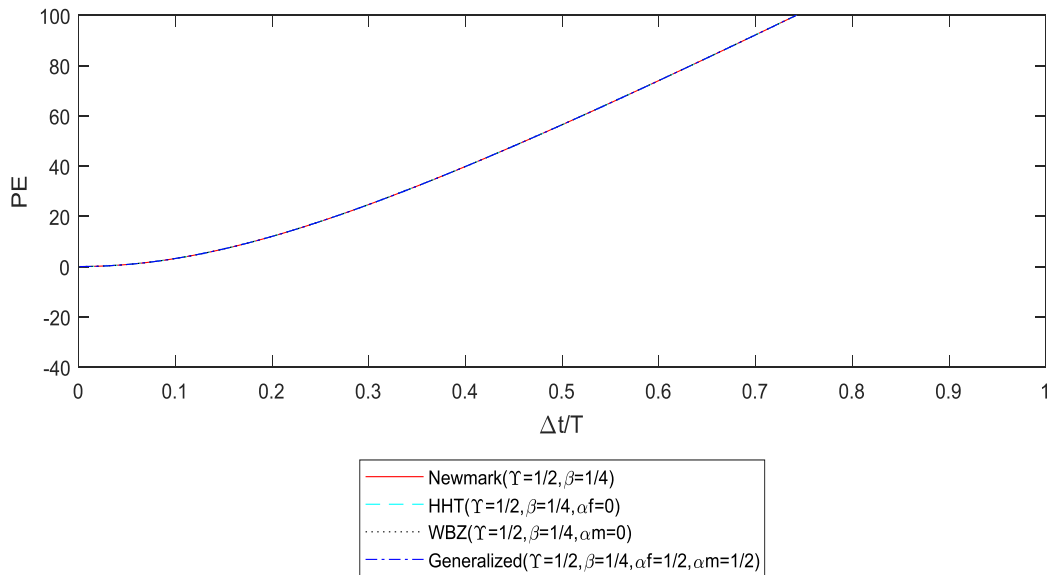


Figure 5.21 Period Elongation of N-M, HHT-M, WBZ-M and G-M, case $\xi=0$ and $\rho_{inf}=1$

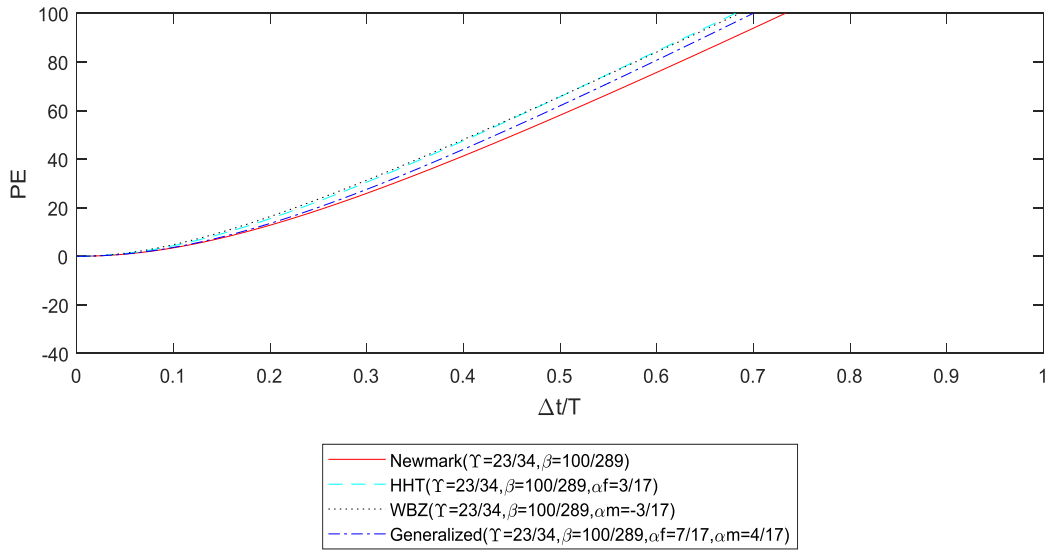


Figure 5.22 Period Elongation of N-M,HHT-M,WBZ-M and G-M,case $\xi=0$ and $\rho_{inf}=0.7$

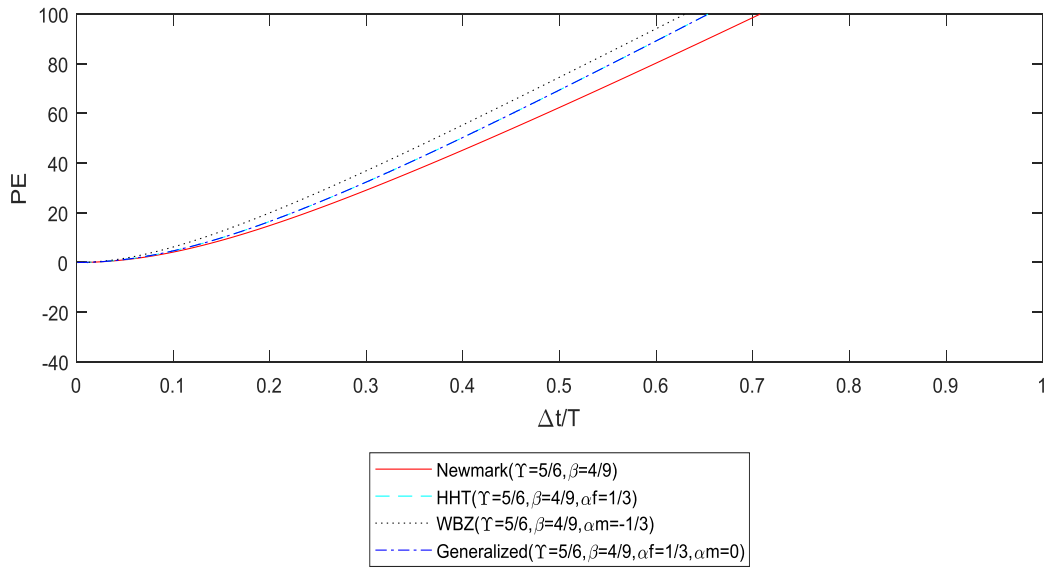


Figure 5.23 Period Elongation of N-M,HHT-M,WBZ-M and G-M,case $\xi=0$ and $\rho_{inf}=0.5$

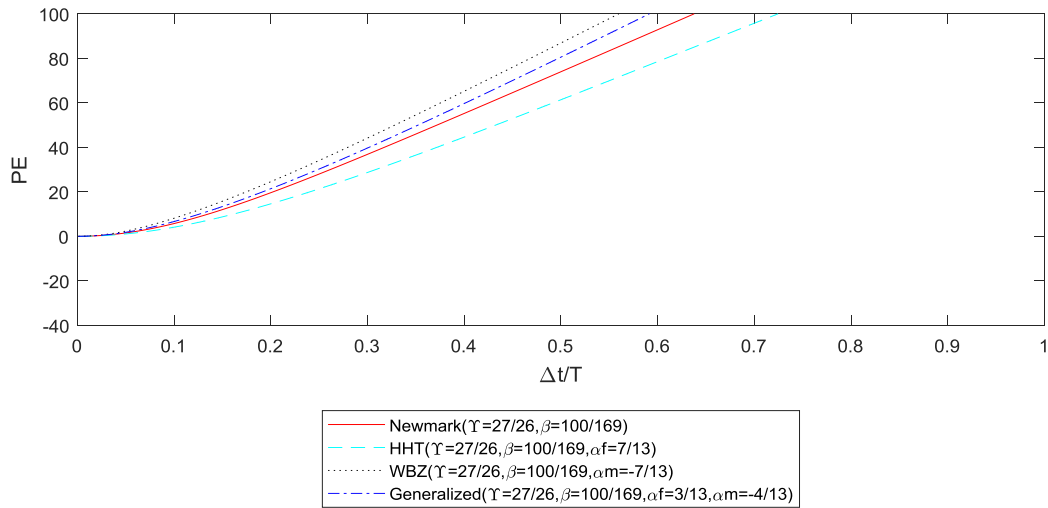


Figure 5.24 Period Elongation of N-M,HHT-M,WBZ-M and G-M,case $\xi=0$ and $\rho_{inf}=0.3$

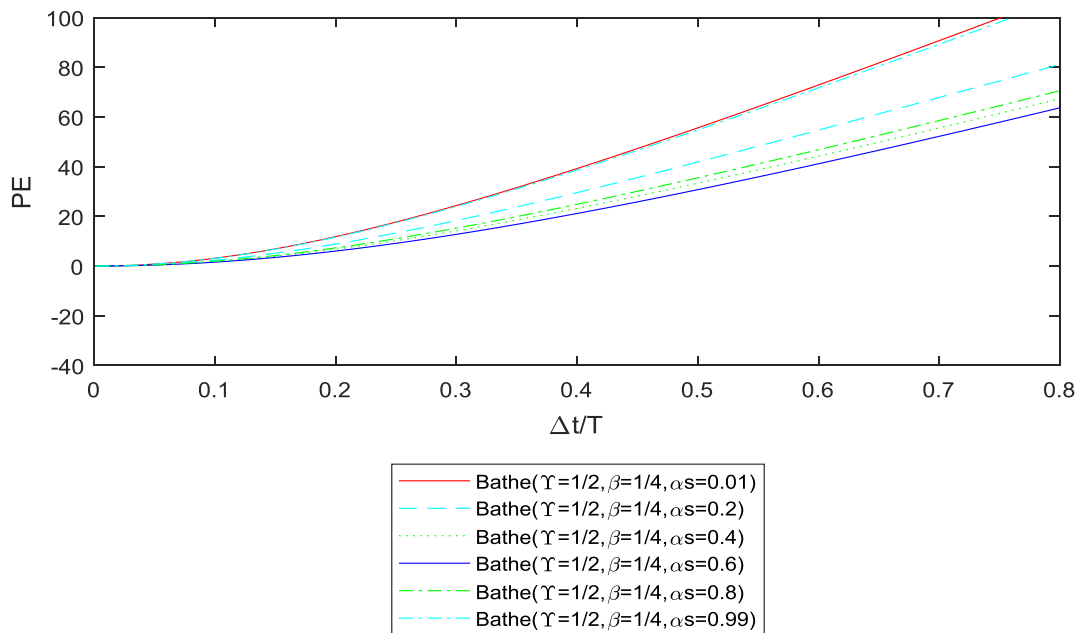


Figure 5.25 Period Elongation of Bathe-M,case $\xi=0$ and $0 < \alpha_s < 1$

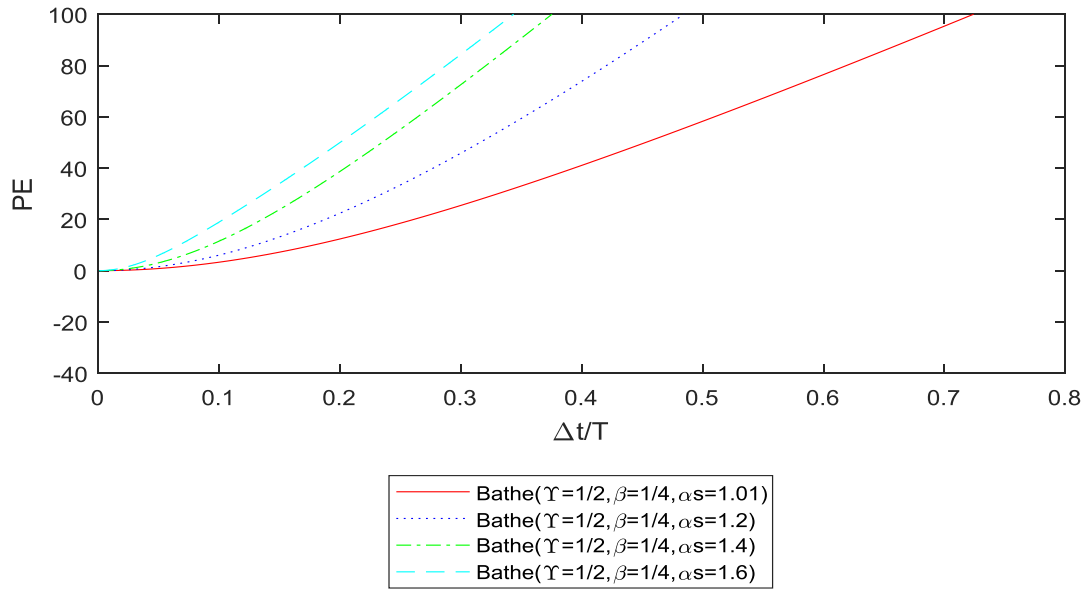


Figure 5.26 Period Elongation of Bathe-M, case $\xi=0$ and $\alpha s > 1$

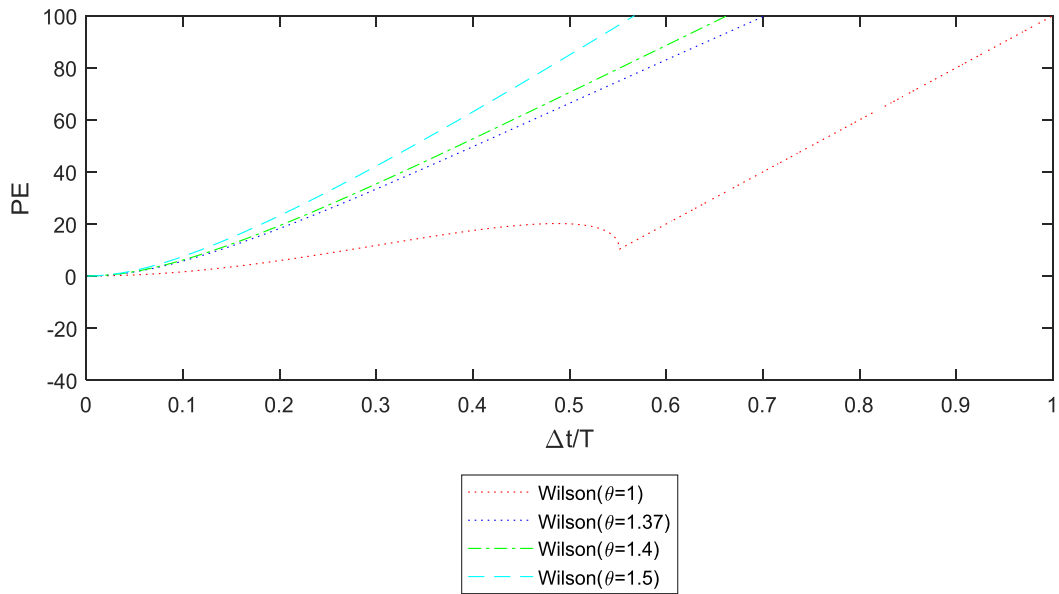


Figure 5.27 Period Elongation of Wilson-M, case $\xi=0$ and $\theta=1, 1.37, 1.4, 1.5$

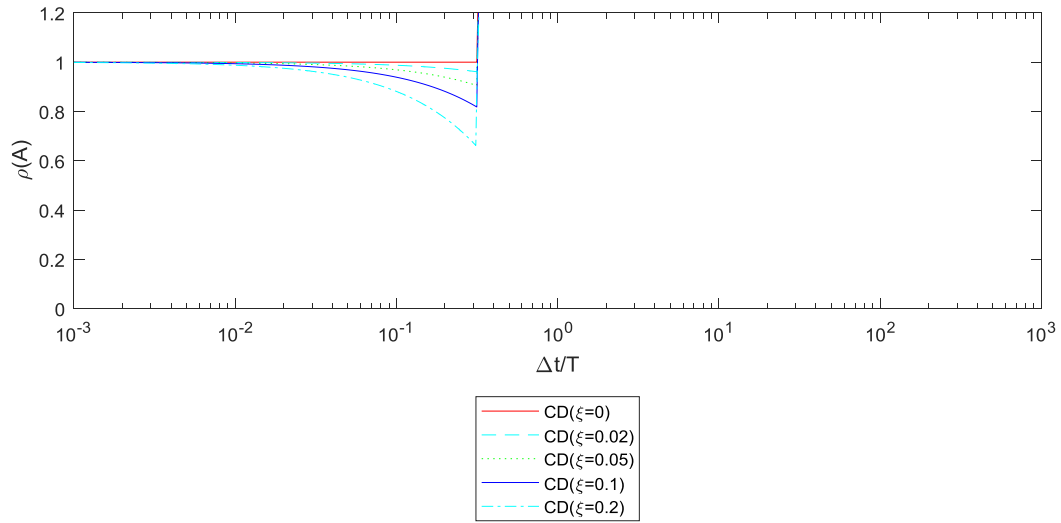


Figure 5.28 Spectral radii of Central Difference Method, case ($\xi=0,0.02,0.05,0.1,0.2$)

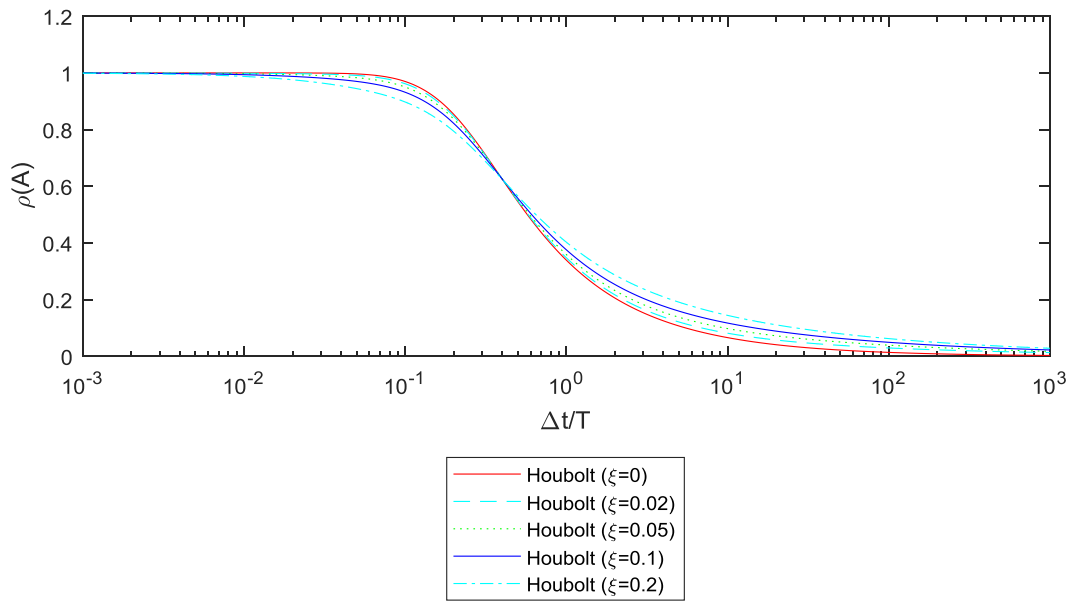


Figure 5.29 Spectral radii of Houbolt Method, case ($\xi=0,0.02,0.05,0.1,0.2$)

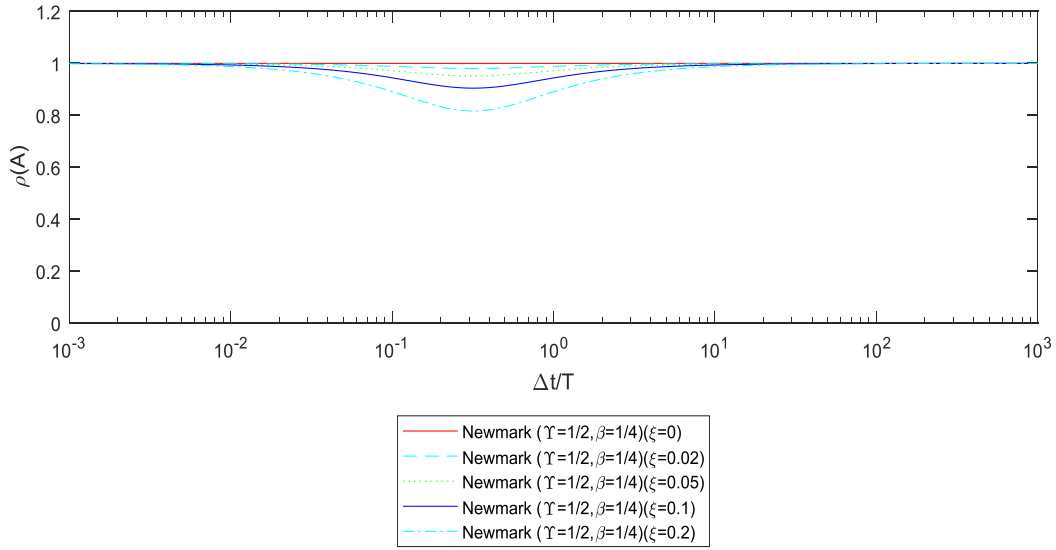


Figure 5.30 Spectral radii of Newmark Method ($\gamma=1/2, \beta=1/4$), case ($\xi=0, 0.02, 0.05, 0.1, 0.2$)

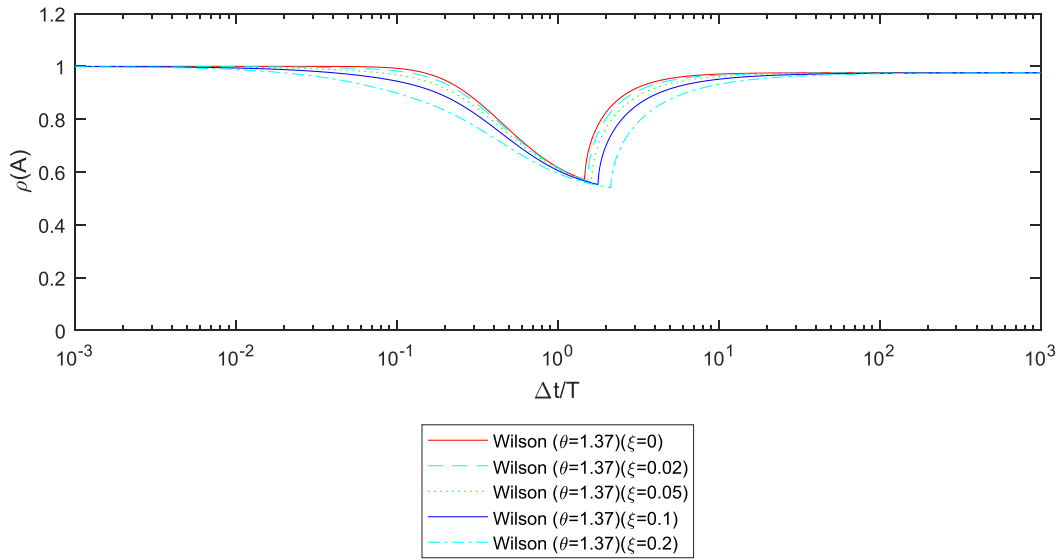


Figure 5.31 Spectral radii of Wilson Method ($\theta=1.37$), case ($\xi=0, 0.02, 0.05, 0.1, 0.2$)

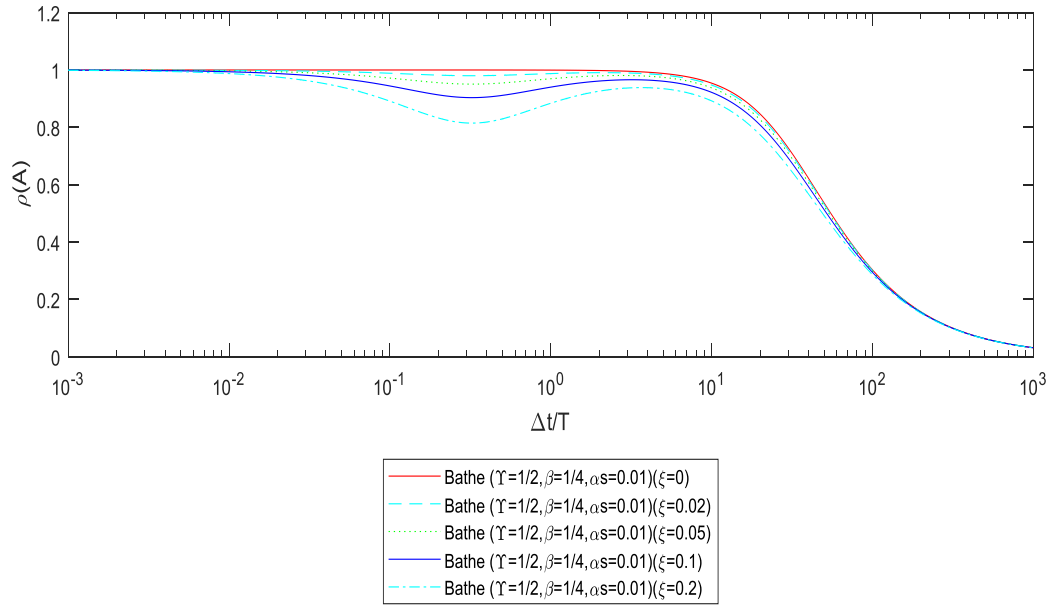


Figure 5.32 Spectral radii of Bathe Method ($\gamma=1/2, \beta=1/4, \alpha s=0.01$), case ($\xi=0, 0.02, 0.05, 0.1, 0.2$)

6. Illustrative example solutions

6.1 Single degree of freedom system

Let us consider the following equilibrium equation:

$$2\ddot{U} + 8U = 0$$

$$U(0) = 2$$

$$\dot{U}(0) = 0$$

The analytical solution of the above equation is:

$$U(t) = 2 \cos 2t$$

$$w_n = 2$$

$$T_n = \frac{2\pi}{w_n} = \pi$$

We determine the numerical solutions by using Bathe method, central difference method, Generalized- α method, Houbolt method, Newmark method, Wilson method and proposed method 1. We use the time steps ($\Delta t = 0.3, 0.5, 1.2$) and the choice of the time step ($\Delta t = 1.2$) is based on the fact that it should be greater than Δt_{cr} (for central difference method).

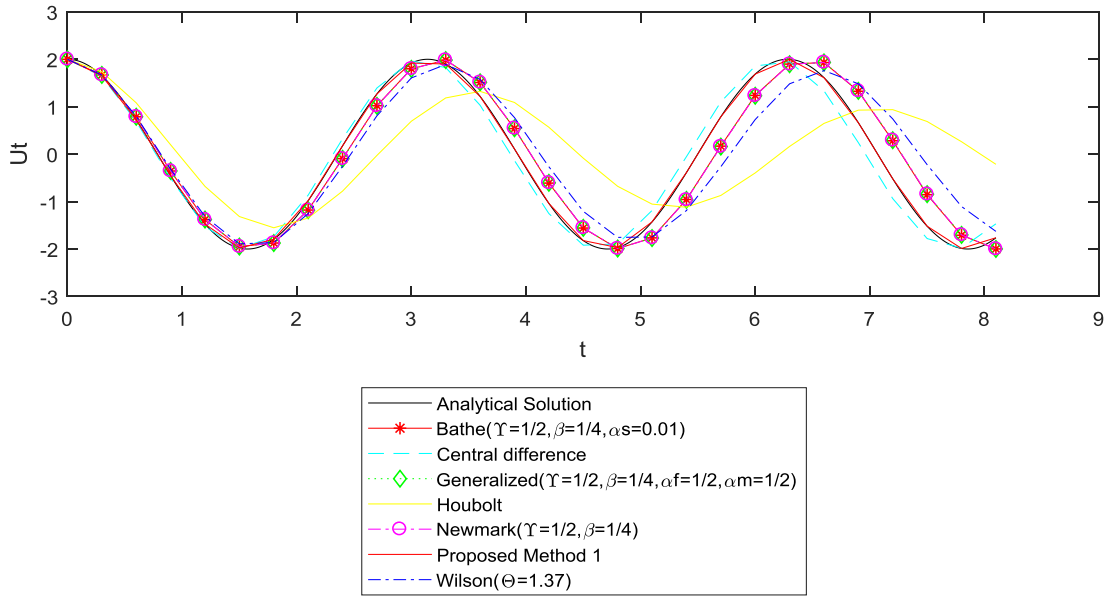


Figure 6.1.1 Displacement response of single degree of freedom system, $\Delta t=0.3$

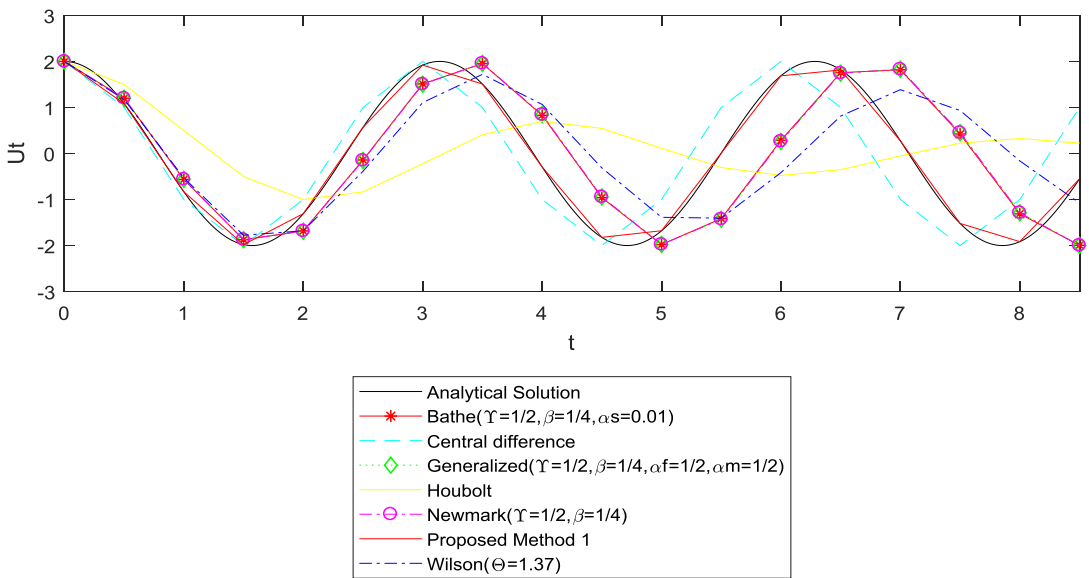


Figure 6.1.2 Displacement response of single degree of freedom system, $\Delta t=0.5$

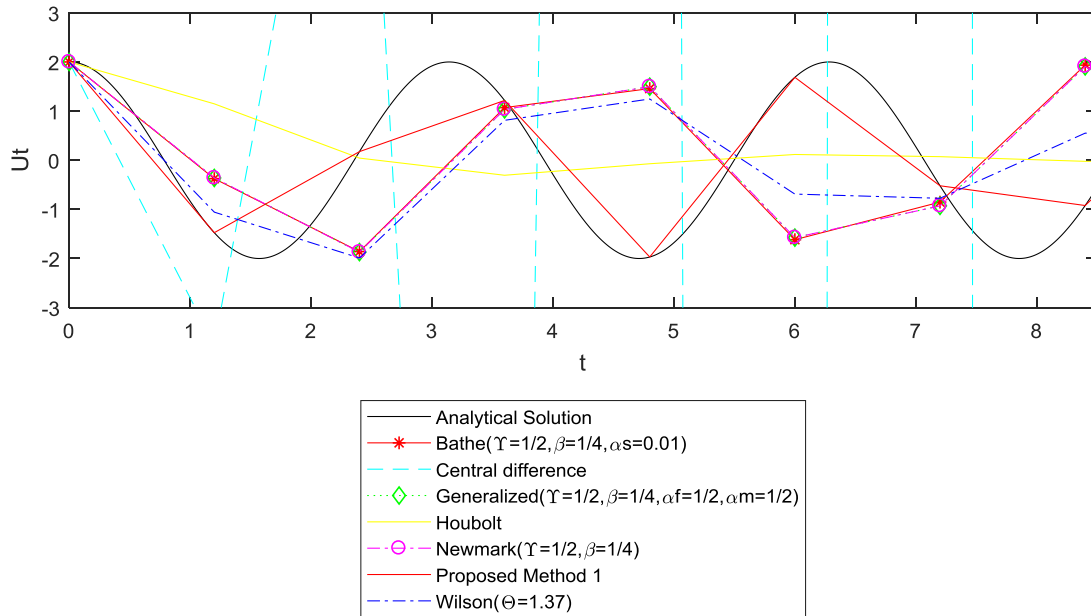


Figure 6.1.3 Displacement response of single degree of freedom system, $\Delta t=1.2$

As evidenced in the above figures, the methods exhibit different characteristics as the time step increases.

Figs 34, 35 and 36 show that as expected, no amplitude decay is observed for the Bathe method ($\gamma=1/2, \beta=1/4, \alpha_s=0.01$), Generalized- α method ($\gamma=1/2, \beta=1/4, \alpha_f=1/2, \alpha_m=1/2$) and Newmark method ($\gamma=1/2, \beta=1/4$). Furthermore, as shown in Fig 34 and 35, the central difference method introduces no amplitude decay. But the central difference method gives meaningless results when the time step is equal to 1.2. As the chosen time step is greater than Δt_{cr} , the central difference method becomes unstable. (Fig 36)

The Wilson method introduces less amplitude decay and period elongation than the Houbolt method.

As expected, the results of proposed method 1 are identical to the exact solutions and this shows that the method is efficient and accurate.

6.2 Multi-degree of freedom system (Undamped)

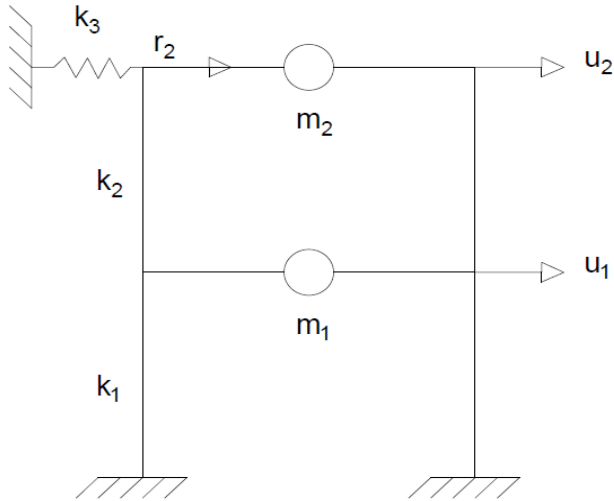


Figure 6.2 (a)

For the system shown in Figure 5.4, the mass and stiffness matrices are:

$$\mathbf{M} = \begin{bmatrix} m_1 & 0 \\ 0 & m_2 \end{bmatrix} \text{ and } \mathbf{K} = \begin{bmatrix} k_1 + k_2 & -k_2 \\ -k_2 & k_2 + k_3 \end{bmatrix}$$

Where

$$m_1 = 3, m_2 = 1, k_1 = 5, k_2 = 2, k_3 = 4 \text{ and } r_2 = 8$$

The equation of the multi-degree system can be written as follows:

$$\begin{bmatrix} 3 & 0 \\ 0 & 1 \end{bmatrix} \ddot{U} + \begin{bmatrix} 7 & -2 \\ -2 & 6 \end{bmatrix} U = \begin{bmatrix} 0 \\ 8 \end{bmatrix}$$

$$\mathbf{k} - \omega^2 \mathbf{m} = \begin{bmatrix} 7 - 3\lambda & -2 \\ -2 & 6 - \lambda \end{bmatrix}$$

where $\lambda = \omega^2$

$$\det[\mathbf{k} - \omega^2 \mathbf{m}] = 0$$

which has two solutions: $\lambda_1 = 2$ and $\lambda_2 = \frac{19}{3}$

If $\phi_{11} = 1$ then $\phi_{21} = \frac{1}{2}$

and if $\phi_{12} = 1$ then $\phi_{22} = -6$

$$\mathbf{U}(0) = \begin{bmatrix} 0 \\ 0 \end{bmatrix} \quad \text{and} \quad \mathbf{U}'(0) = \begin{bmatrix} 0 \\ 0 \end{bmatrix}$$

$$M_1 = \phi_1^T m \phi_1 = \begin{bmatrix} 1 & \frac{1}{2} \end{bmatrix} \begin{bmatrix} 3 & 0 \\ 0 & 1 \end{bmatrix} \begin{bmatrix} 1 \\ \frac{1}{2} \end{bmatrix} = \frac{13}{4}$$

$$M_2 = \phi_2^T m \phi_2 = \begin{bmatrix} 1 & -6 \end{bmatrix} \begin{bmatrix} 3 & 0 \\ 0 & 1 \end{bmatrix} \begin{bmatrix} 1 \\ -6 \end{bmatrix} = 39$$

$$P_1(t) = \phi_1^T \begin{bmatrix} 0 \\ 8 \end{bmatrix} = \begin{bmatrix} 1 & \frac{1}{2} \end{bmatrix} \begin{bmatrix} 0 \\ 8 \end{bmatrix} = 4$$

$$P_2(t) = \phi_2^T \begin{bmatrix} 0 \\ 8 \end{bmatrix} = \begin{bmatrix} 1 & -6 \end{bmatrix} \begin{bmatrix} 0 \\ 8 \end{bmatrix} = -48$$

The modal equations are:

$$\ddot{q}_1 + 2q_1 = \frac{16}{13}$$

$$\ddot{q}_2 + \frac{19}{3}q_2 = -\frac{48}{39}$$

The solutions of the modal equations are:

$$q_1 = \frac{8}{13}(1 - \cos \sqrt{2}t)$$

$$q_2 = -\frac{48}{247}(1 - \cos \sqrt{\frac{19}{3}}t)$$

The displacement response can be expressed as follows:

$$U_1(t) = \frac{8}{13}(1 - \cos \sqrt{2}t) - \frac{48}{247}(1 - \cos \sqrt{\frac{19}{3}}t)$$

$$U_2(t) = \frac{4}{13}(1 - \cos \sqrt{2}t) + \frac{288}{247}(1 - \cos \sqrt{\frac{19}{3}}t)$$

For this multi-degree of freedom system, time steps ($\Delta t = 0.3, 0.5, 1$) are utilized. Bathe method, central difference method, Generalized- α method, Houbolt method, Newmark, Wilson method and proposed method 1 are employed to determine the numerical solution of the problem.

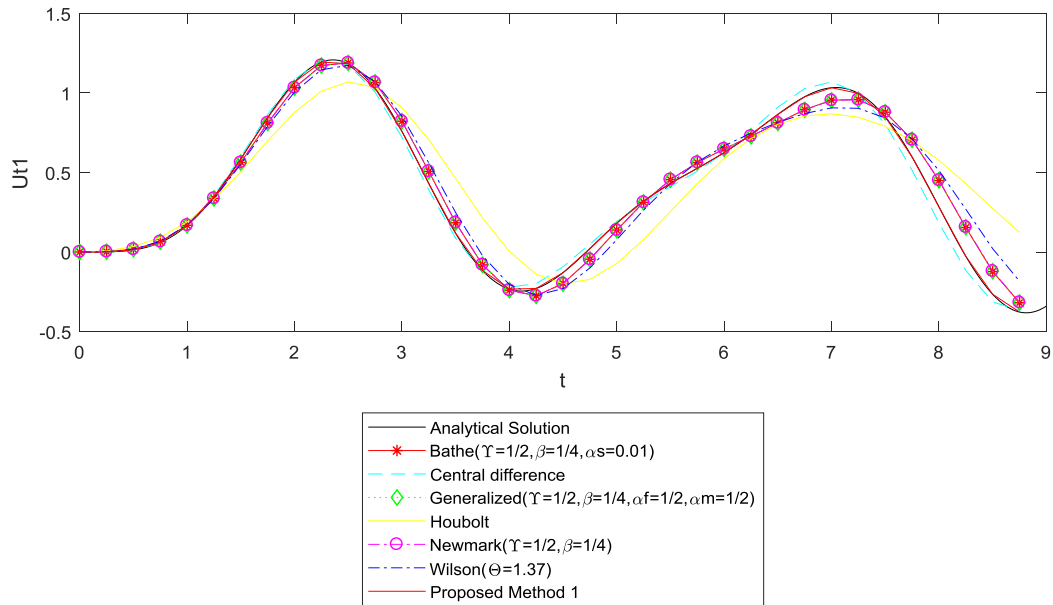


Figure 6.2.1 Displacement response of multi degree of freedom system Ut1, $\Delta t=0.25$

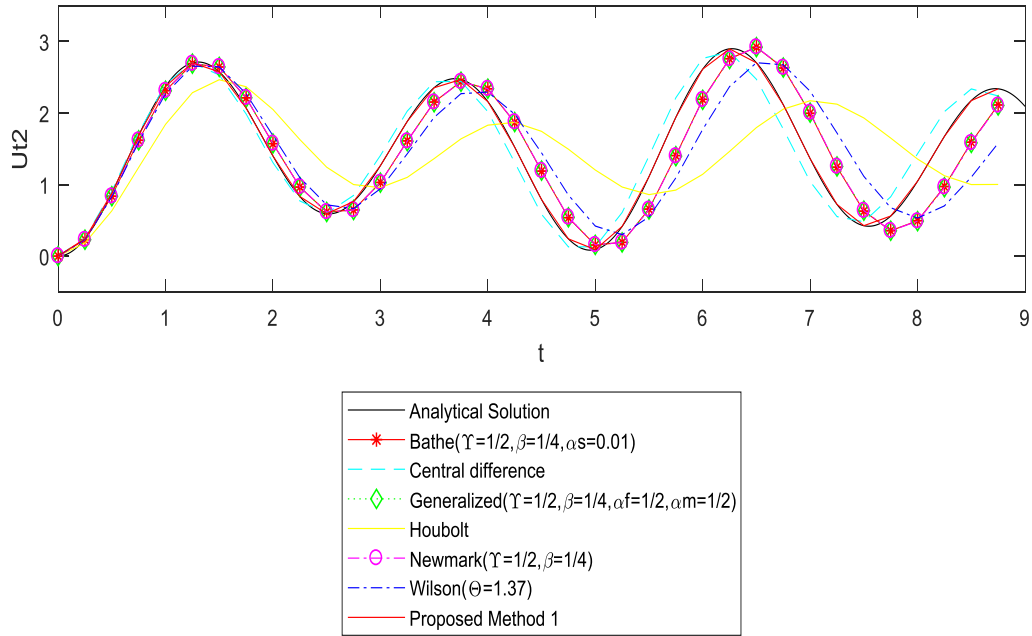


Figure 6.2.2 Displacement response of multi degree of freedom system $U_{t2}, \Delta t=0.25$

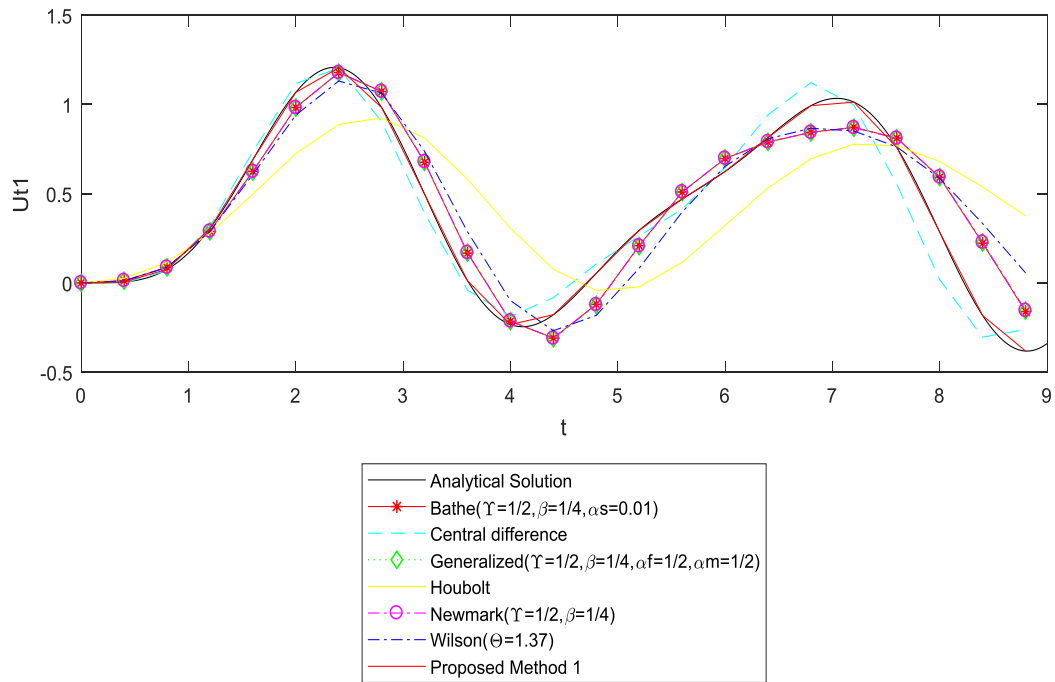


Figure 6.2.3 Displacement response of multi degree of freedom system $U_{t1}, \Delta t=0.4$

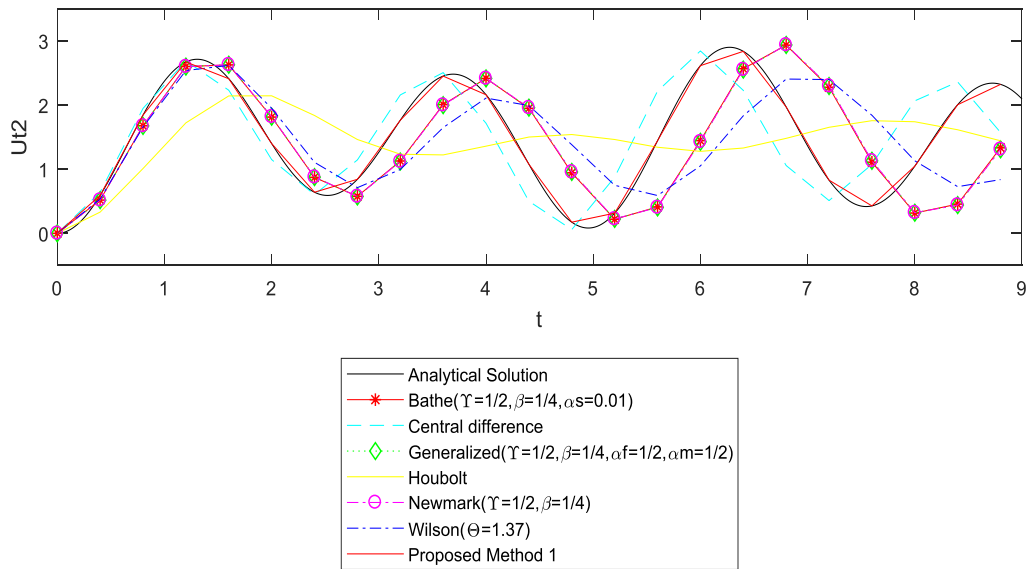


Figure 6.2.4 Displacement response of multi degree of freedom system $U_{t2}, \Delta t=0.4$

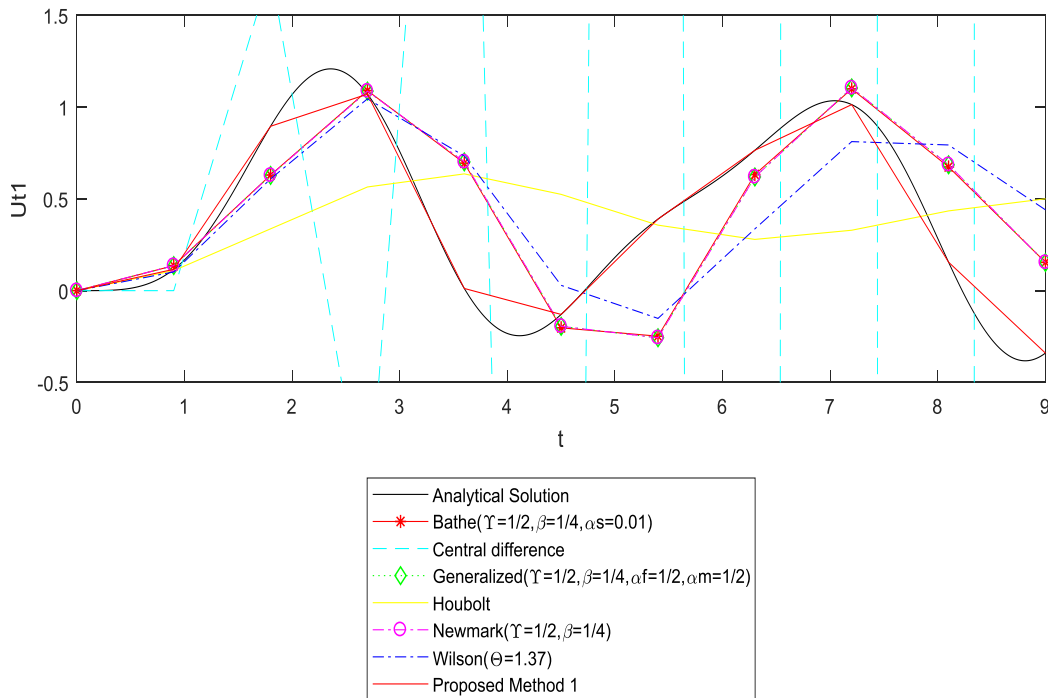


Figure 6.2.5 Displacement response of multi degree of freedom system $U_{t1}, \Delta t=0.9$

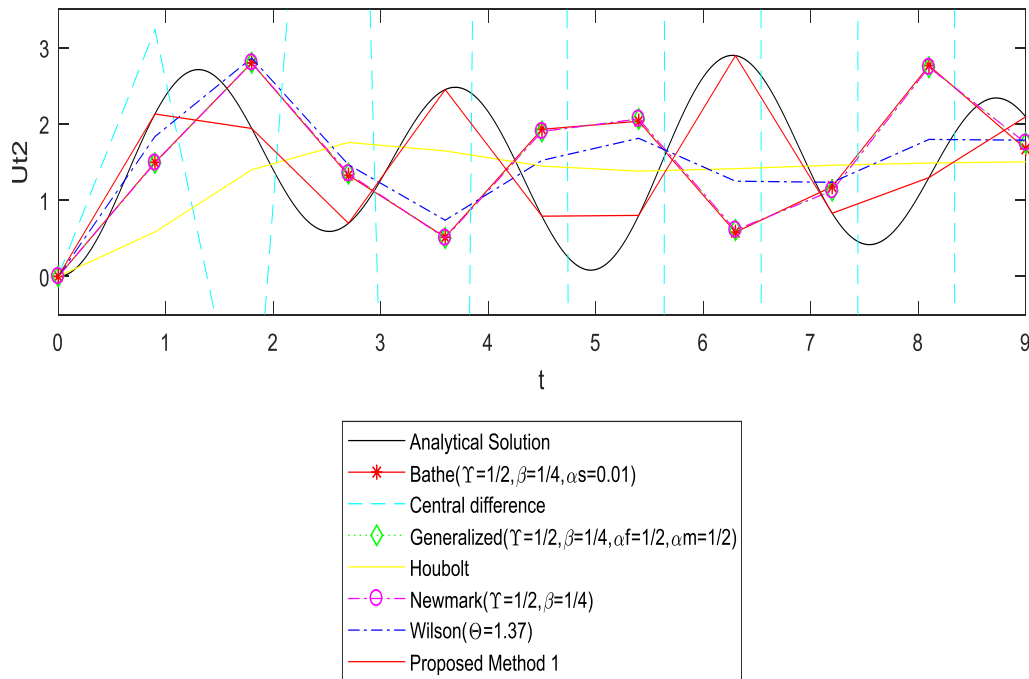


Figure 6.2.6 Displacement response of multi degree of freedom system $U_{t2}, \Delta t=0.9$

According to Figs 37, 38, 39 and 40, the central difference method yields more accurate result compared to other existing methods. But it gives erratic responses when the time step exceeds a critical value Δt_{cr} .

If we consider the responses in all figs (37, 38, 39, 40, 41, 42), the amplitude error of Bathe method ($\gamma=1/2, \beta=1/4, \alpha s=0.01$), Generalized- α method ($\gamma=1/2, \beta=1/4, \alpha f=1/2, \alpha m=1/2$) and Newmark method ($\gamma=1/2, \beta=1/4$) is lesser than that of Houbolt method and Wilson method. The mentioned methods introduce results - which agree with the analytical solutions – even though the time step is long.

As the time step increases, a significant damping is observed in Houbolt and Wilson methods.

As stated in section 2.3, the analysis of stability and accuracy of single degree of freedom system can shed light on the efficacy of the numerical methods in a multi-degree of freedom system.

The reason for the above idea is that if the same integration and the same time step is used for each modal equation, the mode superposition analysis is equivalent to the direct integration method.

Consequently, when studying the stability and accuracy of direct integration methods, it suffices to consider the equilibrium equation of a single degree of freedom system.

Regarding proposed method 1, no amplitude decay and period elongation are observed. This demonstrates that the method provides very accurate results.

6.3 Multi-degree of freedom system (Non-classically damped)

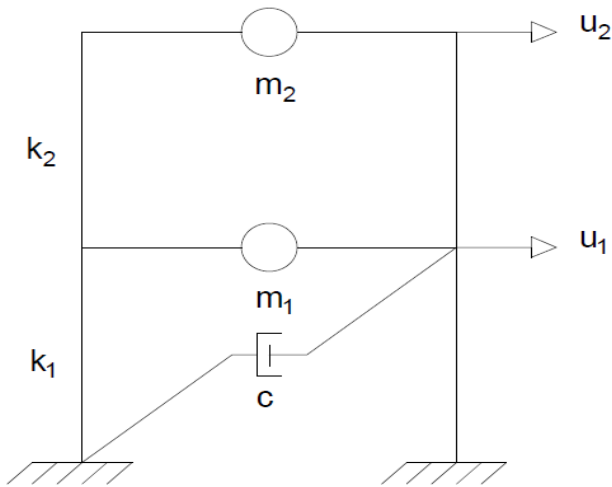


Figure 6.3 (a)

For the system shown in Figure 5.11, the mass and stiffness matrices are:

$$\mathbf{M} = \begin{bmatrix} m_1 & 0 \\ 0 & m_2 \end{bmatrix}, \mathbf{C} = \begin{bmatrix} c & 0 \\ 0 & 0 \end{bmatrix} \text{ and } \mathbf{K} = \begin{bmatrix} k_1 + k_2 & -k_2 \\ -k_2 & k_2 \end{bmatrix}$$

Where

$$m_1 = 3, m_2 = 2, c = 0, k_1 = 6 \text{ and } k_2 = 3$$

The equation of the multi-degree system can be written as follows:

$$\begin{bmatrix} 3 & 0 \\ 0 & 2 \end{bmatrix} \ddot{U} + \begin{bmatrix} 6 & 0 \\ 0 & 0 \end{bmatrix} \dot{U} + \begin{bmatrix} 9 & -3 \\ -3 & 3 \end{bmatrix} U = \begin{bmatrix} 0 \\ 10 \end{bmatrix}$$

$$\mathbf{m} = \begin{bmatrix} 3 & 0 \\ 0 & 2 \end{bmatrix} \quad \mathbf{c} = \begin{bmatrix} 6 & 0 \\ 0 & 0 \end{bmatrix} \quad \mathbf{k} = \begin{bmatrix} 9 & -3 \\ -3 & 3 \end{bmatrix}$$

The eigenvectors of the associated undamped system are:

$$\phi_1 = \begin{bmatrix} 0.4574 \\ 1 \end{bmatrix} \quad \text{and} \quad \phi_2 = \begin{bmatrix} -1.4574 \\ 1 \end{bmatrix}$$

$$cm^{-1}k = \begin{bmatrix} 18 & -6 \\ 0 & 0 \end{bmatrix}$$

$$km^{-1}c = \begin{bmatrix} 18 & 0 \\ 6 & 0 \end{bmatrix}$$

$$cm^{-1}k \neq km^{-1}c$$

Thus, the system is non-classically damped.

For non-classically damped system, the eigenvalue problem to be solved is defined by the following equation:

$$\lambda \mathbf{a} \mathbf{k} + \mathbf{b} \mathbf{k} = \mathbf{0}$$

where the matrices a and b defined in the following manner,

$$a = \begin{bmatrix} 0 & m \\ m & c \end{bmatrix} = \begin{bmatrix} 0 & 0 & 3 & 0 \\ 0 & 0 & 0 & 2 \\ 3 & 0 & 6 & 0 \\ 0 & 2 & 0 & 0 \end{bmatrix}$$

$$b = \begin{bmatrix} -m & 0 \\ 0 & k \end{bmatrix} = \begin{bmatrix} -3 & 0 & 0 & 0 \\ 0 & -2 & 0 & 0 \\ 0 & 0 & 9 & -3 \\ 0 & 0 & -3 & 3 \end{bmatrix}$$

The eigenvalue problem can be solved using Matlab function eig(b,-a):

$$\lambda_1, \bar{\lambda}_1 = -0.7590 \pm 1.4317i$$

$$\lambda_2, \bar{\lambda}_2 = -0.2410 \pm 1.0414i$$

From these eigenvalues, w_n and ξ_n can be determined in the following manner:

$$w_1 = |\lambda_1| = 1.6204$$

$$w_2 = |\lambda_2| = 1.0689$$

$$\xi_1 = -\frac{\text{Re}(\lambda_1)}{|\lambda_1|} = 0.4684$$

$$\xi_2 = -\frac{\text{Re}(\lambda_2)}{|\lambda_2|} = 0.2255$$

The corresponding frequencies $w_n D$ of the damped system are determined as follows:

$$w_1 D = \text{Im}(\lambda_1) = 1.4317$$

$$w_2 D = \text{Im}(\lambda_2) = 1.0414$$

Solutions of the eigenvalue problem also provide the 4x1 eigenvectors, but only the third and fourth components are relevant and shown below:

$$\psi_1 = \begin{Bmatrix} 0.0176 - 1.4488i \\ 1 \end{Bmatrix}$$

$$\psi_2 = \begin{Bmatrix} 0.3158 - 0.3346i \\ 1 \end{Bmatrix}$$

To verify that the eigenvectors ψ_n are orthogonal, we compute the following terms:

$$\psi_1^T m \psi_2 = \begin{Bmatrix} 0.0176 - 1.4488i \\ 1 \end{Bmatrix}^T \begin{bmatrix} 3 & 0 \\ 0 & 2 \end{bmatrix} \begin{Bmatrix} 0.3158 - 0.3346i \\ 1 \end{Bmatrix} = 0.5621 - 1.3901i$$

$$\psi_1^T k \psi_2 = \begin{Bmatrix} 0.0176 - 1.4488i \\ 1 \end{Bmatrix}^T \begin{bmatrix} 9 & -3 \\ -3 & 3 \end{bmatrix} \begin{Bmatrix} 0.3158 - 0.3346i \\ 1 \end{Bmatrix} = -2.3136 + 1.1800i$$

$$\psi_1^T c \psi_2 = \begin{Bmatrix} 0.0176 - 1.4488i \\ 1 \end{Bmatrix}^T \begin{bmatrix} 6 & 0 \\ 0 & 0 \end{bmatrix} \begin{Bmatrix} 0.3158 - 0.3346i \\ 1 \end{Bmatrix} = -2.8758 - 2.7803i$$

$$\begin{aligned} (\lambda_1 + \lambda_2) \psi_1^T m \psi_2 + \psi_1^T c \psi_2 &= (-1 + 2.4731i)(0.5621 - 1.3901i) + (-2.8758 - 2.7803i) \\ &= 0 \end{aligned}$$

$$\begin{aligned} \psi_1^T k \psi_2 - \lambda_1 \lambda_2 \psi_1^T m \psi_2 &= (-2.3136 + 1.1800i) - (-0.7590 + 1.4317i)(-0.2410 + \\ & 1.0414i)(0.5621 - 1.3901i) = 0 \end{aligned}$$

The initial displacement and velocity vectors are:

$$\mathbf{u}(0) = \begin{bmatrix} 0.2 \\ 0.5 \end{bmatrix} \quad \text{and} \quad \dot{\mathbf{u}}(0) = \begin{bmatrix} 0 \\ 0 \end{bmatrix}$$

$$B_1 = \frac{\lambda_1 \psi_1^T m \mathbf{u}(0) + \psi_1^T c \mathbf{u}(0) + \psi_1^T m \dot{\mathbf{u}}(0)}{2\lambda_1 \psi_1^T m \psi_1 + \psi_1^T c \psi_1} = -0.398 + 0.0222i$$

$$B_2 = \frac{\lambda_2 \psi_2^T m \mathbf{u}(0) + \psi_2^T c \mathbf{u}(0) + \psi_2^T m \dot{\mathbf{u}}(0)}{2\lambda_2 \psi_2^T m \psi_2 + \psi_2^T c \psi_2} = 0.2898 - 0.0685i$$

$$\beta_1 = Re(2B_1\Psi_1) = \begin{Bmatrix} 0.0628 \\ -0.0796 \end{Bmatrix}$$

$$\beta_2 = Re(2B_2\Psi_2) = \begin{Bmatrix} 0.1372 \\ 0.5796 \end{Bmatrix}$$

$$\gamma_1 = Im(2B_1\Psi_1) = \begin{Bmatrix} 0.1162 \\ 0.0443 \end{Bmatrix}$$

$$\gamma_2 = Im(2B_2\Psi_2) = \begin{Bmatrix} -0.2372 \\ -0.1371 \end{Bmatrix}$$

The free vibration response is expressed in the following manner:

$\mathbf{u}(t) =$

$$e^{-0.759t} \left[\begin{Bmatrix} 0.0628 \\ -0.0796 \end{Bmatrix} \cos 1.4317t - \begin{Bmatrix} 0.1162 \\ 0.0443 \end{Bmatrix} \sin 1.4317t \right] + e^{-0.241t} \left[\begin{Bmatrix} 0.1372 \\ 0.5796 \end{Bmatrix} \cos 1.0414t + \begin{Bmatrix} 0.2372 \\ 0.1371 \end{Bmatrix} \sin 1.0414t \right]$$

The displacement responses (U_{t1} and u_{t2}) are determined using Bathe method, central difference method, Generalized- α method, Houbolt method, Newmark method, Wilson method and proposed method 1 for time steps ($\Delta t = 0.3, 0.5, 1.5$). Afterward, a comparison is made between the analytical and numerical solutions.

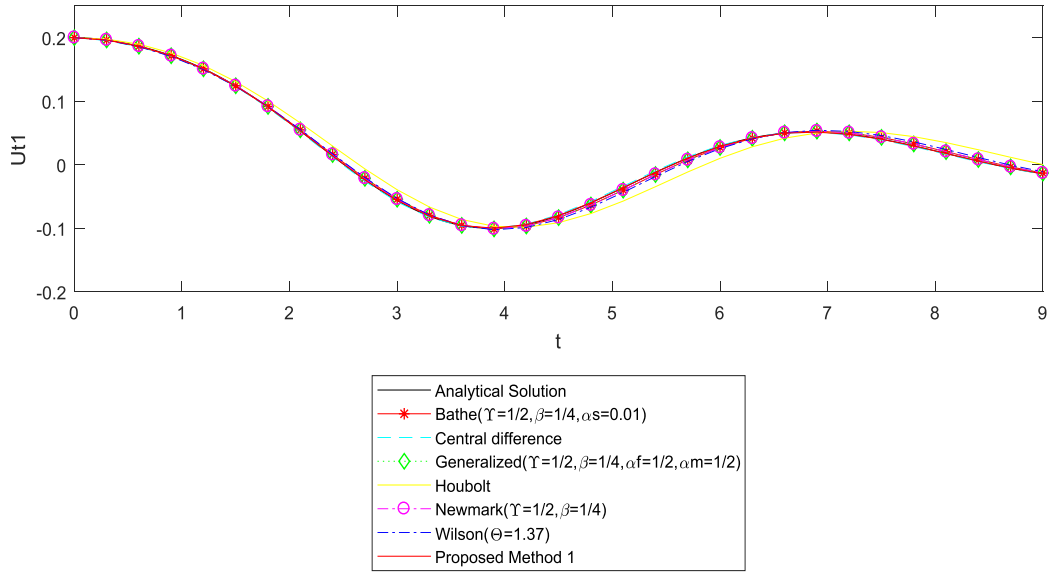


Figure 6.3.1 Displacement response of multi degree of freedom system (NCD) $U_{t1}, \Delta t=0.3$

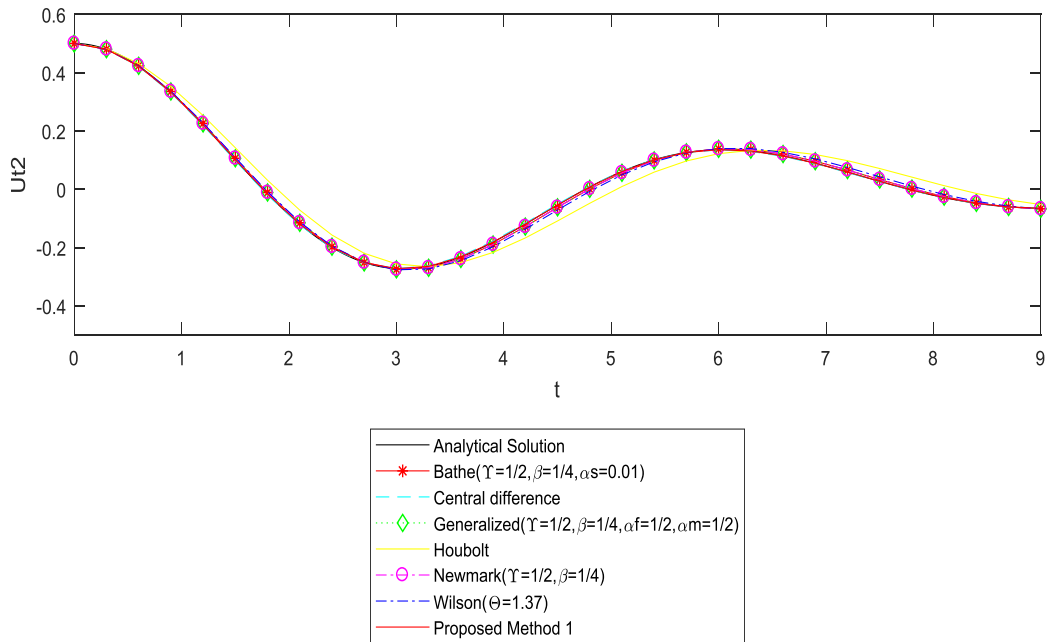


Figure 6.3.2 Displacement response of multi degree of freedom system U_{t2} (NCD), $\Delta t=0.3$

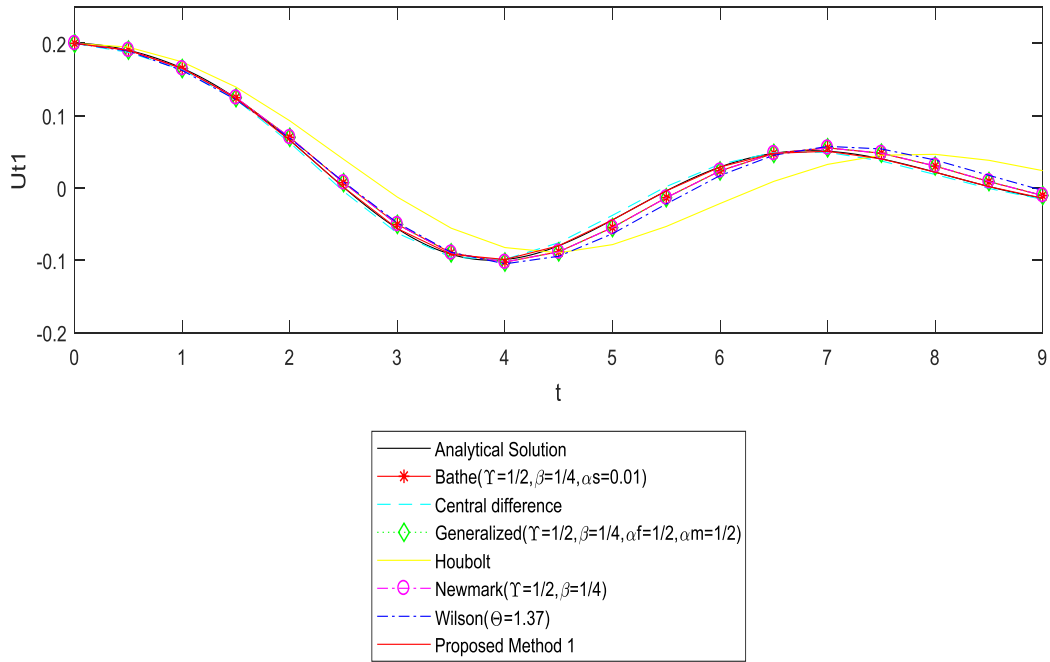


Figure 6.3.3 Displacement response of multi degree of freedom system (NCD) $Ut_1, \Delta t=0.5$

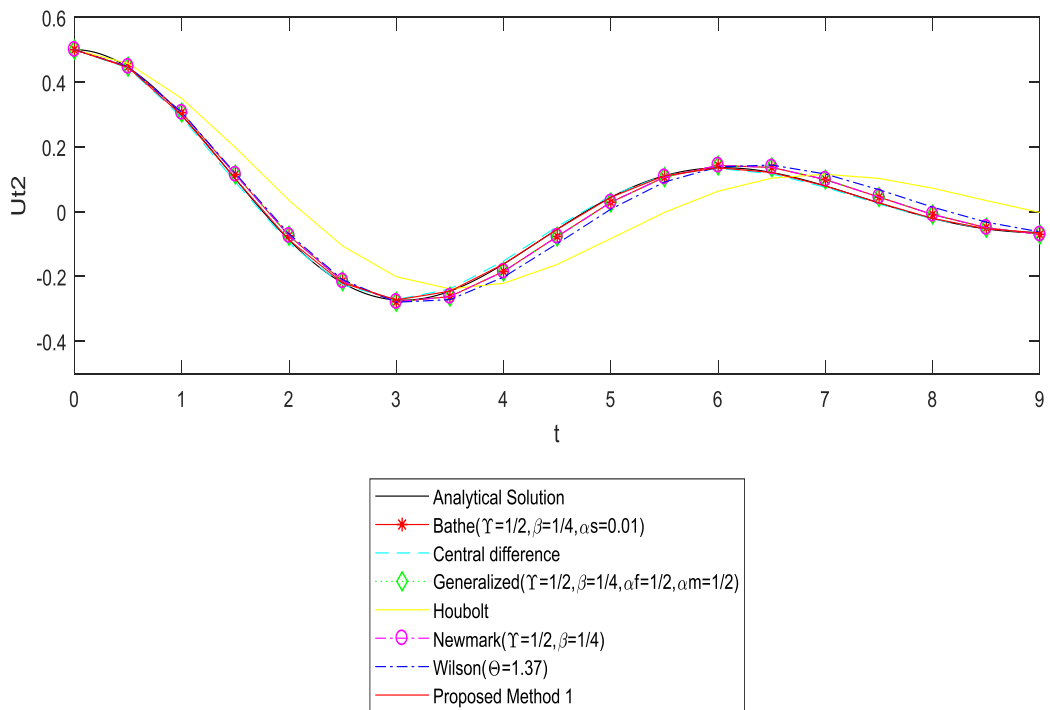


Figure 6.3.4 Displacement response of multi degree of freedom system Ut_2 (NCD), $\Delta t=0.5$

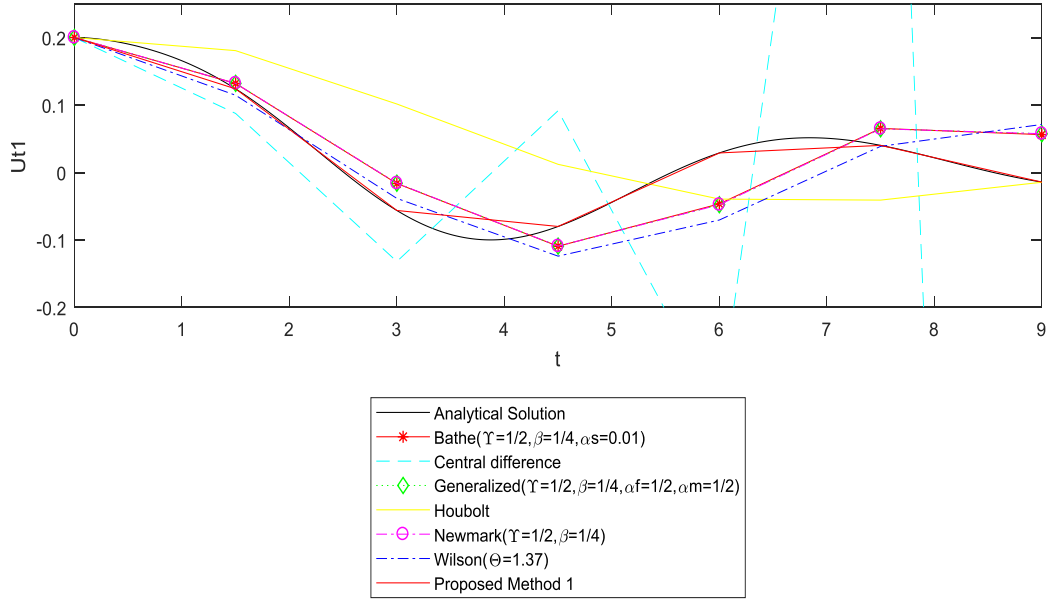


Figure 6.3.5 Displacement response of multi degree of freedom system (NCD) $U_{t1}, \Delta t=1.5$

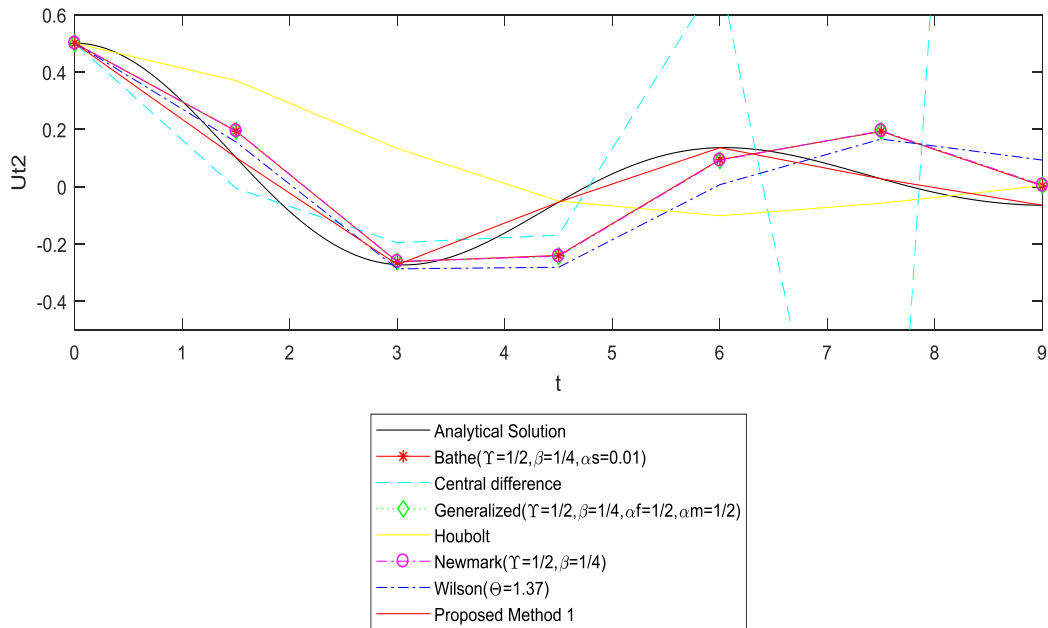


Figure 6.3.6 Displacement response of multi degree of freedom system U_{t2} (NCD), $\Delta t=1.5$

For time steps ($\Delta t = 0.3, 0.5$), all numerical methods give solutions that agree with the analytical responses. But a slight period elongation is observed in the responses of Houbolt method.

However, for time step ($\Delta t = 1.5$), the results obtained from Bathe method, Generalized- α method and Newmark method are found to be more accurate than other existing methods. Houbolt method introduces significant numerical damping and period elongation.

Furthermore, the results determined using the central difference method increase without bound as the time step increases. By trial and error, it is determined that the central difference method becomes unstable when the time step is greater than 1.01 which differs from the critical time step ($\Delta t = T/\pi$). We can conclude that the stability and accuracy analysis of a single degree of freedom system doesn't predict exactly the behavior of a numerical method in a non-classically damped system. But, most of the numerical methods exhibit the characteristics predicted in the analysis of the stability and accuracy of the algorithms.

With regard to proposed method 1, the results given by the method are similar to the exact solutions. It should be noted that the method based on interpolation of excitation (piece-wise exact method) is not suitable for non-classically damped systems. Alternatively, proposed method 1 can be considered as an extension of the method based on interpolation of excitation which can be used for non-classically damped systems.

6.4 Clamped-free bar

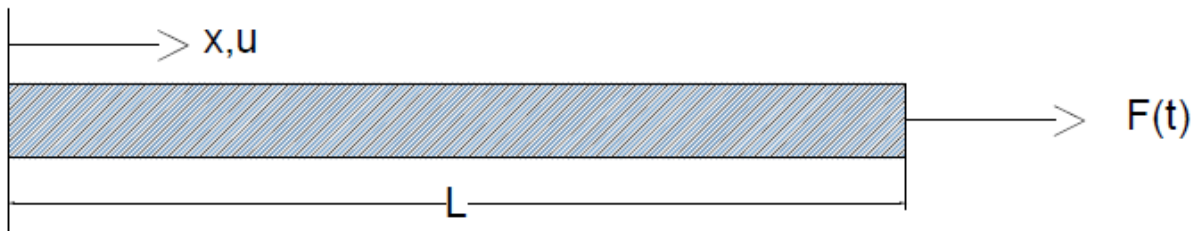


Figure 6.4 (a) Clamped-free bar excited by an end load

For the finite element system of the clamped-free bar shown in Figure 6.4 (a), the mass and stiffness matrices are:

$$\mathbf{M} = \frac{\rho A l}{2} \begin{bmatrix} 2 & & & & 0 \\ & 2 & & & \\ & & \ddots & & \\ & & & \ddots & \\ & & & & 2 \\ 0 & & & & & 1 \end{bmatrix}, \text{ and } \mathbf{K} = \frac{EA}{l} \begin{bmatrix} 2 & -1 & & & & 0 \\ -1 & 2 & -1 & & & \\ & -1 & \ddots & & & \\ & & & \ddots & -1 & \\ & & & & -1 & 2 & -1 \\ 0 & & & & & -1 & 1 \end{bmatrix}$$

where the bar is divided into N finite elements and l is equal to $\frac{L}{N}$.

The material and geometrical properties are presented as follows:

$$E = 4 \times 10^7, \rho = 0.0008, A = 1, \text{ and } L = 400$$

The load applied at the end of the bar amounts to 50,000 and the value of N selected for the analysis of the finite element system is 100.

The exact solutions of the continuous system of the clamped-free bar are determined based on the procedure described in **Mechanical Vibrations (Michel Geradin and Daniel J. Rixen)**.

The displacement and velocity responses (at $x=200$) are calculated by using the following methods with a time step ($\Delta t=0.001$):

- Proposed Method 1 (The first 49 modes are taken into account to get rid of the spurious modes)
- Central difference method
- Newmark method ($\rho_{inf}=1, 0.7, 0.5, 0.3, 0$)
- HHT- α method ($\rho_{inf}=0.7, 0.5, 0.3, 0$)
- WBZ- α Method ($\rho_{inf}=0.7, 0.5, 0.3, 0$)
- Generalized- α method ($\rho_{inf}=0.7, 0.5, 0.3, 0$)
- Standard Bath method
- Houbolt method

The results in Fig 6.4.1 show that the central difference method gives unreliable solutions. This phenomenon is associated to the fact that the selected time step is greater than the critical time step.

The displacement responses of all methods -except Newmark ($\rho_{inf}=0.3, 0$) method, central difference method and HHT- α ($\rho_{inf}=0$) method - are accurate. (See Fig 6.4.1-10).

However, the velocity responses of most methods – except the proposed method 1 and Newmark ($\rho_{inf}=0.7$) – include noticeable unwanted frequencies. A decay is observed in the velocity responses of Newmark method ($\rho_{inf}=0, 0.3, 0.5$). This shows that Newmark method ($\rho_{inf}=0, 0.3, 0.5$) affects the important modes. (See Figs 6.4.6, 6.4.8, 6.4.10)

Proposed method 1 and Newmark ($\rho_{inf}=0.7$) provide accurate velocity responses compared to other methods.

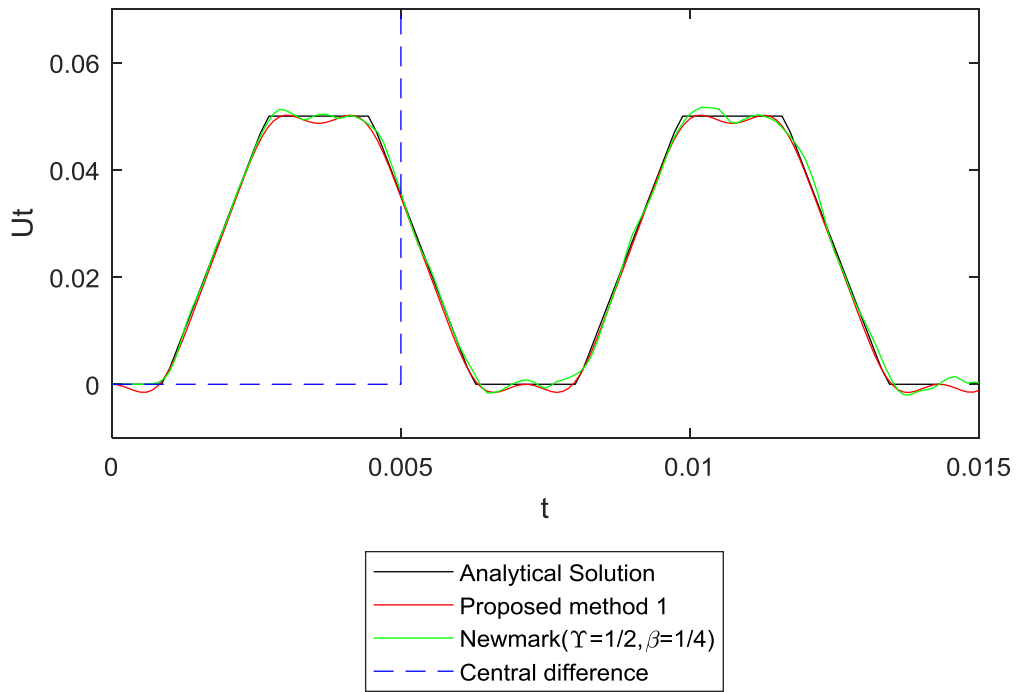


**Figure 6.4.1 Displacement response of clamped-free bar - Analytical Solution
Proposed method 1,Newmark,Central difference**

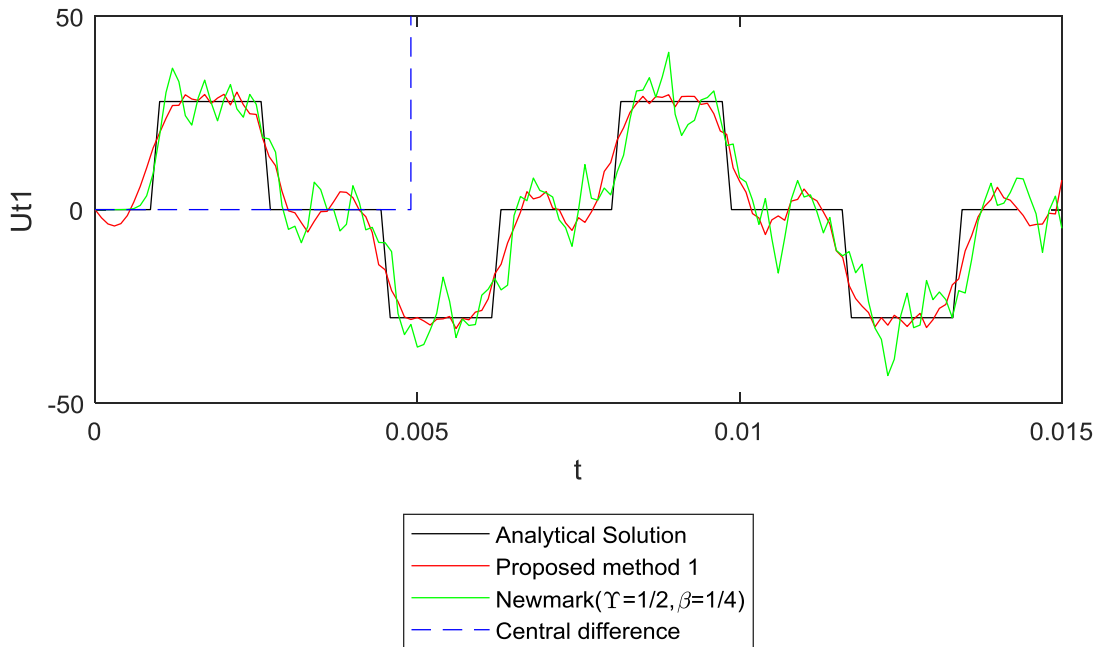


**Figure 6.4.2 Velocity response of clamped-free bar - Analytical Solution
Proposed method 1,Newmark,Central difference**

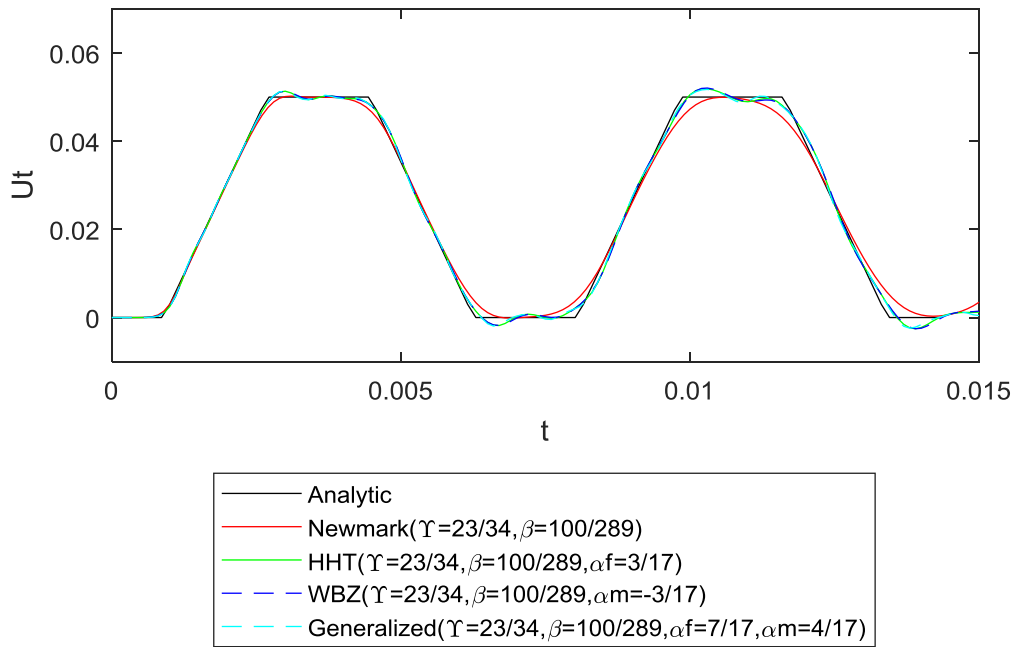


Figure 6.4.3 Displacement response of clamped-free bar -Analytic,N-M,HHT-M WBZ-M and G-M, $\rho_{inf}=0.7$

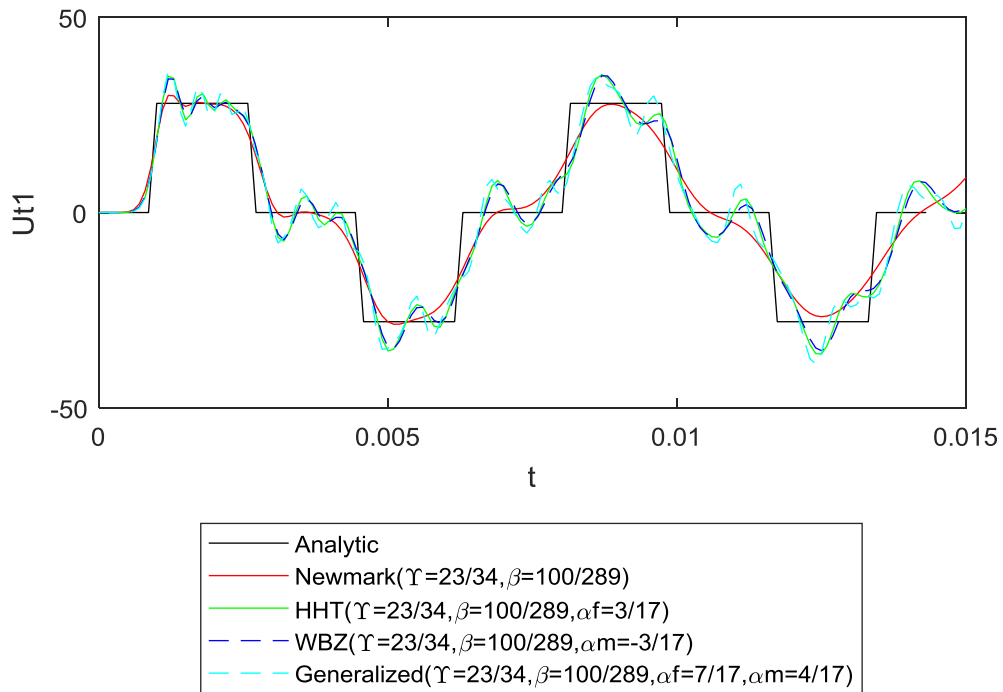


Figure 6.4.4 Velocity response of clamped-free bar -Analytic,N-M,HHT-M WBZ-M and G-M, $\rho_{inf}=0.7$

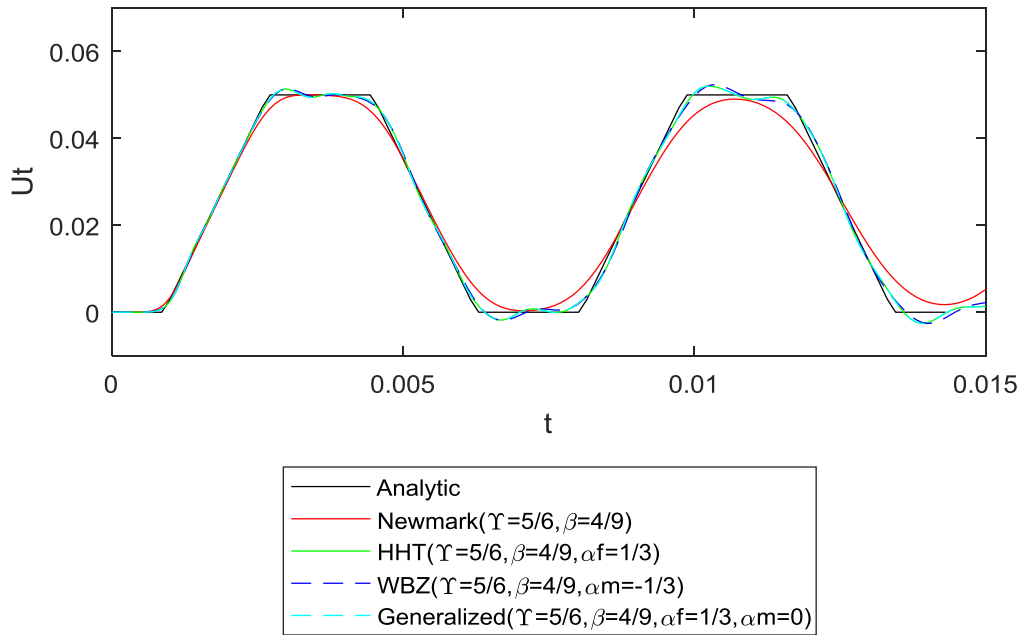


Figure 6.4.5 Displacement response of clamped-free bar -Analytic,N-M,HHT-M WBZ-M and G-M, $\rho_{inf}=0.5$

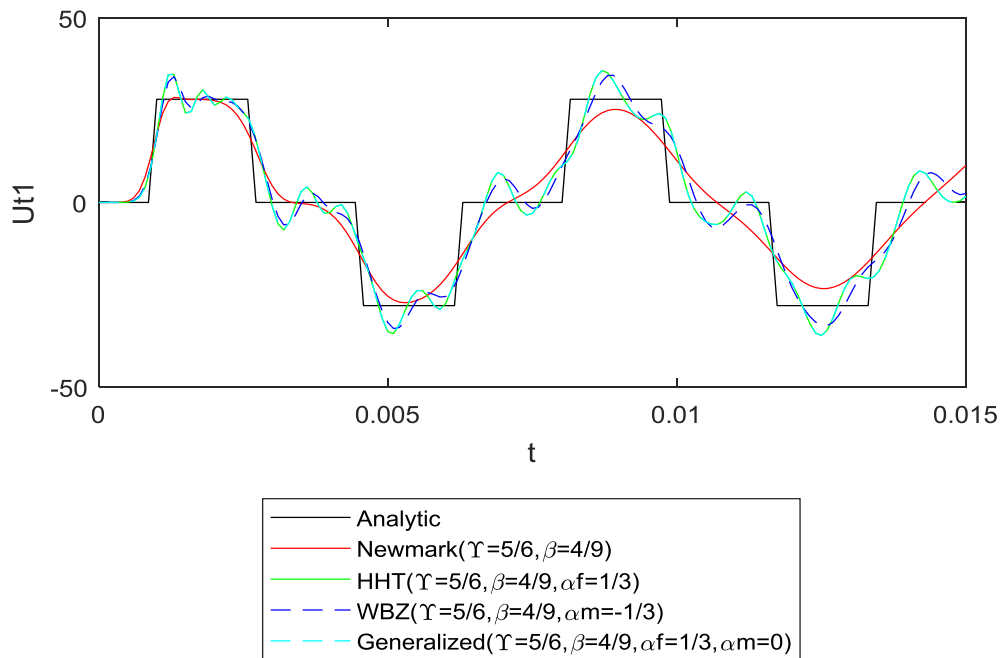


Figure 6.4.6 Velocity response of clamped-free bar -Analytic,N-M,HHT-M WBZ-M and G-M, $\rho_{inf}=0.5$

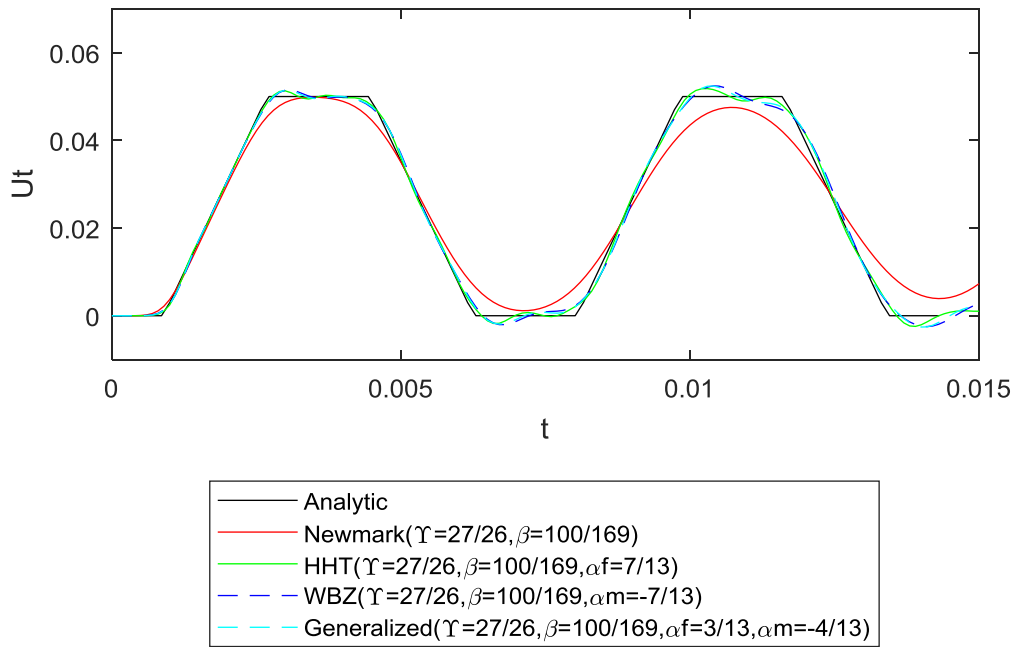


Figure 6.4.7 Displacement response of clamped-free bar -Analytic,N-M,HHT-M WBZ-M and G-M, $\rho_{inf}=0.3$

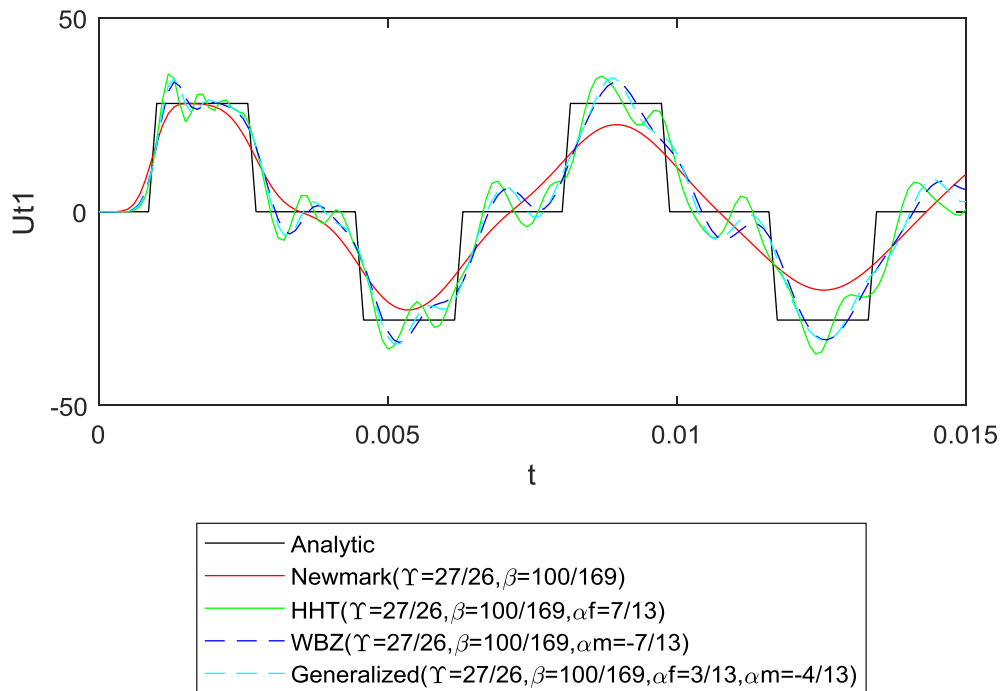


Figure 6.4.8 Velocity response of clamped-free bar -Analytic,N-M,HHT-M WBZ-M and G-M, $\rho_{inf}=0.3$

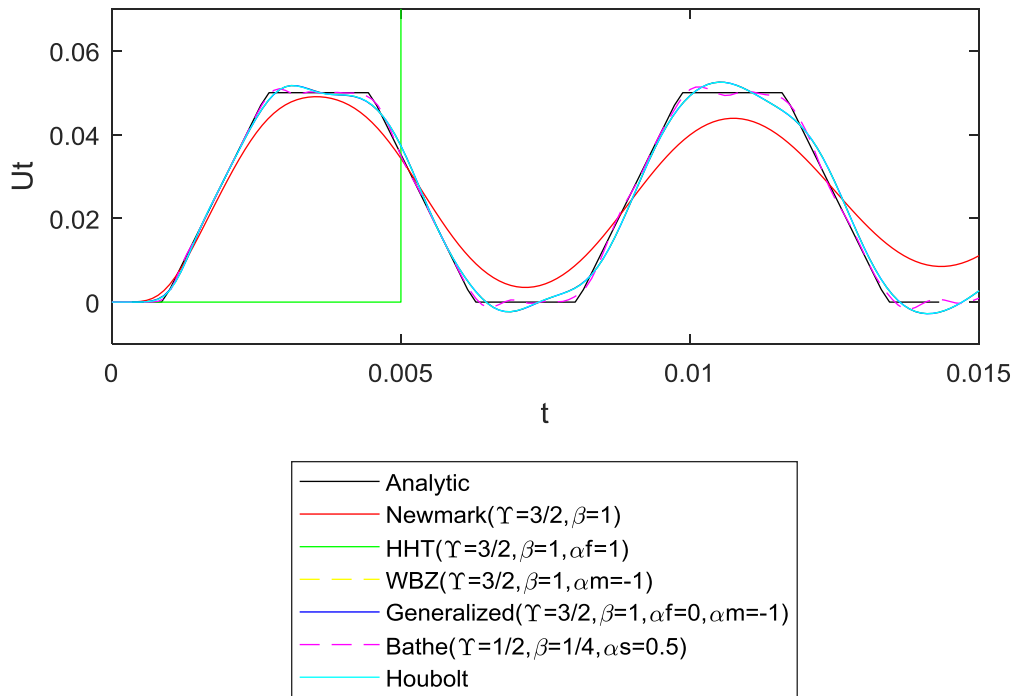


Figure 6.4.9 Displacement response of clamped-free bar -Analytic,N-M,HHT-M WBZ-M and G-M, $\rho_{inf}=0$ with Standard Bathe and Houbolt

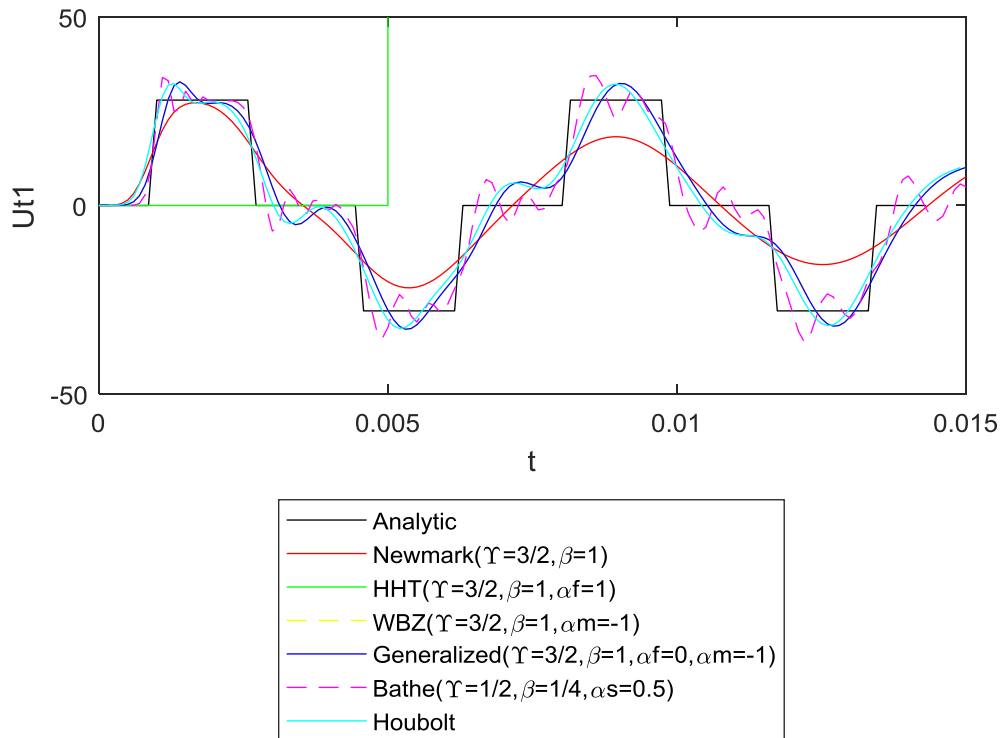


Figure 6.4.10 Velocity response of clamped-free bar -Analytic,N-M,HHT-M WBZ-M and G-M, $\rho_{inf}=0$ with Standard Bathe and Houbolt

6.5 Two-story-building system (dissipation of unwanted frequencies)

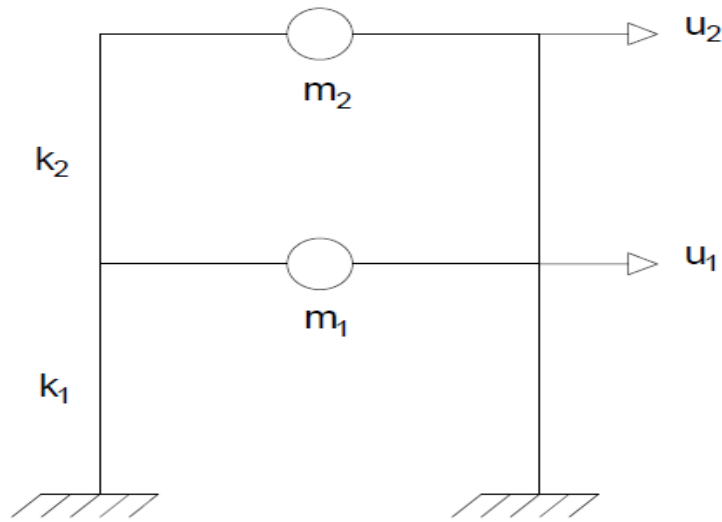


Figure 6.5 (a)

This system is established in such a way that it describes the dynamic behavior of a typical large system. The first mode represents the modes that are important and must be accurately determined. The second mode represents the spurious frequencies that must be dissipated.

For the system shown in Figure 6.5 (a), the mass and stiffness matrices are:

$$\mathbf{M} = \begin{bmatrix} m_1 & 0 \\ 0 & m_2 \end{bmatrix}, \text{ and } \mathbf{K} = \begin{bmatrix} k_1 + k_2 & -k_2 \\ -k_2 & k_2 \end{bmatrix}$$

where

$$m_1 = 25 \times 10^3 \text{ kg}, m_2 = 25,000 \text{ kg}, k_1 = 25 \times 10^6 \text{ and } k_2 = 25 \times 10^9$$

The equation of the multi-degree system can be written as follows:

$$25 \times 10^3 \begin{bmatrix} 1 & 0 \\ 0 & 1 \end{bmatrix} \ddot{U} + 25 \times 10^6 \begin{bmatrix} 1001 & -1000 \\ -1000 & 1000 \end{bmatrix} U = \begin{bmatrix} 0 \\ 0 \end{bmatrix}$$

The initial conditions of the system are defined as follows:

$$U_0 = \begin{bmatrix} 0 \\ 0.4 \end{bmatrix} \text{ and } \dot{U}_0 = \begin{bmatrix} 0 \\ 0 \end{bmatrix}$$

A time step of 0.01s is used when evaluating the response of the system.

For this two-story building system, Bathe method (standard), central difference method, Generalized- α method (pinf=0.7), Houbolt method, Newmark method (pinf=1, 0.9), Wilson method and proposed method 1 are utilized to determine the response of the system.

According to Fig 6.5.1, the response determined based on Bathe method (standard) yields accurate response.

The central difference method provides an erroneous result due to the fact that the selected time step exceeds the critical limit Δt_{cr} . (Fig 6.5.2)

Generalized- α method (pinf=0.7) and Newmark method (pinf=0.9) gives acceptable results compared to Houbolt and Wilson methods. (Figs 6.5.3 and 6.5.6)

Even though the higher mode is filtered out in the result of Houbolt method, amplitude decay is observed in the lower mode. In this case, the most important mode is not accurately determined. (Fig 6.5.4)

As expected, the higher mode is not removed in the response of Newmark method (pinf=1) which is a non-dissipative algorithm. (Fig 6.5.5)

In the Wilson method, an overestimation of the displacement response is observed in the first few steps. This property is described as the tendency to overshoot significantly the exact solutions. (**Collocation, Dissipation and 'Overshoot' for time integration schemes in structural dynamics; Hans M. Hilber and Thomas J. R. Hughes**)

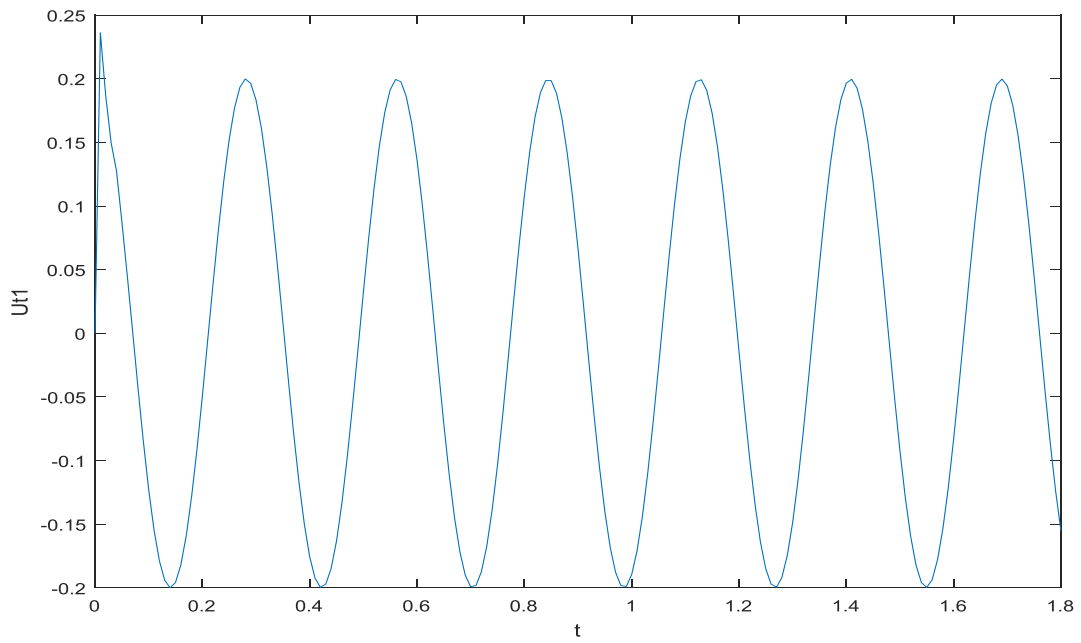


Figure 6.5.1 Two-story-building system, Bathe Method($\gamma=1/2, \beta=1/4, \alpha s=0.5$)

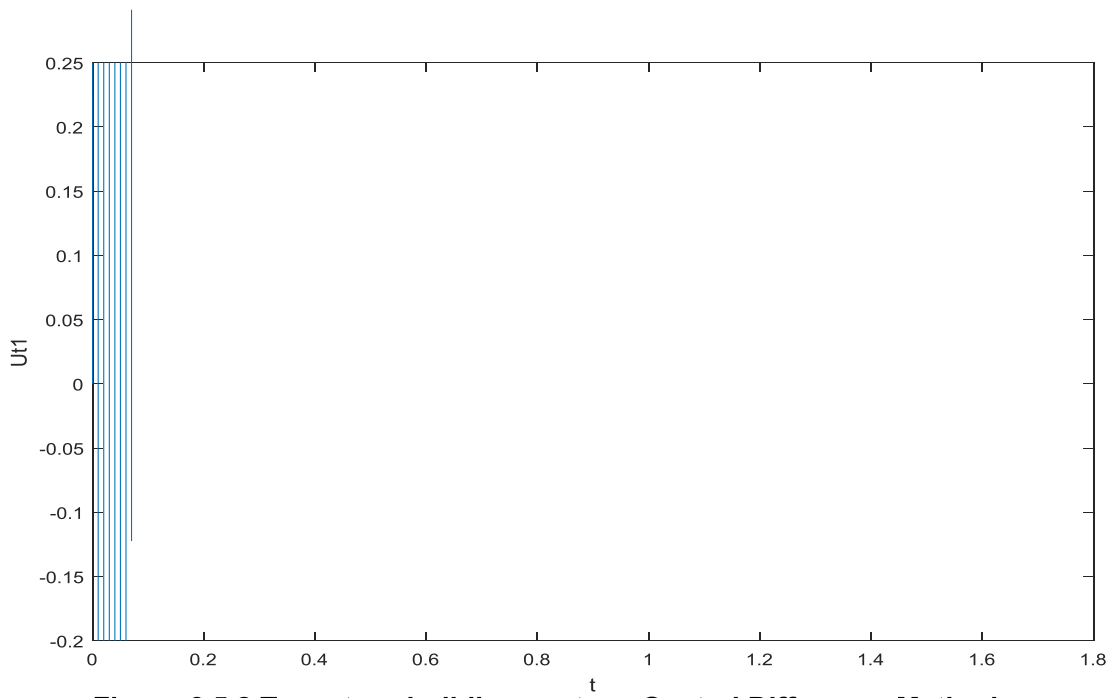


Figure 6.5.2 Two-story-building system, Central Difference Method

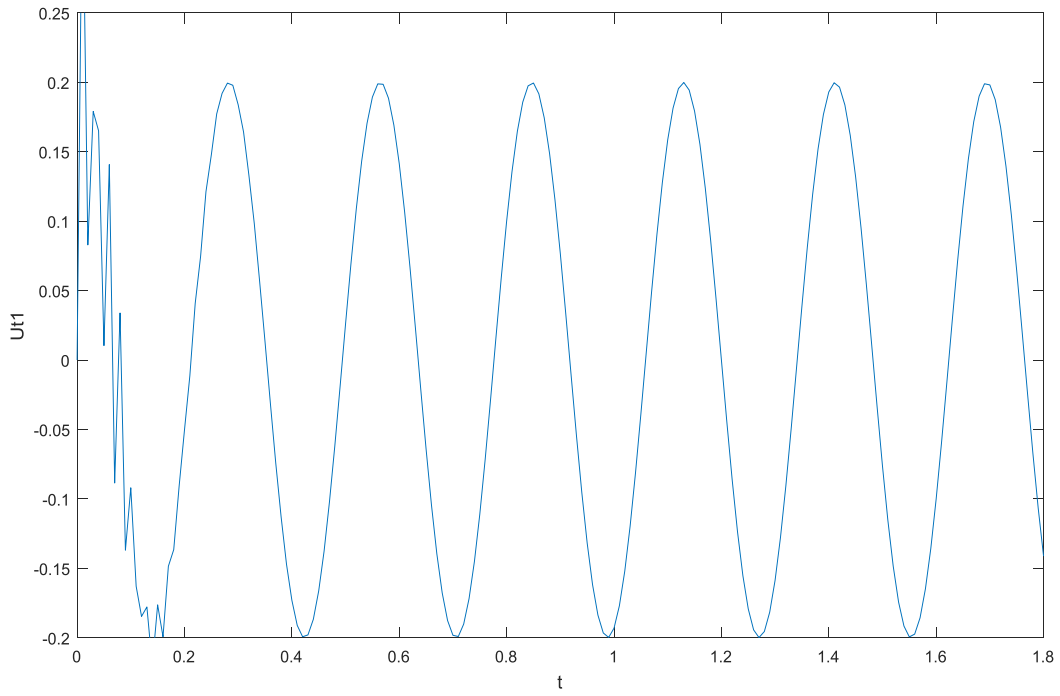


Figure 6.5.3 Two-story-building system, Generalized-alpha Method($\gamma=1/2, \beta=1/4, \alpha f=1/2, \alpha m=1/2$)

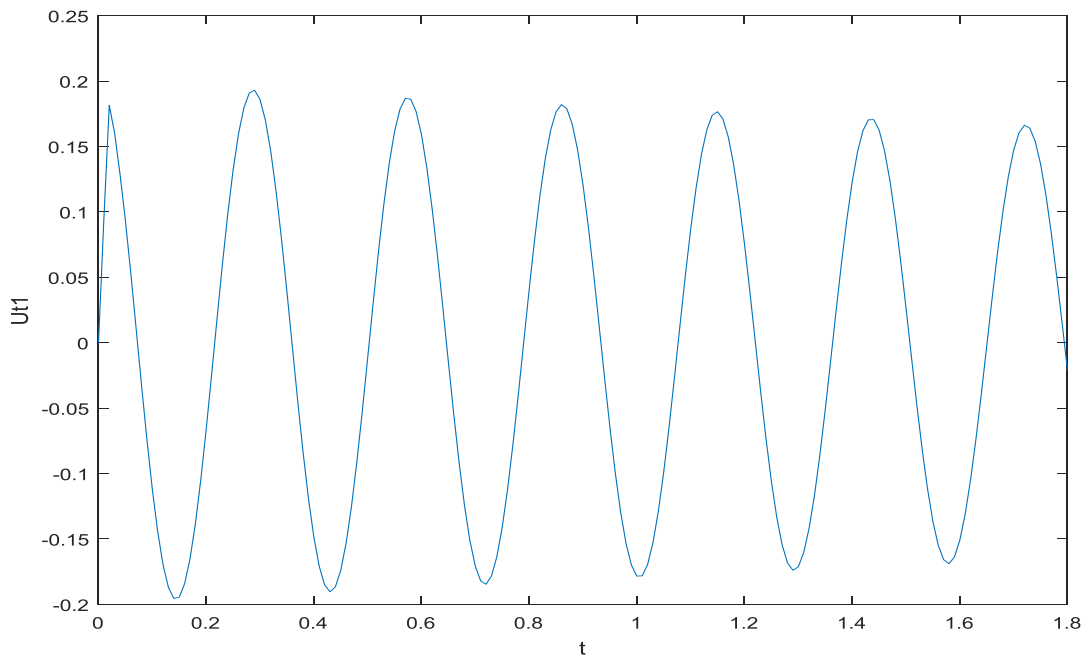


Figure 6.5.4 Two-story-building system, Houbolt Method

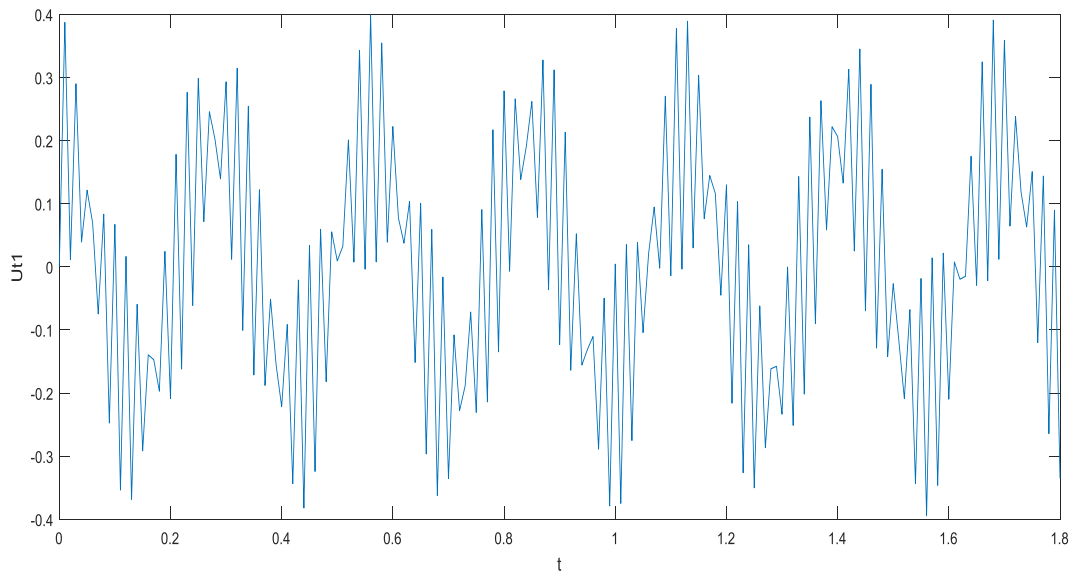


Figure 6.5.5 Two-story-building system, Newmark Method($\gamma=1/2, \beta=1/4$)

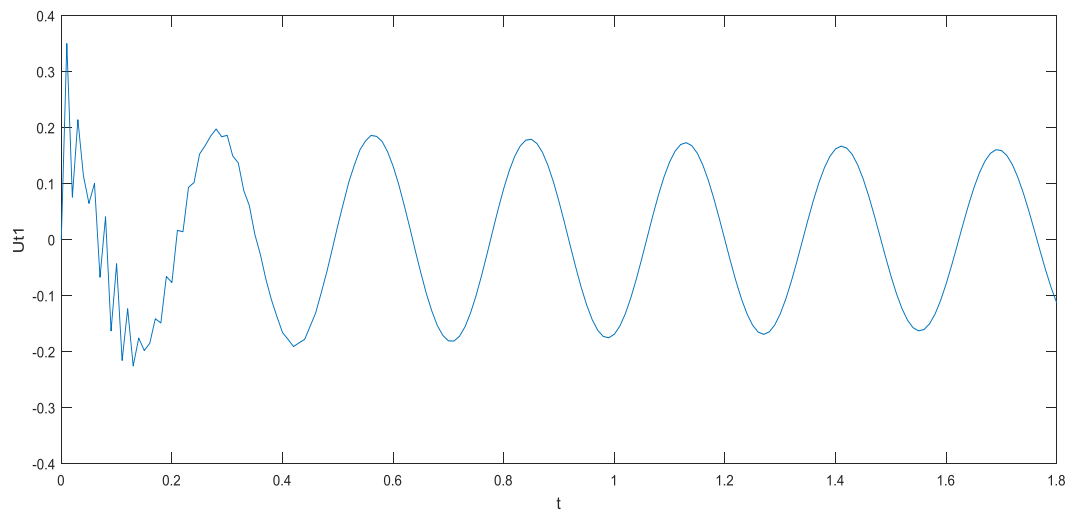


Figure 6.5.6 Two-story-building system, Newmark Method($\gamma=21/38, \beta=100/361$)

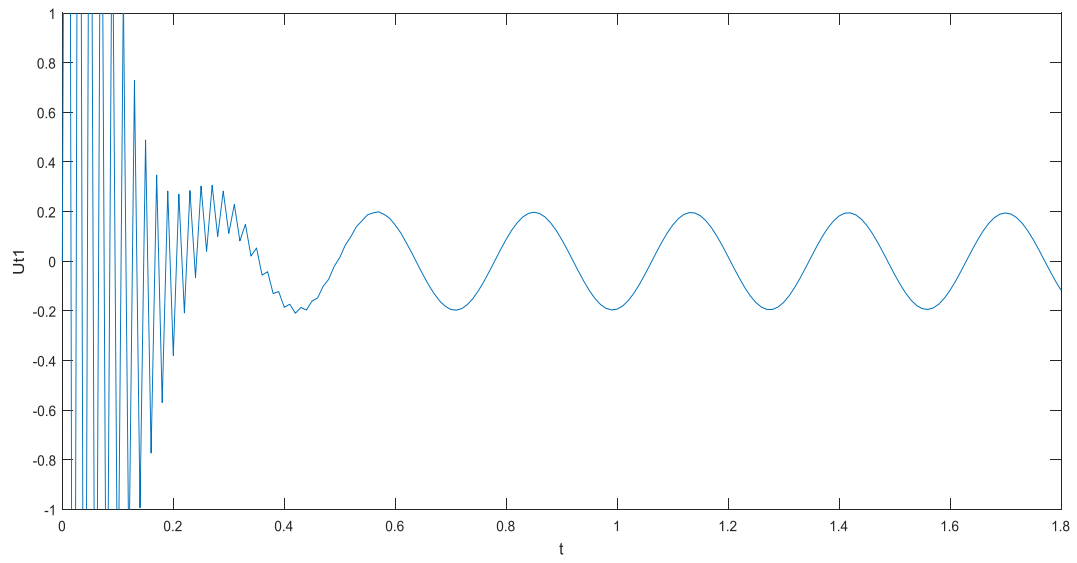


Figure 6.5.7 Two-story-building system, Wilson Method($\theta=1.37$)

6.6 Non-linear spring system

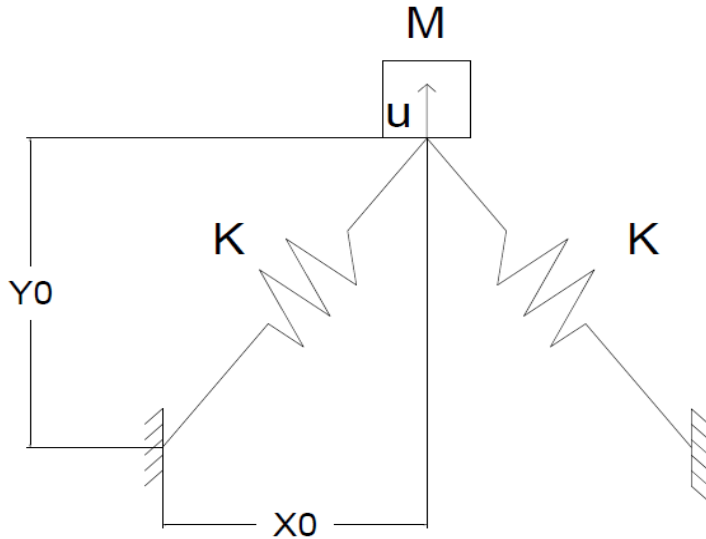


Figure 6.6 (a) Non-linear spring

For the system shown in Figure 6.6 (a), the mass and stiffness matrices are:

$$m\ddot{U} + F(U) = R$$

where

$$F(U) = 2k(l - l_0) \frac{y_0 + U}{l}, \quad l_0 = \sqrt{x_0^2 + y_0^2}, \quad l = \sqrt{x_0^2 + (y_0 + U)^2},$$

$$k = 100, \quad x_0 = 3, \quad y_0 = 4$$

The numerical solutions are determined by using central difference method, Newmark method, Proposed Method 2 and Proposed Method 3. The time steps ($\Delta t = 0.1, 0.3, 0.5$) are used for the calculation of the displacement response.

The central difference method (with a time step equal to 0.001s) is used in order to find the highly precise solution which can serve as a reference.

According to Fig 6.6.1, all methods yield accurate result when the time step is equal to 0.1s. As shown in Figs 6.6.2 and 6.6.3, the central difference method and Newmark

method introduce significant period elongation. However, no significant amplitude is observed in the responses of the Newmark method in spite of the increase of the time step. Conversely, the central difference method becomes unstable when the time step is increased to 0.5s.

As shown in all figures, Proposed Method 2 provides accurate results compared to the central difference method and Newmark method.

As expected, the results determined based on Proposed Method 3 are almost identical to the highly precise solution of the differential equation. But, the determination of the response (by using Proposed method 3) is found to be costly because it is difficult to determine the derivatives of the force function in each time step.

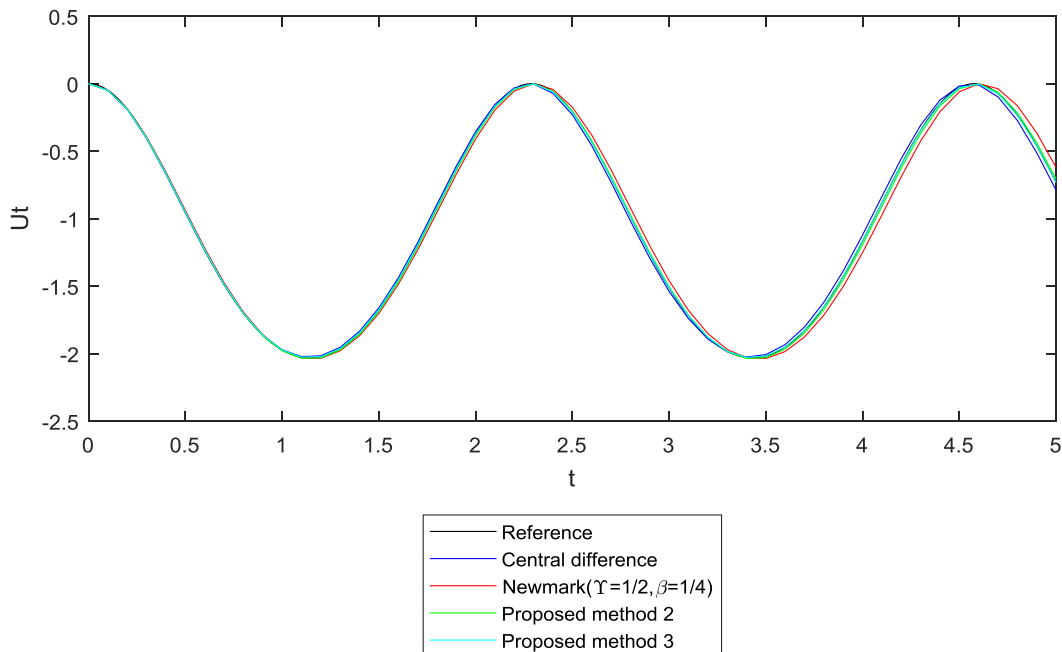


Figure 6.6.1 Displacement response of Non-linear spring -Reference,CD-M,N-M,PM2,PM3- time step (0.1s)

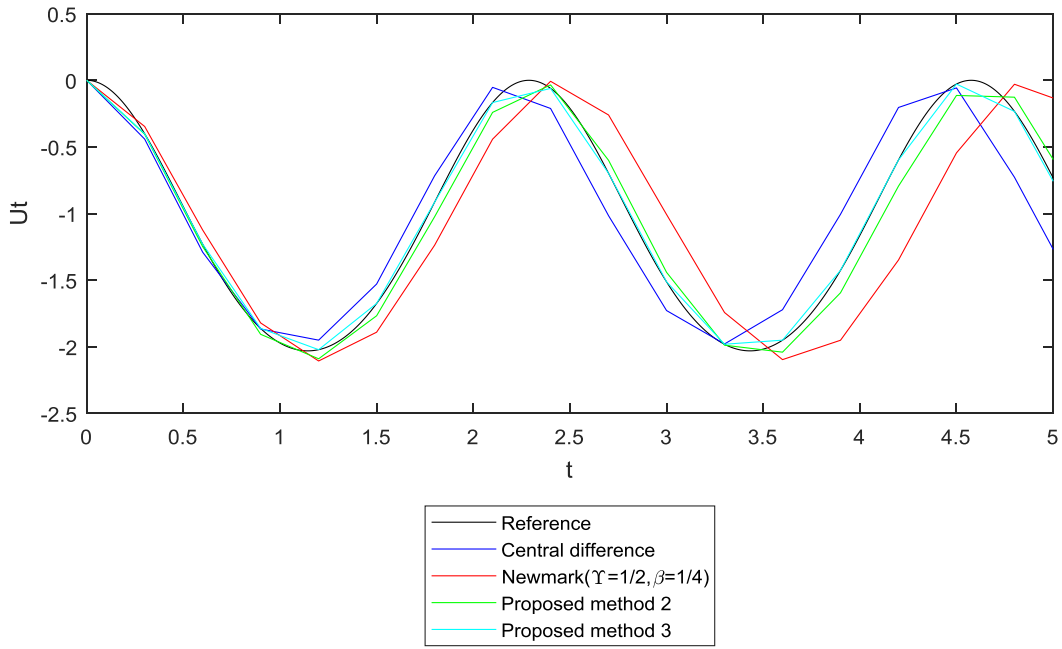


Figure 6.6.2 Displacement response of Non-linear spring -Reference,CD-M,N-M,PM2,PM3- time step (0.3s)

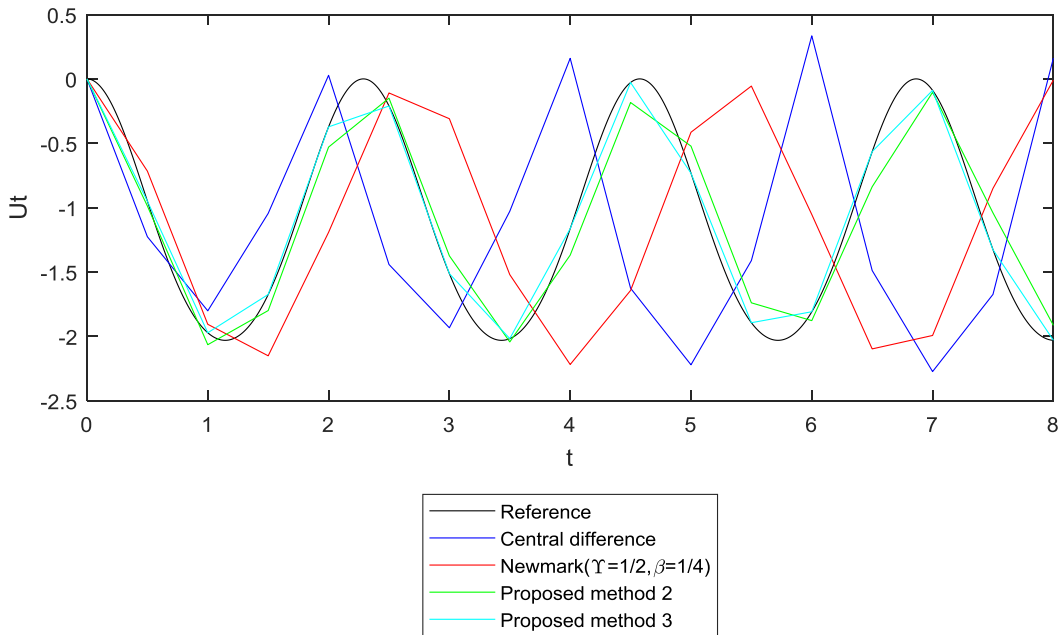


Figure 6.6.3 Displacement response of Non-linear spring -Reference,CD-M,N-M,PM2,PM3- time step (0.5s)

6.7 Five-story shear building (Non-linear)

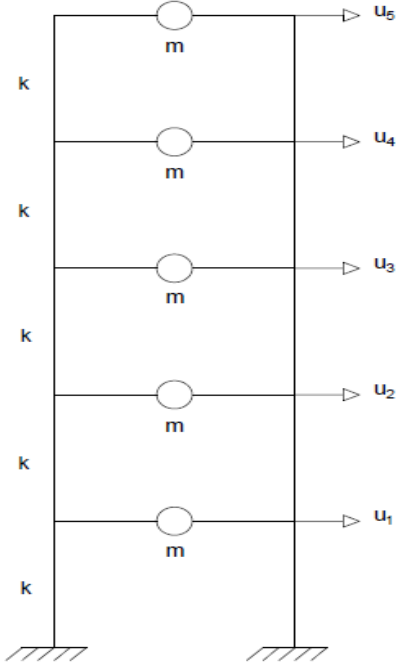


Figure 6.7 (a)

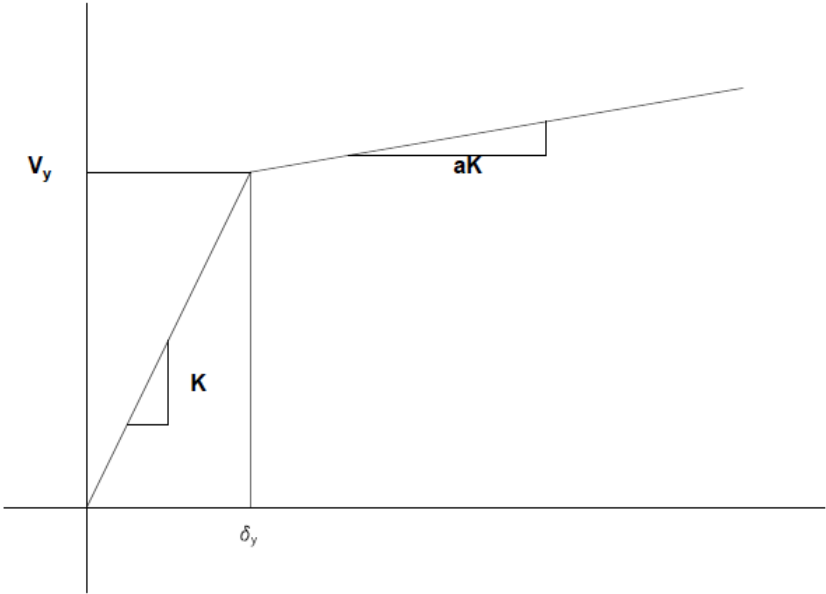


Figure 6.7 (b)

The five-story shear building shown in Figure 6.7 (a) is subjected to an earthquake load with a ground acceleration $\ddot{u}_g(t)$ expressed by the following formula:

$$\ddot{u}_g(t) = \ddot{u}_{go} \sin 2\pi t$$

where

$$\ddot{u}_{go} = 200 \text{ cm/s}^2$$

The damping matrix is derived by assuming that the damping ratio ξ_n is 5% for all modes.

$$\mathbf{C} = \begin{bmatrix} 0.8314 & -0.2383 & -0.0408 & -0.0165 & -0.0105 \\ & 0.7905 & -0.2548 & -0.0514 & -0.0270 \\ & & 0.7800 & -0.2653 & -0.0678 \\ (sym) & & & 0.7635 & -0.3062 \\ & & & & 0.5252 \end{bmatrix}$$

The mass matrix is defined as follows:

$$\mathbf{M} = \begin{bmatrix} m & 0 & 0 & 0 & 0 \\ 0 & m & 0 & 0 & 0 \\ 0 & 0 & m & 0 & 0 \\ 0 & 0 & 0 & m & 0 \\ 0 & 0 & 0 & 0 & m \end{bmatrix}$$

Where

$$m = 0.3 \text{ KNsec}^2/\text{cm}$$

The story shear-drift is the same for all stories and bilinear (as shown in Figure 6.7 (b)) with:

$$k = 125 \text{ KN/cm}$$

$$\alpha = 0.05$$

$$V_y = 150 \text{ KN}$$

The central difference method, Newmark method and Proposed Method 2 are employed to determine the displacement of the fifth floor.

The central difference method (with a time step equal to 0.001s) is utilized to obtain the highly precise solution which can be considered as a reference.

Fig 6.7.1 shows that all methods provide results which agree with the highly precise solution when the time step is equal to 0.05s. Particularly, the result of Proposed Method 2 is similar to the correct solution.

In Fig 6.7.2, Proposed Method 2 remains accurate while deviations are observed in the solutions of the central difference method and Newmark method.

While the time step is equal to 0.2s, all methods become unstable. However, the solution provided by Proposed Method 2 is found to be more accurate than those resulting from the other methods.

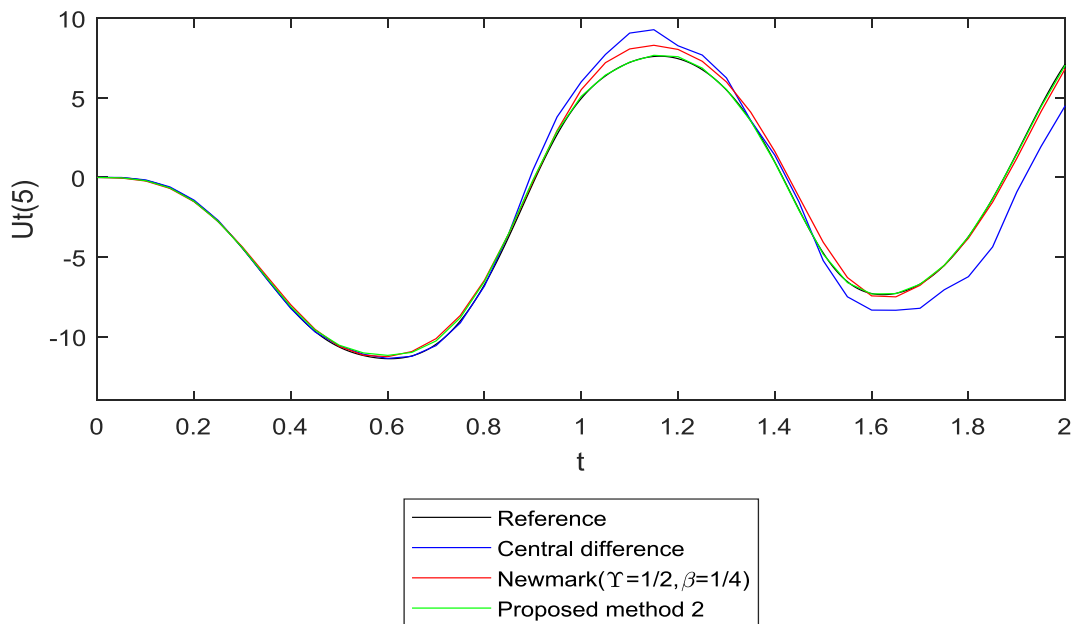


**Figure 6.7.1 Displacement response (5) of five story shear building
Reference,CD-M,N-M,PM2- time step (0.05s)**

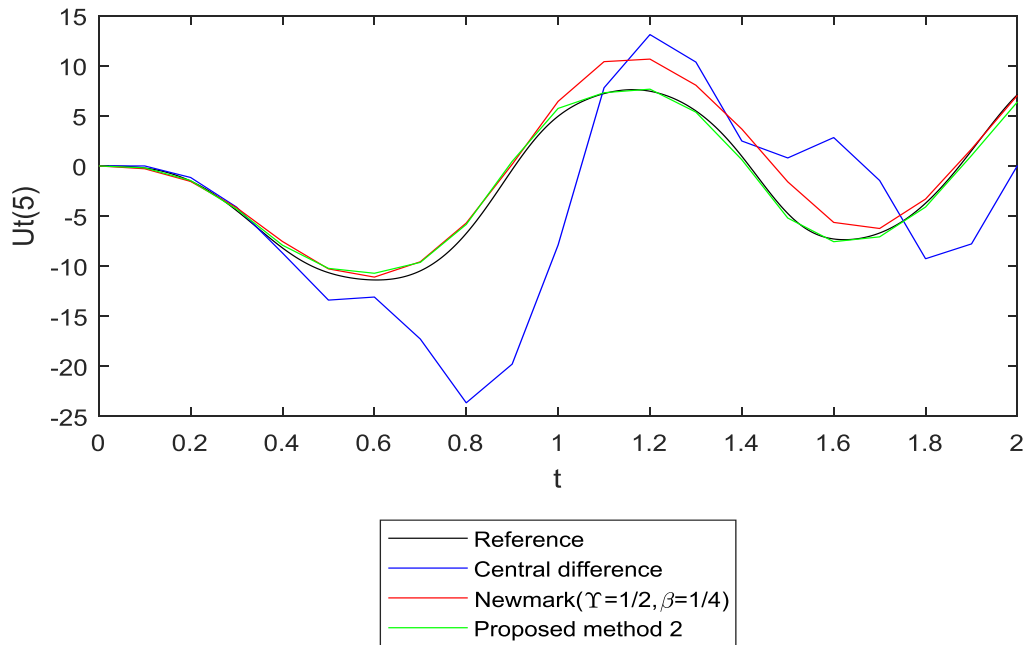


**Figure 6.7.2 Displacement response (5) of five story shear building
Reference,CD-M,N-M,PM2- time step (0.1s)**

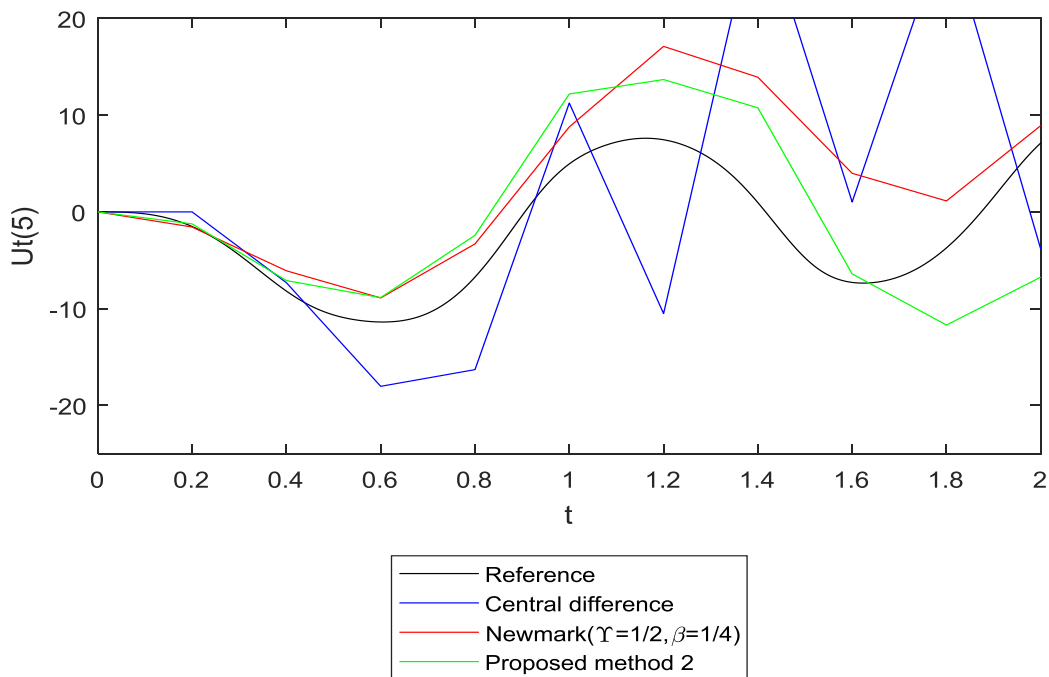


**Figure 6.7.3 Displacement response (5) of five story shear building
Reference,CD-M,N-M,PM2- time step (0.2s)**

7. Conclusion

According to our analysis, we can conclude that:

- In truncated modal space (where modal superposition is used and unwanted frequencies are removed), Newmark method ($\gamma=1/2$, $\beta=1/4$), the method based on interpolation of excitation and Proposed Method 1 can be recommended for the determination of the response. Newmark method ($\gamma=1/2$, $\beta=1/4$) is unconditionally stable and doesn't introduce numerical damping. The method based on interpolation of excitation and Proposed Method 1 are highly accurate methods that don't result in periodicity error. However, Proposed Method 1 demonstrates superior performance because it is suitable for non-classical damping system.
- Among the algorithms having numerical dissipation (where direct integration method is used), Generalized- α method and Bathe method are efficient in accurately integrating the lower modes and filtering out higher modes (which are usually the artifacts of the finite element meshing). They seem to have superior spectral performance compared to HHT- α and WBZ- α methods. The Houbolt method is found to affect the lower modes even though it is effective in removing the higher modes.
- In the analysis of non-linear system, Proposed Method 2 provides results that are more accurate than those determined by Newmark method ($\gamma=1/2$, $\beta=1/4$) and Central difference method.
- Proposed Method 3 can be considered as an unconditionally stable algorithm for non-linear system. However, the determination of the derivatives in each time step is a tedious task. Further researches are required to make the algorithm practical and efficient.

8. References

1. Bathe, K.-J., Finite Element Procedures, Prentice Hall, Englewood Cliffs, N.J., 1996, Chapter 9.
2. Filippou, F. C., and Fenves, G. L., "Methods of Analysis for Earthquake-Resistant Structures,"
3. E. L. Wilson, I. Farhoomand, and K. J. Bathe, "Nonlinear dynamic analysis of complex structures,"
4. N. M. Newmark, "A Method of Computation for Structural Dynamics"
5. Anil K. Chopra, "Dynamics of structure (Fourth Edition)"
6. Anestis S. Veletsos and Carlos E. Venturas, "Modal Analysis of non-classically damped linear systems"
7. Hans M. Hilber and Thomas G. R. Hughes, Collocation, Dissipation and Overshoot for Time Integration Schemes in Structural Dynamics
8. Hans M. Hilber, Thomas G. R. Hughes and Robert L. Taylor, "Improved Numerical Dissipation for Time Integration Algorithms in Structural Dynamics"
9. Houbolt, J. C. "A Recurrence Matrix Solution for the Dynamic Response of Elastic Aircraft," Journal of the Aeronautical Sciences, Vol. 17, pp. 540-550, 1950.
10. K. J. Bathe and E. L. Wilson "Stability and accuracy analysis of direct integration methods" Earthquake Engineering and Structural dynamics, Vol. 1, 283-291, 1973
11. G. Noh and K.-J. Bathe, "Further insights into an implicit time integration scheme for structural dynamics," June 2018.
12. M. Géradin and D.J. Rixen, "Mechanical Vibrations, Theory and Application to Structural Dynamics", 2015
13. Patrick Paultre, "Dynamics of Structures", 2011
14. W. L. Wood, M. Bossak, and O. C. Zienkiewicz, "An alpha modification of Newmark's method," 1980
15. J. Chung and G. M. Hulbert, "A Time Integration Algorithm for Structural Dynamics With Improved Numerical Dissipation: The Generalized- α Method," 1993